Modeling and Optimization of Reversed-Phase Chromatography

Effects of Modulators and Temperature

Arkell, Karolina

2017

Document Version:
Publisher's PDF, also known as Version of record

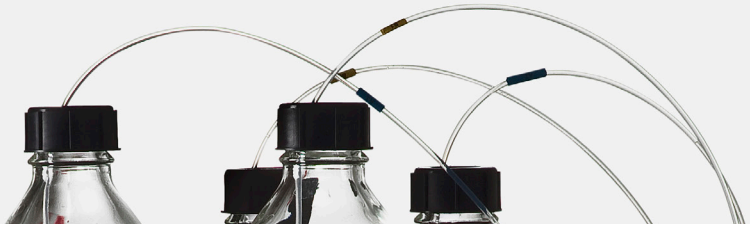

Modeling and Optimization of Reversed-Phase Chromatography

Effects of Modulators and Temperature

DEPARTMENT OF CHEMICAL ENGINEERING | LUND UNIVERSITY
KAROLINA ARKELL

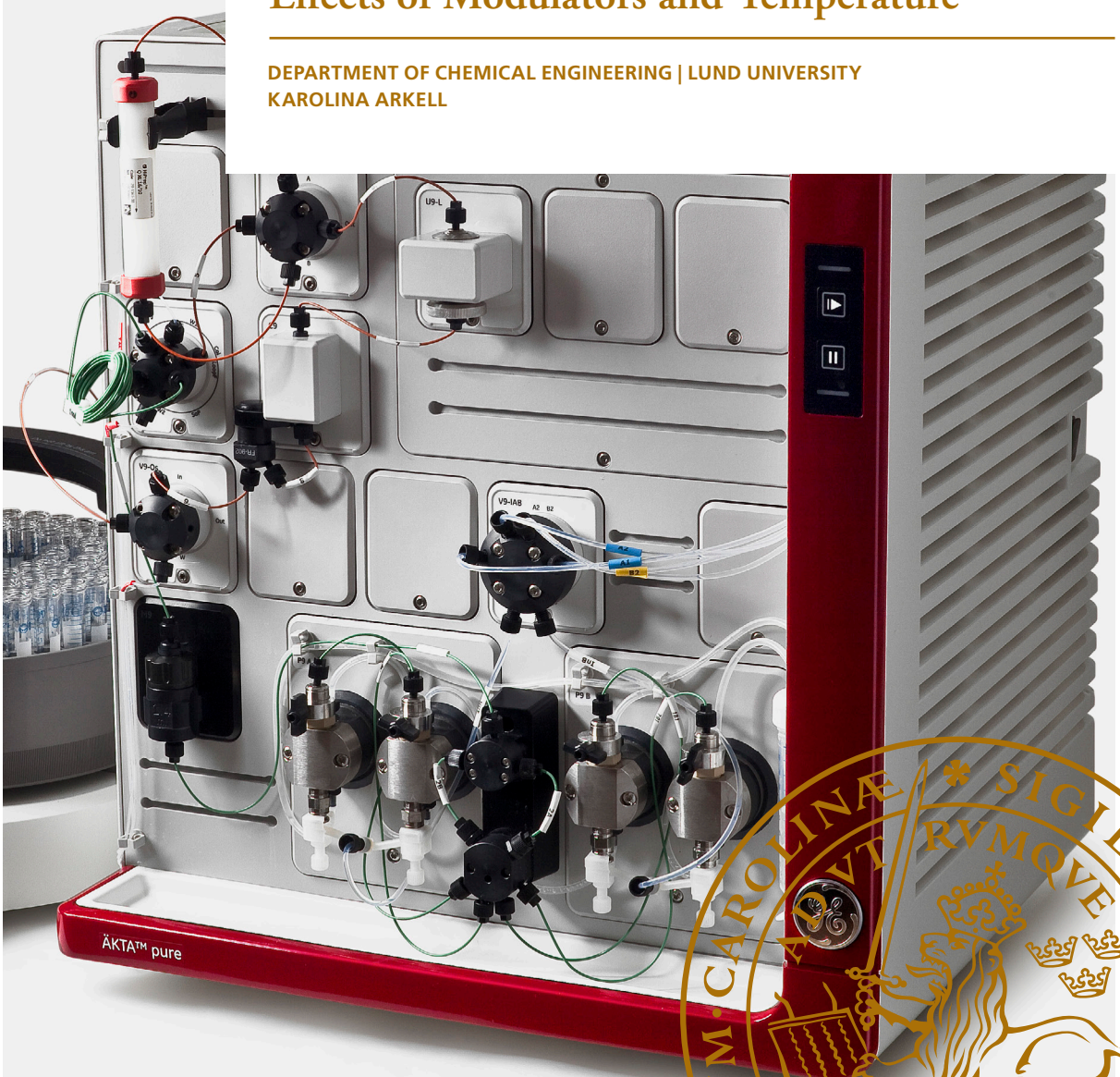

Modeling and Optimization of Reversed-Phase Chromatography

Effects of Modulators and Temperature

Karolina Arkell

Department of Chemical Engineering
Lund University, Sweden
2017

LUND
UNIVERSITY

Academic thesis, which, by due permission of the Faculty of Engineering of Lund University, will be publicly defended on December 1, 2017 at 13:15 in lecture hall K:B at the Centre for Chemistry and Chemical Engineering, Getingevägen 60, Lund, for the degree of Doctor of Philosophy in Engineering.

The faculty opponent is Prof. Abraham M. Lenhoff, Department of Chemical & Biomolecular Engineering, University of Delaware, USA.

Modeling and Optimization of Reversed-Phase Chromatography
Effects of Modulators and Temperature

Picture on front cover: ÄKTA™ pure chromatography system

Department of Chemical Engineering
Lund University
P.O. Box 124
SE-221 00 Lund

ISBN: 978-91-7422-547-1 (print)
ISBN: 978-91-7422-548-8 (pdf)

Printed in Sweden by Media-Tryck, Lund University, Lund, 2017

Success is not final, failure is not fatal:
it is the courage to continue that counts.

Winston Churchill

Abstract

Many widespread diseases, such as diabetes, various types of cancer, and aggressive versions of influenza, are treated or prevented with biopharmaceuticals. Biopharmaceuticals are drugs that are based on proteins, peptides, antibodies, attenuated viruses (vaccines), and other biomolecules that are synthesized predominately in bacteria, yeast, and mammalian cells. The first biopharmaceutical was introduced to the market in the early 1980s, and in the past several years, approximately 10 new compounds have reached the market annually. If this trend continues, rapid development of production processes for these new biopharmaceuticals will be required.

One important method by which biomolecules are purified is preparative chromatography. Although it is a well-established approach, the phenomena on which it is based are still incompletely understood. Knowledge about the effects of the process setup and operating conditions is crucial to design new chromatographic processes efficiently and streamline existing processes.

In the work presented in this thesis, the influence of the adsorbent and process conditions on the chromatographic separation of three insulin variants was examined. Two adsorbents each for reversed-phase chromatography (RPC) and hydrophobic interaction chromatography (HIC) were tested, and the effects of temperature and the concentrations of the two modulators, KCl and ethanol, were examined.

The retention of the insulin variants on the RPC adsorbents decreased as the temperature and concentrations of the modulators rose. On the HIC adsorbents, the retention declined with higher ethanol concentrations and increased with higher KCl concentrations. Consequently, KCl caused salting-in at the high ethanol concentrations that were required for elution from the RPC adsorbents and induced salting-out at the low ethanol concentrations that were needed to achieve retention on the HIC adsorbents. These data are consistent with predictions by other groups. Due to the severe self-association of insulin molecules in the HIC experiments, these two process setups were not examined further.

In a comparison between the solubility data for insulin and its chromatographic retention, the influence of ethanol on the latter was significantly stronger and thus was attributed not only to its effect on the mobile phase — the most likely explanation is that ethanol molecules adsorbed onto the ligands and were displaced by adsorbing insulin molecules. A semi-empirical RPC model that was based on thermodynamic theories was derived from the adsorption equilibrium. This model assumed adsorption of ethanol and included the activity coefficients of all involved species.

The effect of temperature on the equilibrium constant can be satisfactorily described by a linear variation of the change in Gibbs free energy on adsorption — i.e., assuming that the changes in enthalpy and entropy are temperature-independent. Because the estimated values of the enthalpy and entropy are negative, the adsorption must be enthalpy-driven. Apart from the effect of temperature on the equilibrium constant, the activity coefficients of the ethanol and insulin variants varied significantly with temperature. These effects should be separated if the temperature and modulator concentrations are varied and if several combinations of adsorbates, adsorbents, and modulators are compared.

A satisfactory model fit was achieved for variations in the concentrations of KCl and ethanol with regard to calculation of the linear-range retention and the dynamic simulations at high load. The effect of changes in temperature is less well described, albeit sufficiently, by the model. Considering that the values of the model parameters that are related to the influence of the modulators were not adjusted to the data from the temperature study, the fit is impressive.

The applicability of the final model was demonstrated in a model-based multi-objective optimization study. Pareto fronts, showing the optimal combinations of yield and productivity, were generated for both RPC adsorbents. Due to the higher selectivity between the insulin variants on the C_{18} versus C_4 adsorbent, the former effected greater productivities at a higher yield. The effect of a constraint on the Pareto fronts, with regard to the solubility of the insulin variants, was examined by comparing Pareto fronts that were based on constrained versus unconstrained optimizations. The Pareto fronts diverged when the constraint became active, and the productivity was nearly constant, with decreasing yield for the constrained optimizations, whereas that for the unconstrained optimizations continued to rise steadily.

Due to the halt in increased productivity, an alternative to performing constrained optimizations could be to select the operating point from an unconstrained optimization that lies just below the solubility limit, which yielded approximately the same result in this case study.

Populärvetenskaplig sammanfattning

Att utveckla tillverkningsmetoden för ett nytt läkemedel är dyrt och tidskrävande. Det är svårt att hitta en metod som ger ett läkemedel av hög kvalitet utan att en stor mängd kemikalier förbrukas. Datorsimuleringar kan användas för att effektivisera både nya och redan existerande tillverkningsmetoder. Då kan kostnaden för tillverkningen och dess miljöpåverkan minskas, utan att säkerheten hos läkemedlet äventyras.

Forskningen som presenteras i den här avhandlingen handlar om att bättre förstå vad som händer i ett särskilt steg i tillverkningsmetoden för insulin och liknande läkemedel. Resultaten visar hur olika faktorer påverkar läkemedlets kvalitet och hur mycket tid och kemikalier som går åt. Den modell som har utvecklats kan användas för att förbättra metoden. Då kan tiden och mängden kemikalier som går åt reduceras, samtidigt som en hög läkemedelskvalitet bibehålls. Det går också att minska den andel av läkemedlet som inte uppfyller kvalitetskraven, och därför måste kasseras. På så sätt kan den här sortens läkemedel bli både billigare, säkrare och mer miljövänliga.

Varför är detta så viktigt? Mer än var 20:e person i världen lider av diabetes och andelen ökar snabbt. Diabetes kan orsaka allvarliga komplikationer, exempelvis blindhet, njursvikt eller hjärtattack. Därför är det viktigt med effektiv behandling. Det finns olika sorters diabetes och en av de vanligaste, diabetes typ 1, går ännu inte att bota. Diabetes typ 1 beror på att kroppen inte producerar *insulin*, ett protein som behövs för att cellerna ska kunna använda sockret i maten som vi äter. Enkelt uttryckt svälter man ihjäl om kroppen inte kan utnyttja sockret, samtidigt som det gör skada i blodådrorna.

Det vanligaste sättet att behandla diabetes typ 1 är genom att ta sprutor med insulin före varje måltid. Tyvärr går det inte att ta insulinet i tablettform, eftersom det skulle brytas ner i matsmältningssystemet. När ett läkemedel sprutas rakt in i kroppen är det extra viktigt att det är rent, för att undvika att immunförsvaret reagerar på föroreningar.

Hur har föroreningarna hamnat där? Många av dagens läkemedel består av proteiner eller andra komplexa ämnen som friska människor själva producerar. Proteiner är väldigt svåra att tillverka genom att låta olika kemikalier reagera. Därför används oftast *skräddarsydda mikroorganismer*, exempelvis bakterier eller jäst. Deras arvsmassa har ändrats så att de producerar proteinet till läkemedlet i fråga. Tyvärr måste mikroorganismerna även producera många andra ämnen för att överleva. Dessa ämnen kan förorena läkemedlet och flera olika separationsmetoder krävs för att rena läkemedelsproteinet från dem. En vanlig sådan metod är *kromatografi*.

Kromatografi är en separationsmetod som kan beskrivas med följande liknelse. Anta att en stor grupp människor går in samtidigt på ett köpcentrum. Beroende på hur mycket de gillar att shoppa, så kommer de att gå in i olika många affärer och stanna där olika länge. De som inte gillar shopping lär komma ut först och vi kan på så sätt ”separera” dem från de som älskar att shoppa. Ungefär så fungerar kromatografi och proteinerna separeras utifrån sina egenskaper. Det går dock att påverka hur bra och snabb separationen blir, exempelvis genom att ändra temperaturen. Att ändra sådana förhållanden motsvarar att exempelvis få människorna att stanna längre i köpcentret genom att ha rea, respektive kortare genom att sänka temperaturen till 15°C.

Effekterna i kromatografi är dock svåra att förutsäga. Därför har ett stort antal experiment vid olika förhållanden gjorts. Sedan har en modell som beskriver kromatografiprocessen utvecklats. Den här sortens modell består av många ekvationer som kan användas i datorsimuleringar som förutspår resultatet av olika experiment. Genom jämförelse av resultaten från experimenten med dem från simuleringarna har modellen anpassats så att den stämmer bra överens med verkligheten. Med modellen går det att hitta det bästa sättet att rena läkemedelsproteinet.

Acknowledgments

It feels like it's been a hard day's night, although I've only been working like a dog for certain periods during my PhD project[1]. Looking back while exiting the thesis-writing tunnel, there are many things that I wish I had done differently, and I feel that I should have taken more time to reflect upon my work. Hopefully, I have still learned a lot in the process. I owe thanks to many people for helping and supporting me along the way, especially those mentioned below.

First of all, I want to thank my main supervisor, Professor Bernt Nilsson, for enabling this journey and always inspiring me to find alternative ways when I found myself in a dead end. Thank you for also letting me visit the US and several European cities for the first time to attend conferences. I want to thank my former assistant supervisor, Dr. Marcus Degerman, for trying to boost my creativity, always bringing positive energy, and listening when I needed it the most. Dr. Mats Galbe: Thank you for taking over for Marcus when he left academia, for useful comments on my manuscripts and abstracts, and for helping me with computer-related problems.

To my unofficial, but very important, assistant supervisors at Novo Nordisk, Dr. Søren Søndergaard Frederiksen and Dr. Martin Breil: Thank you for all your help with my PhD project. Thank you, Søren, for sharing your deep knowledge of chromatography and for often being the one asking the difficult questions. Thank you, Martin, for your devotion in scrutinizing my manuscripts, finding references for me, and helping me find a way through the maze known as thermodynamics.

In addition to Bernt, Søren, and Martin, I would like to thank Dr. Jørgen Mollerup and Dr. Arne Staby for initiating my PhD project. Jørgen: Thank you for your brutal better-late-than-never honesty. Arne: Thank you for always being helpful and for all the good times at conferences.

Thank you, Jan Sternby, for your good advice as my mentor in the MentLife program. I would also like to thank Lars Erik Edholm for initiating and organizing MentLife, and Anders Nilsson for helping me to widen my circle of contacts.

I am very grateful to all the current and former employees at Novo Nordisk whose acquaintance I have made, especially those in Departments 4606 and 4545 in Bagsværd. Despite my being an external, you have always welcomed me as one of your own. Special thanks to Nanna Mikkelsen, Anna-Margrethe Flarup, and Mette Lund for helping me with experiments. Thank you, Dorte Lunøe Dünweber, Karol Lacki, Ernst Broberg Hansen, and Mattias Hansson, my former bosses-in-practice

[1] Some phrases borrowed from *A Hard Day's Night* by J. Lennon and P. McCartney

at Novo Nordisk, for your support and for your interest in my project and my work situation.

I also want to thank all my current and former colleagues in the Department of Chemical Engineering at Lund University. Thank you for contributing to a good atmosphere, for enjoyable coffee room discussions, and for being helpful in general. I especially want to thank:

- Hans-Kristian "Hasse" Knutson, for giving me a good starting point for my last paper and for good company when we were officemates
- Niklas Andersson, for helping me with `pcs` and Matlab coding in general and for always doing it with a smile
- Anton Sellberg, for gladly helping me with Matlab coding and for being a nice traveling companion during conference journeys
- Frida Ojala, for being an excellent officemate who listened to my problems and supported me when I needed it and for letting me do the same for you
- Mikael Nolin, for nice discussions about topics ranging from wedding planning to programming and for enduring my moodiness as my officemate during pregnancy and thesis writing
- Maria Messer, Lena Nilsson, and Lill Dahlström for your help with all administrative issues

Thank you, Paula Leckius, for your devotion to making my thesis look professional and aesthetically appealing.

Novo Nordisk A/S, The Swedish Foundation for Strategic Research (SSF), the Swedish Innovation Agency (Vinnova), The Process Industry Centre at Lund University (PIC-LU), and the initiative Process Industrial IT and Automation (PiiA) are gratefully acknowledged for their financial support.

I want to thank all my friends, especially Anna and Tina, for always supporting me and taking my mind off work with your delightful company. I owe my parents many thanks for always believing in me and making me feel that I can become whatever I want. A warm thanks to my parents and my in-laws for all your love.

Anders, my better half, and Alice, my lovely daughter: You are the sunshine of my life! Thank you, Anders, for making me smile even when I don't really want to and for pushing me to continue when my motivation is low. And, of course, for loving me despite all my shortcomings. Thank you, Alice, for being my greatest accomplishment and for giving me the joy of seeing your daily progress and growth. All your smiles, hugs, and kisses make me feel all right. ♪♫

Karolina Arkell
October 2017, Lund

List of Publications

This thesis is based on the papers below, which will be referred to by their Roman numerals in the text.

I. **Johansson, K.**, Frederiksen, S. S., Degerman, M., Breil, M. P., Mollerup, J. M., Nilsson, B.
Combined effects of potassium chloride and ethanol as mobile phase modulators on hydrophobic interaction and reversed-phase chromatography of three insulin variants
J. Chromatogr. A, 2015. **1381**(1): p. 64-73

II. **Arkell, K.**, Breil, M. P., Frederiksen, S. S., Nilsson, B.
Mechanistic modeling of reversed-phase chromatography of insulins with potassium chloride and ethanol as mobile-phase modulators
ACS Omega, 2017, **2**(1), p. 136-146

III. **Arkell, K.**, Breil, M. P., Frederiksen, S. S., Nilsson, B.
Mechanistic modeling of reversed-phase chromatography of insulins within the temperature range 10-40°C
Submitted for publication

IV. **Arkell, K.**, Knutson, H.-K., Frederiksen, S. S., Breil, M. P., Nilsson, B.
Pareto-optimal reversed-phase chromatography separation of three insulin variants with a solubility constraint
Submitted for publication

My Contributions to the Studies

I. I planned the study and evaluated the results with my co-authors. I performed most of the experiments, analyzed the data, and wrote the manuscript.

II. I planned the study and evaluated the results with my co-authors. I performed all of the chromatography experiments, analyzed the data, developed the model, and wrote the manuscript.

III. I planned the study and evaluated the results with my co-authors. I performed all of the experimental work, analyzed the data, developed the model, and wrote the manuscript.

IV. I planned the study and evaluated the results with my co-authors. I implemented the model and performed the optimizations, with help from one of my co-authors. I wrote the manuscript.

Abbreviations and Symbols

Abbreviations

AC	Affinity chromatography
`act`	Applied Chromatography Toolbox
aq	In (mainly) aqueous solution
But	Butyl (ligands)
CV	Column volume
FVM	Finite volume method
HIC	Hydrophobic interaction chromatography
IEX	Ion-exchange chromatography
IMAC	Immobilized metal ion affinity chromatography
NPC	Normal-phase chromatography
ODE	Ordinary differential equation
`pcs`	Preparative Chromatography Simulator
PDE	Partial differential equation
Ph	Phenyl (ligands)
RI	Refractive index
RPC	Reversed-phase chromatography
s	Solid state
SEC	Size-exclusion chromatography
SMA	Steric mass-action
VLE	Vapor–liquid equilibrium
WENO	Weighted essentially non-oscillatory

Symbols

a	Activity [-]
A	Thermodynamic retention factor [-]
A_0	Constant part of thermodynamic retention factor [-]
A'_0	Lumped parameter with constants for thermodynamic retention factor [-]
c	Concentration in solution or mobile phase [mol/m^3]
c_{tot}	Total molarity of solution or mobile phase [mol/m^3]
C_p	Heat capacity [J/(mol·K)]
d_p	Particle diameter [m]
D_{app}	Apparent axial dispersion coefficient [m^2/s]
D_{ax}	Axial dispersion coefficient [m^2/s]
E	Internal energy [J/mol]
$E_{i,j}$	Binary interaction parameter for species i and j [-]
$E_{0,i,j}$	Reference value for binary interaction parameter for species i and j [-]
f_{cal}	Objective function for calibration

f_{con}	Constraint function for optimization
f_{obj}	Objective function for optimization
F	Faraday's number [C/mol]
G	Gibbs free energy [J/mol]
H	Enthalpy [J/mol]
k	Retention factor [-]
k_{ads}	Adsorption rate [s^{-1}]
k_D	Exclusion factor [-]
k_{des}	Desorption rate [s^{-1}]
k_{kin}	Kinetic constant for adsorption/desorption process [-]
K	Association equilibrium constant [-]
K_{ads}	Adsorption equilibrium constant [-]
K_{sol}	Dissolution equilibrium constant [-]
L	Column length [m]
N	Number of adsorbate types, grid points, process conditions, or data sets
N_A	Avogadro's number [mol^{-1}]
$\boldsymbol{p}$	(Set of) decision variables
P	Productivity [$kg/(m^3 \cdot h)$]
Pe	Péclet number [-]
q	Concentration in stationary phase [mol/m^3]
q_{max}	Saturation capacity of adsorbent [mol/m^3]
Q	Volumetric flow of mobile phase [m^3/s]
R	Ideal gas constant [J/(mol·K)]
S	Entropy [J/mol]
t	Time [s]
T	Temperature [K]
T_H	Reference temperature for change in enthalpy [K]
T_S	Reference temperature for change in entropy [K]
$U_{i,j}$	Parameter for temperature dependence of binary interaction parameter for species i and j [-]
v_{sup}	Superficial velocity of mobile phase [m/s]
V	Volume [m^3]
V_0	Residence volume of mobile phase [m^3]
V_{col}	Column volume [m^3]
V_m	Molar volume [m^3/mol]
V_{NR}	Non-retained volume [m^3]
V_{pore}	Pore volume (in stationary phase) [m^3]
V_R	Retention volume [m^3]
w	Weight fraction [-]
x	Amount-of-substance fraction in liquid [-]
$\boldsymbol{x}$	(Set of) process conditions
X	(Product) purity [-]
y_{exp}	Experimental result

y_{mod}	Model response
Y	(Product) yield [-]
z	Axial coordinate in column [m]
α	Lumped parameter for simplified Wilson's equation [-]
β	Valence of ion [-]
γ	Activity coefficient [-]
δ	Lumped parameter for simplified Wilson's equation [-]
Δ	Difference [-]
ε_0	Permittivity of vacuum [$C^2/(N \cdot m^2)$]
ε_c	Interstitial column porosity [-]
ε_D	Permittivity [$F/m=C^2/(N \cdot m^2)$]
ε_p	Particle porosity [-]
ζ	Lumped parameter for simplified Wilson's equation [-]
η	Salting-in parameter related to adsorbate size and dipole moment [C^2/m^3]
κ	Inverse of the Debye length [m^{-1}]
Λ	Ligand density [mol/m^3]
ν	Stoichiometric coefficient, ligands per protein molecule [-]
ξ	Stoichiometric coefficient, modulator molecules per ligand [-]
σ	Shielding factor [-]
τ	Salting-in parameter related to adsorbate size [m^2]
ϕ	Phase ratio [-]
χ	Lumped parameter for simplified Wilson's equation [-]
ψ	Lumped salting-in parameter related to adsorbate size and dipole moment [C^2m]
ω	Weight factor for multi-objective optimization [-]

Indices

c	First cut point, pooling begins
f	Last cut point, pooling and elution ends
i,j	Index for adsorbate, grid point, process condition, or data set
L	Ligand
M	Mobile phase modulator
P	Protein
W	Water

Contents

Chapter 1

Introduction

The first scientifically documented application for chromatography was the separation of plant pigments, performed by the botanist Mikhail Tswett, at the start of the 20th century [1]. Tswett used a primitive type of column chromatography, in which separation was based on the tendency of substances to adsorb to porous particles, called the *adsorbent*, or to dissolve in the liquid that was passing through the column [2]. Tswett also coined the term chromatography — a combination of the Greek words for *color* and *to write* [1]. Tswett's work, however, was not recognized by his contemporaries, in part because it was only published in Russian. Consequently, the development of chromatographic technology stalled for three decades, until Kuhn and Lederer demonstrated its value in separating carotenes and pigments [3].

In the 1940s and 1950s, this technology was further developed by Archer Martin and Richard Synge, who received the Nobel Prize in Chemistry in 1952 "for their invention of partition chromatography" [4]. At that time, research in the field of chemistry was focused on the extraction and characterization of substances, such as peptides and proteins, from living organisms. Martin and Synge reported that filter-paper chromatography was an excellent method for analyzing complex mixtures from various plants, animals, and microorganisms. In filter-paper chromatography, the substances in a sample form separate bands, based on their tendency to travel with liquid that is drawn up by the paper [4].

Martin and Synge, however, did not invent filter-paper chromatography but proved its value in studies of biomolecules. Their theory on partition chromatography — that substances are separated because they partition between water and the other solvent in the liquid, which are drawn up at disparate speeds — earned them the Nobel Prize. Using this method, Frederick Sanger determined the structure of insulin, for which he received the Nobel Prize in Chemistry in 1958 [4]. In 1982, human insulin, produced in genetically modified microorganisms, was the first biopharmaceutical to be approved for clinical treatment [5].

If insulin-based pharmaceuticals were to be formulated as tablets, the insulin would be digested, like any other protein that passes through the digestive system. Therefore, to achieve a sufficiently high dose, these pharmaceuticals are generally administered as subcutaneous injections, often into the stomach or thigh. Any remaining impurities — e.g., other proteins that are produced by the microorganism — thus remain intact and might cause adverse effects. Consequently, purification is a vital step in the production of biopharmaceuticals, and column chromatography is an essential separation method for purifying the active ingredients. Generally, several types of chromatography are included in this process [6].

To ensure the safety of all pharmaceuticals, they must be approved by certain regulatory bodies, such as the US Food and Drug Administration (FDA), the European Medicines Agency (EMA), and the Medical Products Agency in Sweden, before they are introduced to the market. Traditionally, the strategy for producing a safe and efficacious pharmaceutical has been to develop a process that yields the desired quality, using the same operating conditions for each batch. This homogeneity does not necessarily guarantee the same behavior by the microorganisms, and the purification process is designed to handle the smaller variations that arise. However, these fixed processes are generally designed to effect a higher quality of the final product in most cases, in order for it to be sufficient in the worst cases. This design approach results in an unnecessarily high proportion of active ingredient ending up in the waste stream.

In the past several decades, a new strategy has emerged that focuses on understanding and modeling the process and using control strategies to counteract variations in the feed for each process step, thereby ensuring a product that meets the quality criteria. Naturally, processes that are based on this approach must also aim to exceed the required product quality, but the ability of the process to adapt mitigates this need. The adaptive strategy is encouraged by the International Council for Harmonisation (ICH), a cooperative project between regulatory bodies in Europe, Northern America, and Japan [7].

The use of models for process development, optimization, and robustness analysis can save time and resources. An experiment that takes several hours to perform can be simulated in minutes, or even seconds, without the consumption of chemicals and depreciation of equipment. A model can be used to study the effects of many process parameters, for example, on yield and productivity under certain constraints. Based on the optimization or robustness analysis in silico, the theoretical optimum or correlations between process conditions and product quality can be verified or rejected experimentally.

Experimental validation and verification are especially important if extrapolations are made — i.e., if the process conditions of interest are outside of the intervals that are used to estimate the process parameters. Most phenomena in chromatography

can be modeled, but all models are simplifications of reality, and the assumptions that are made affect their predictive ability. *Black box models* are models that only describe a simplified correlation between inputs, such as process conditions, and outputs, such as product quality. These models provide limited information about the process properties and merely describe the types of changes for which they have been calibrated. However, models that are based on knowledge of the mechanisms that cause such phenomena could allow one to extrapolate, and for these models, there is often a clear connection between a parameter and the related physical properties. Mechanistic modeling is thus a more robust approach than black box modeling for creating a representation of the process in silico.

With a mechanistic model, it is possible to separate the effects of the properties of *adsorbates* (the substances that are to be separated), the *adsorbent* (what adsorbates adsorb to), and *modulators* (the substances that are used to tune the adsorption)[2] [8-10]. If only the parameters that are affected by the modulators or adsorbent must be re-estimated when either is exchanged, this type of model would be useful for screening of new purification processes. Existing models for RPC tend to incorporate parameters that are difficult to estimate from experimental data [11] or are not clearly linked to the properties of the adsorbate, adsorbent, and modulators [12].

1.1 Aim and Scope

The aim of the work described in this thesis was to examine the combined effects of a salt and an organic solvent, as modulators, on hydrophobic interaction chromatography (HIC) and reversed-phase chromatography (RPC) and explore the possibilities to develop a model that combines these types of chromatography, focusing on the effects on the retention of and selectivity between adsorbates. The criteria for the model were that it had to: 1. be based on thermodynamics; 2. describe the effect of changes in modulator concentrations, temperature, and the type of adsorbent; and 3. be sufficiently simple for use in process development in the biopharmaceutical industry. Data from chromatographic experiments were to be combined with supplementary data, primarily from solubility experiments, to discriminate between phenomena and facilitate the estimation of parameters.

The secondary goals were to determine whether the organic modulator adsorbed to the stationary phase and demonstrate the applicability and value of the final model in a multi-objective optimization study.

The model combined existing thermodynamic theories with suitable modifications and thus was not a completely new theory. A mixture of three insulin variants — insulin aspart, desB30 insulin, and an insulin ester — were used to represent the

[2] The terms adsorbate, adsorbent, and modulator are properly defined in Chapter 2.

typical feed in a purification step during the production of a biopharmaceutical. Four adsorbents were used — two for HIC with butyl and phenyl functionalities[3] and two for RPC with C_4 and C_{18} functionalities. Ethanol and potassium chloride (KCl) were used as modulators for all adsorbents, and a range of temperatures was tested. This separation problem was not drawn from an existing industrial process, but it resembles one of the final steps in the purification of insulin from genetically modified yeast [13]. The development of the model focused on the linear adsorption range, but the model was extended to preparative load levels.

The calibrated model was used to perform multi-objective optimization, in which a set of weighted combinations of productivity and yield were maximized. By varying the weight factor, a Pareto front[4] was created for each adsorbent. The Pareto front shows the optimal combinations of productivity and yield for various prioritizations between these two objectives. The decision variables were the load factor and the concentrations of ethanol and KCl in the elution buffers. In addition to the purity constraint and the upper limits of the impurity levels, the solubility of the insulin variants in the product pool was applied as a constraint. The effect of the solubility constraint on the shape of the Pareto front was studied by comparing the results of the optimization with and without this constraint. Also, an alternative to traditional constrained optimization was evaluated.

1.2 Outline of Thesis

This thesis consists of nine chapters and the four papers on which it is based. The first four chapters after the introduction provide background information for this thesis and briefly describe the theory and methods that are applied in this work. Chapter 2 summarizes the fundamentals and explains the important concepts of chromatography, and Chapter 3 presents various applications for this technology. Modeling of chromatography is described in Chapter 4, and Chapter 5 discusses how models are calibrated and how they can be used for simulation and optimization. Chapter 6 contains the results of the HIC experiments, and Chapters 7 and 8 present the findings from the modeling and optimization, respectively, of the RPC separations. The thesis closes with conclusions, a brief evaluation of the certainty of those conclusions, and suggestions for future work in Chapter 9.

[3] The more general term ‘functionality’ is used here, instead of ligand, because this concept is introduced and defined in Chapter 2.

[4] The term ‘Pareto front’ is explained more thoroughly in Chapter 5.

Chapter 2

Fundamentals of Chromatography

Chromatography is a separation method that is based on the variation in the distribution equilibria of different compounds between two phases — the *stationary phase* and the *mobile phase*. It can be used for *preparative* and *analytical* purposes, as described and exemplified in the next chapter. A schematic of a chromatography system is shown in Figure 2.1. The stationary phase consists of porous particles, typically 10-100 µm in diameter, which are made from silica, a polymer, or a gel, such as agarose. The surface of these particles, most of which lie inside of the pores, is covered with *ligands* (brown lines in lower right part of Figure 2.1) [14].

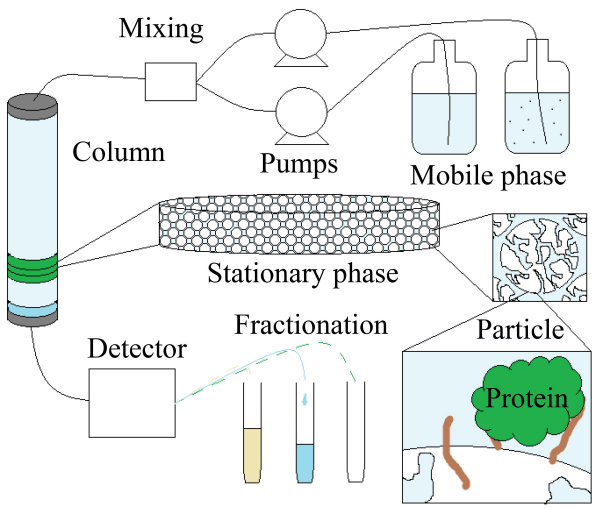

Figure 2.1: Basic equipment for chromatography. Sample injection is performed by stopping the flow of the mobile phase and adding feed mixture at the inlet of the column.

The ligands are functional groups that are bound covalently to the particle surface, and their functionality — e.g., electric charge or hydrophobicity — mediates their interaction with *adsorbates* — i.e., the compounds that are being separated. The strength of this interaction determines the distribution equilibrium; one exception is

size-exclusion chromatography (SEC), in which the distribution equilibrium depends on the size of the substances that are to be separated. A stronger interaction results in a longer *retention time* — the adsorbate spends more time in the stationary phase and exits the column (i.e., is *eluted*) later [14, 15].

In Figure 2.1, the beige adsorbate is most weakly retained by the stationary phase and has thus been eluted first, into the vial on the left. The blue adsorbate is intermediately retained and is just being eluted into the vial in the middle, whereas the green adsorbate is the most strongly retained and has not begun to be eluted. The collection of eluted mobile phase into different containers is called *fractionation* or *pooling*. The point at which the pooling into one container ends and that into the next container starts is determined by the *cut points*, which can be fixed or calculated using a control strategy and based on, for example, the eluted volume or detector signal. Most of the eluted liquid, however, is collected as waste.

The strength of the adsorbate–ligand interaction, and thus the retention time, can be tuned using *mobile phase modulators*. In most cases, the mobile phase that is used in chromatographic separation is a liquid, consisting primarily of water. The mobile phase can also be a gas (gas chromatography), which is often the case for analytical purposes, or a supercritical fluid, such as highly compressed carbon dioxide; but non-liquid mobile phases are rarely used in preparative chromatography. In addition to water, the mobile phase usually contains a buffering agent to maintain the pH and one or more mobile phase modulators to adjust the retention [14]. One exception is the normal-phase chromatographic (NPC) mode, in which the mobile phase is a weakly polar organic solvent that has a more polar organic solvent as the modulator [16].

The mobile phase modulator is often a salt, an organic solvent, or an acid or base (Table 2.1). If *isocratic* elution is applied, the modulator concentration is constant during the elution. Elution is commonly performed with a *gradient* or by stepwise changes in the modulator concentration. The gradient is usually linear and is achieved by mixing two buffer solutions with different modulator concentrations but otherwise identical compositions (Figure 2.1) [15].

Isocratic elution yields wider peaks at higher retention times, due to band-broadening that is caused by the mixing effects of dispersion, film mass transfer, and pore diffusion. Gradient elution counteracts band-broadening by gradually decreasing the adsorbate–ligand interaction, thus increasing the desorption rate [15, 17]. Gradient elution is also faster than isocratic elution, resulting in higher productivity. Occasionally, step elution is more suitable, for example, if the adsorbates differ significantly in binding strength. More advanced nonlinear gradients with many stepwise changes, such as the M-shaped elution curves that were introduced by Sellberg, Holmqvist, and colleagues [18, 19], can further optimize the elution.

2.1 Adsorbate–Ligand Interactions

The nature of the modulator depends on the chromatographic mode — i.e., the type of interaction between adsorbates and ligands. Table 2.1 lists the most common modes and the corresponding type of adsorbate–ligand interaction and modulator. The curious term 'reversed-phase chromatography' stems from its opposing nature to normal-phase chromatography: the mobile phase consists primarily of water, which is more polar than the modulator, which should be slightly hydrophobic. NPC was termed "normal" because it was common in the early history of chromatography [16].

Table 2.1: Common chromatographic modes, the interactions on which they are based, and the type of mobile phase modulator used [14].

Chromatographic mode	Interaction	Modulator
Size-exclusion (SEC)	None	None
Normal phase (NPC)	Polar	Organic solvent
Reversed-phase (RPC)	Hydrophobic (strong)	Organic solvent
Hydrophobic interaction (HIC)	Hydrophobic (weak)	Salt
Ion-exchange (IEX)	Electrostatic	Salt
Immobilized metal ion affinity (IMAC)	Metal ion–protein	pH/chelating agent/etc.
Affinity (AC)	Functional pairs	Varying

As discussed, size-exclusion chromatography differs significantly from the other modes, because it does not involve any interaction. The stationary phase lacks ligands, and separation in SEC is mediated by differences in adsorbate size — larger adsorbates access a smaller quantity of pores in the stationary phase and thus are eluted earlier, because they pass through a smaller volume. Conversely, affinity chromatography is based on specific interactions, such as that between an antibody and antigen, inhibitor and enzyme, or hormone and receptor [20]. A recent advance is mixed-mode chromatography, in which adsorbents with both HIC and IEX functionalities are used. This property significantly increases the possibility of separating similar adsorbates, and the number of studies on mixed-mode chromatography [21-25] and its applications is increasing rapidly [26, 27].

2.1.1 HIC and RPC

There are two chromatographic modes that are based on hydrophobicity — HIC and RPC — but the hydrophobic interactions in each differ in strength. The ligand density of RPC adsorbents is 5-100 times higher than that of HIC adsorbents [28-31], potentially forming an organic phase on the particle surface. With the possibility of developing a two-phase system, the mechanism in RPC might be partitioning rather than adsorption [32]. No consensus, however, has been reached regarding this issue [33], and the mechanism might vary between different

adsorbates and adsorbents. Due to the strongly hydrophobic interactions in RPC, an organic solvent, such as ethanol and acetonitrile, must be used as the modulator. The retention declines with increasing modulator content, because the mobile phase becomes more hydrophobic. RPC is not always appropriate for separating proteins, because the high content of organic solvent can denature the protein; HIC can be applied as an alternative, because it does not require an organic solvent [34].

Due to the low hydrophobicity of HIC adsorbents, it is sufficient to use a salt as the modulator. As opposed to most modes, retention increases with higher modulator concentrations, via the salting-out phenomenon. Salting-out generally refers to the decrease in protein solubility with rising salt concentrations that is observed at high salt contents. The concomitant increase in salt concentration and retention in HIC has been attributed to the salting-out effect, as supported by published comparisons of protein retention and solubility [10, 35, 36]. The retention in HIC is thus mediated by the repulsion between the adsorbate and mobile phase, rather than by the attraction between the adsorbate and ligands. At very low salt concentrations, the opposite effect is seen — termed salting-in — and the opposing effects of salting-in and salting-out cause a maximum in the solubility, corresponding to a minimum in retention in HIC [6].

2.2 Isotherms

The association equilibrium for a combination of an adsorbate and adsorbent is often described by an isotherm. An isotherm describes the equilibrium between the concentrations of adsorbate in the mobile (c) and stationary phases (q). As its name implies, the correlation is valid for constant temperature, but constant mobile phase composition, pH, and pressure are also presumed, because all of these factors affect the equilibrium [14]. The most common type of isotherm has a concave curvature (Equation 1), which is often referred to as the Langmuir isotherm, having first been described by Irving Langmuir in 1918 [37]:

$$q = \frac{q_{max} K c}{1 + K c} \tag{1}$$

K is the association equilibrium constant, and q_{max} is the saturation capacity — i.e., the highest achievable concentration of adsorbate in the stationary phase. Examples of concave isotherms, with various values for K and q_{max}, are given in Figure 2.2.

The other primary model is the convex isotherm, which has a negative sign in front of the second term (Kc) in the denominator (Equation 1) and is thus a mirror image of the concave isotherm. A combination of concave and convex intervals, forming several plateaus, can be observed if multilayers are formed or if saturation occurs [15]. Isotherms exist in other shapes, such as the Toth and Freundlich isotherms [38], but the Langmuir isotherm is the most commonly applied model for protein chromatography, which is the focus of this thesis.

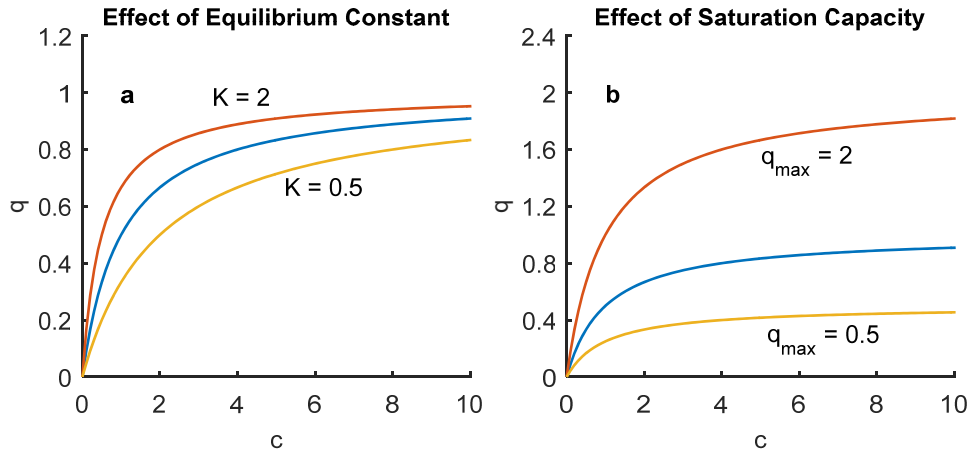

Figure 2.2: Concave isotherms for different values of a) adsorption equilibrium constant and b) saturation capacity. If not specified, the value of the parameter is unity.

2.2.1 Chromatograms and Peak Shapes

The course of a chromatographic run is often depicted by a chromatogram — reflecting the detector response (generally UV absorbance for proteins) as a function of time or the volume that has passed through the column. The response is proportional to the concentration of each adsorbate, according to the Lambert-Beer law, and the chromatogram can be decomposed into individual peaks — for example, skewed Gaussian peaks — using a suitable fitting algorithm [39] (Figure 2.3a).

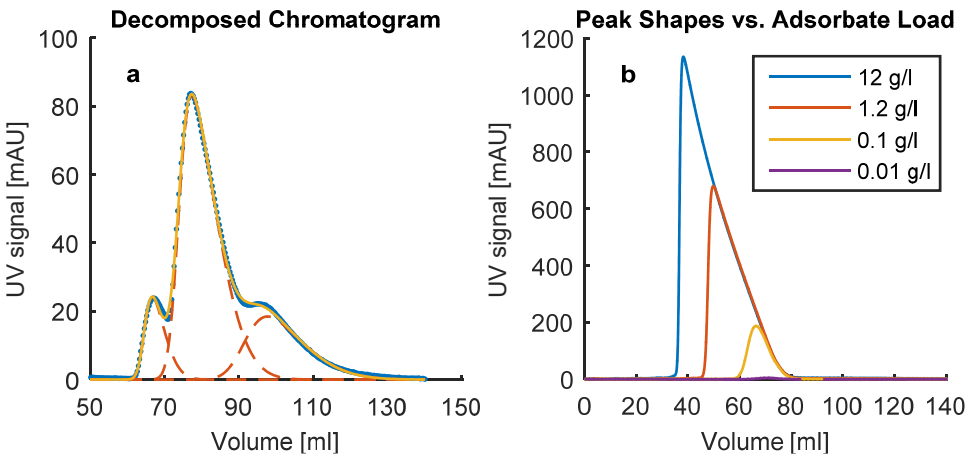

Figure 2.3: a) Chromatogram of low-load separation of insulin variants on an RPC adsorbent (blue dotted curve), decomposed into skewed Gaussian peaks (red dashed curves) that together yield the yellow solid curve. Adapted from Paper I [40]. b) Chromatogram of separation of insulin variants on an RPC adsorbent at varying adsorbate loads. The injection volumes have been subtracted.

At low adsorbate loads, the eluted peaks should assume a Gaussian shape. The peaks in Figure 2.3a exhibit slight *tailing* — i.e., they are skewed to the left. This pattern indicates that the adsorption kinetics or the mass transfer between, on the surface of, or inside of the particles is slow compared with the bulk flow of the mobile phase [15]. Another explanation is adsorption to secondary sites [41]. Tailing can also be caused by a high adsorbate load (Figure 2.3b), and for concave isotherms, the peaks generally have a common trailing edge, whereas the leading edge moves farther to the left with increasing adsorbate loads.

For convex isotherms, the peaks move in the opposite direction, resulting in *fronting* peaks and a mirror image of Figure 2.3b. Double-layer isotherms, generated by self-association of adsorbates, show more complex high-load behavior with peaks that become increasingly fronting at low to medium loads and exhibit tailing behavior at medium to high loads [15]. Examples of this pattern are found in Paper I [40].

Chapter 3

Applications of Chromatography

As discussed, chromatography can be divided into two categories based on its application — *analytical* and *preparative*. Analytical chromatography is used to analyze the composition of a sample. The adsorbate load is relatively low in analytical chromatography. Thus, there are no effects of capacity on the position or shape of the peaks, enabling identification of the adsorbates based on retention volume, and minimizing overlap between peaks. Because the aim is to identify and quantify adsorbates, widely separated Gaussian peaks are preferred, and the adsorbate load need only be sufficiently high to ensure the required precision [1, 3].

The goal of preparative chromatography is to purify one or more target adsorbates from various impurities in a sample, with minimal loss of target adsorbates. Productivity is an important factor in preparative chromatography; thus, the adsorbate load is relatively high. Because maximum recovery of the product is desired, preparative chromatography should not damage the target adsorbate, whereas the remains of the sample in analytical chromatography are discarded [1, 3]. Because the scope of this work was limited to preparative chromatography, analytical applications are not presented.

3.1 Applications of Preparative Chromatography

Based on its versatility and unique separation power, preparative chromatography has many industrial applications, ranging from the purification of high-value products, such as active ingredients for pharmaceuticals, food additives, and rare-earth elements using designed adsorbents, to potable and waste water treatment using activated carbon and bentonites [3, 42]. The applicability of advanced types of chromatography, however, is limited by the high investment and operating costs for complex equipment, expensive adsorbents with a limited life span, and high solvent consumption. Consequently, in the past several decades, purification processes for enantiomers, peptides, and proteins have been the focus of research and development efforts, primarily in the pharmaceutical industry [3, 43, 44].

3.1.1 Separation of Biopharmaceuticals

Preparative chromatography is a crucial technology for the production of biopharmaceuticals, and most purification processes for such substances include several chromatographic steps [45]. A biopharmaceutical is a drug that is based on an active ingredient that is partly or entirely produced by cells, such as bacteria, yeast, and mammalian cells — not from chemicals. This term encompasses blood, tissues, and living cells but usually refers to pharmaceuticals that are based on proteins, peptides, or antibodies. Besides insulin, other examples include growth hormones, vaccines, blood factors for the treatment of hemophilia, and monoclonal antibodies for cancer and autoimmune diseases [46, 47].

The cells for biopharmaceutical production, which are generally genetically modified to synthesize the desired substance, are grown in large tanks that are filled with aqueous solutions of the required nutrients. This initial step in the production process is called *cultivation,* or sometimes *fermentation*, regardless of whether it is performed anaerobically. When the batch cultivation is completed, the tank contains a dilute solution of the active ingredient and numerous impurities, such as product aggregates, host cell proteins, and residual nutrients [48]. It is crucial that the final purity of the active ingredient is high and that the concentration of certain impurities is below specified limits. Any remaining impurities, especially host cell proteins and product aggregates, might cause side effects by triggering the immune system. Because most biopharmaceuticals would be digested if they were to be administered orally, the standard route of administration is injection. Due to lower bioavailability, oral administration would also require a dose that is several times higher [49]. By circumventing the digestive system, the risk of degradation is mitigated, but the risk of the side effects of impurities might increase, because they are also protected from digestion.

To obtain the required purity, the purification of the active ingredient for biopharmaceuticals entails many steps — broadly categorized into *recovery*, *purification*, and *polishing*. The first step is sometimes termed *capture* or *isolation*, and polishing is not always distinguished from purification. During recovery, most of the water and impurities that differ significantly from the target product are removed. This step can be accomplished by flow-through chromatography, in which the active ingredient adsorbs strongly to the column, whereas most impurities flow through it. Alternative separation technologies include solvent extraction, ultrafiltration, and precipitation [6, 50].

The goal of the second category, purification, is to remove product-similar impurities — for example, host cell proteins and other versions of the target product. The purification is expensive and generally requires more than one chromatographic step in combination with, for example, crystallization [6, 13]. HIC, IEX, and affinity chromatography are the most commonly applied modes.

The final steps, called polishing, prepare a substance for *formulation* — i.e., the process in which the active ingredient is packaged as a pharmaceutical, such as tablets, capsules, and solutions for injection. Crystallization and spray-drying are frequently used methods for polishing [6].

Insulin

Type I diabetes has long been known to be caused by the inability of the body to metabolize sugar, due to pancreatic dysfunction, but the missing link between the metabolism of sugar and the pancreas was not found until insulin was discovered by Frederick G. Banting and John Macleod in 1921. Banting and Macleod showed that this type of diabetes could be managed, but not cured, with daily injections of insulin — a protein and hormone [51]. For several decades, insulin was acquired as a by-product from the meat industry, but it became evident that this supply would fail to meet the future demand of diabetic patients [5]. Today, over 400 million people suffer from diabetes [52], many of whom are dependent on insulin-based pharmaceuticals to survive.

Two of the largest insulin producers, Novo Nordisk A/S and Eli Lilly & Co., use genetically modified Saccharomyces cerevisiae (yeast) and Escherichia coli, respectively, for fermentation. The process that is used by Novo Nordisk A/S to recover insulin precursor that is produced by yeast cells, transform it into human insulin, and purify the final product is described below. Because the yeast cells excrete insulin precursor into the fermentation broth, the first step in recovery is thus cell removal, which is performed by centrifugation. The insulin precursor is then captured by cation exchange chromatography, and the remaining cell debris is subsequently removed by filtration. Most residual impurities are removed by crystallization and precipitation, and in the final recovery step, a purity that exceeds 90% is achieved by crystallization of the insulin precursor [13].

The purification begins with two chemical reactions that transform the insulin precursor into an insulin ester and then into human insulin, each of which is followed by two chromatographic steps to remove the enzyme from the first reaction and by-products from both reactions. RPC, followed by anion exchange chromatography, and two RPC steps are used to purify the product after the first and second reactions, respectively [13]. Insulin is one of the few proteins that can tolerate the high concentrations of organic solvent that are required for RPC, primarily due to its small size and globular shape. The purification processes for other proteins are thus generally combinations of IEX and HIC steps. The impurities that are removed in the AIEX and second RPC steps include desB30 insulin and an insulin ester. Both of these variants were used in the work presented in this thesis. Finally, human insulin is crystallized, resulting in a purity above 99.5%, and freeze-dried before formulation [13].

3.1.2 Separation of Small Molecules and Ions

Preparative chromatography is also used to purify non-biological active ingredients, such as pharmaceuticals that are based on substances that are synthesized without cells or other organisms. One common application in this area is the separation of enantiomers — molecules that are mirror images of each other. When substances that have enantiomers are synthesized through chemical reactions — not by an organism — a mixture of the two enantiomers is often obtained. However, only one of them is the desired active ingredient, and the other might have undesirable side effects [43, 44].

An example of such side effects is the teratogenicity of an enantiomer of thalidomide. Thalidomide was the active ingredient of a drug that was commonly prescribed to pregnant women in the 1950s to treat sleeplessness and nausea. Unfortunately, the effects of thalidomide had not been properly investigated and the otherwise inactive enantiomer caused birth defects, primarily severe deformities in the limbs and internal organs. More than 10,000 children were affected worldwide [53].

Preparative chromatography is also used for separation in the food industry, such as the continuous separation of fructose and glucose, using a *simulated moving bed* (SMB). In SMB, several columns are connected in series and switch places sequentially, achieving the apparent effect of countercurrent motion of the stationary and mobile phases [54].

Secondary metabolites from plants are a class of substances that can be used as active ingredients in pharmaceuticals and food additives. Secondary metabolites are substances that organisms produce, although they are not essential to their survival, such as carotene, menthol, and lignin. Analytical chromatography is often used to identify the secondary metabolites in various plants in the search for new active ingredients for pharmaceuticals or suitable food colorants and flavorings. However, the high cost of large-scale preparative chromatography limits its use for production-scale separation of these substances, at least in the food industry [55, 56].

Another application of preparative chromatography that is being commercialized is AC for the separation of rare-earth elements from dissolved ore. Rare-earth elements are metals that are used in many high-tech products, such as batteries, monitors, and superconductors [57]. IEX was used to separate rare-earth elements in the Manhattan Project in the 1940s, but this method never passed the pilot stage [3]. The separation process that is generally applied in industry comprises a multi-step liquid–liquid extraction and a final chromatographic step for polishing. Replacement of the extraction steps with chromatography-based stages significantly reduces the number of steps that is required and the consumption of solvent [57-59].

Chapter 4

Modeling of Preparative Chromatography

In the studies on which this thesis is based, retention is assumed to occur due to adsorption, not partitioning. To avoid confusion with the thermodynamic retention factor and because all adsorbates in these studies are proteins, the adsorbate is henceforth assumed to be a protein and is denoted *P* or adsorbate *i*. Adsorption means that the protein (*P*) is reversibly bound to a number of ligands (*L*), forming a protein–ligand complex (PL_ν), as described by Equation 2a, where ν denotes the stoichiometric coefficient between ligands and protein molecules. Equation 2b describes the process when ξ modulator molecules (M) competitively adsorb to the ligands and are displaced by the adsorbing protein.

$$P + \nu L \rightleftarrows PL_\nu \tag{2a}$$
$$P + \nu LM_\xi \rightleftarrows PL_\nu + \nu\xi M \tag{2b}$$

The adsorption equilibria for these two cases are given by Equation 3, where K_{ads} is the equilibrium constant for the adsorption, a is the activity, γ is the activity coefficient, and x is the amount-of-substance fraction — all of the species that are specified by the index.

$$K_{ads} = \frac{a_{PL_\nu}}{a_P a_L^\nu} = \frac{\gamma_{PL_\nu}}{\gamma_P \gamma_L^\nu}\frac{x_{PL_\nu}}{x_P x_L^\nu} = \frac{\gamma_{PL_\nu}}{\gamma_P \gamma_L^\nu}\frac{q_P}{c_P}x_L^{-\nu} \tag{3a}$$
$$K_{ads} = \frac{a_{PL_\nu}a_M^{\nu\xi}}{a_P a_{LM_\xi}^\nu} = \frac{\gamma_{PL_\nu}\gamma_M^{\nu\xi}}{\gamma_P \gamma_{LM_\xi}^\nu}\frac{x_{PL_\nu}x_M^{\nu\xi}}{x_P x_{LM_\xi}^\nu} = \frac{\gamma_{PL_\nu}\gamma_M^{\nu\xi}}{\gamma_P \gamma_{LM_\xi}^\nu}\frac{q_P}{c_P}\left(\frac{x_M^\xi}{x_{LM_\xi}}\right)^\nu \tag{3b}$$

The equilibria in Equation 3 can be used directly to calculate the retention volume (V_R) for each adsorbate, but estimating the peak shapes and thus the degree of separation requires a dynamic simulation, including the mass transport and the kinetics of the adsorption/desorption.

4.1 Retention Factors

The retention volume of an adsorbate is defined as the first moment of the corresponding peak in the chromatogram, starting from the outset of elution. If the peaks are symmetrical, the first moment coincides with the position of the peak maximum. The most commonly used normalized measure of retention is the retention factor k, which is calculated from experimental data per Equation 4 [15].

$$k_P = \frac{V_{R,P} - V_0}{V_0} = \frac{V_{R,P} - V_{col}\left(\epsilon_c + (1-\epsilon_c)\epsilon_p\right)}{V_{col}\left(\epsilon_c + (1-\epsilon_c)\epsilon_p\right)} \tag{4}$$

V_0 is the residence volume of the mobile phase — i.e., the total void volume of the column — and V_{col} is the total column volume. ε_c is the interstitial column porosity — i.e., the void fraction between the particles — and ε_p is the particle porosity. k is easy to determine and is suitable for small molecules that can access the same fraction of pore volume as the mobile phase. For proteins and other macromolecules, however, the thermodynamic retention factor A [10, 60, 61] might be more suitable (Equation 5).

$$A_P = \frac{V_{R,P} - V_{NR,P}}{V_{pore,P}} = \frac{V_{R,P} - V_{col}\left(\epsilon_c + (1-\epsilon_c)\epsilon_p k_{D,P}\right)}{V_{col}\left((1-\epsilon_c)\epsilon_p k_{D,P}\right)} \tag{5}$$

$V_{NR,P}$ is the non-retained volume — i.e., the residence volume under non-adsorbing conditions — and $V_{pore,P}$ is the accessible pore volume, both for the protein. By introducing the exclusion factor $k_{D,P}$, the limitations in the accessible pore volume due to the shape and size of the protein are taken into consideration. Thus, comparisons between adsorbates and adsorbents are based solely on the adsorption equilibria and are unaffected by shape or size.

The retention factor k_P (Equation 6) is directly proportional to the equilibrium constant for the adsorption but also depends on the phase ratio ϕ, which is the ratio between the volumes of the stationary and mobile phases [62]. The exact definition varies between theories [63, 64]. For the thermodynamic retention factor (Equation 7), the relationship with the equilibrium constant depends on the adsorption mechanism and can be derived from the corresponding equilibrium expression — e.g., Equation 3a or b. The definition of A is based on the adsorption isotherm and is equal to its initial slope — i.e., the q_P/c_P ratio at infinite dilution [65].

$$k_P \equiv K_{ads,P}\phi \tag{6}$$

$$A_P \equiv \lim_{q_P \to 0} \frac{q_P}{c_P} \tag{7}$$

4.2 Thermodynamic Equilibrium Models

As a consequence of the range in theories on hydrophobicity, there are many models that describe the adsorption equilibrium in HIC and RPC. Due to the high ligand density of RPC adsorbents [28, 29, 66], the mechanism of retention in RPC can be viewed as adsorption [11, 12, 33] — i.e., a reaction in which adsorbate molecules and ligands associate reversibly — or as partitioning [12, 32, 33, 67], similar to the phenomenon that underlies liquid–liquid extraction. As discussed in the introduction and earlier in this chapter, in this project, the retention mechanism is regarded as adsorption. For smaller molecules, partitioning might also mediate retention in RPC. However, I find it unlikely that large molecules, such as peptides and proteins, can partition into an organic phase that is formed by ligands due to their sheer size. A selection of equilibrium models that assume adsorption are presented below.

4.2.1 Modulator Effects

The most famous and widely applied [68-70] thermodynamic descriptions of HIC and RPC are the adaptations of the solvophobic theory by Horváth, Melander, and colleagues [11, 35, 71]. The main feature of these models is that the effect of the modulator is attributed primarily to its effect on surface tension, correlated with the change in Gibbs free energy for cavity formation. Van der Waals and electrostatic forces are included in the models, but they are assumed to vary negligibly in RPC when only the mobile phase composition changes. This model structure yields a linear dependence of $\ln(k)$ on surface tension with the change in contact area between the mobile phase and the adsorbate, ligands, and adsorbate–ligand complex on adsorption as a proportionality constant [11].

HIC Models

For HIC, the electrostatic forces are given by a salting-in term per Debye and Hückel and a salting-out term that is related to the dipole moment of the adsorbate. The former is negligible at relevantly high salt concentrations, and the latter is proportional to the molality of the salt, and so is the surface tension. This results in a linear dependence of $\ln(k)$ on the molality of the salt. In this case, the proportionality constant is the difference between the term for the contact area and surface tension increment, and the term for the dipole moment [35]. Despite the success of adaptations of the solvophobic theory with regard to chromatography, these models have received significant criticism [72-75] — for example, claiming that the changes in surface tension are not the only source of the dependence of the retention in HIC on salt concentration.

Another well-known and popular HIC model [76, 77] is the adaptation of the preferential interaction theory [72, 78]. This model is also based on the salting-in and salting-out phenomena but does not correlate them with surface tension. Instead, the variation in the effects of various salts on the retention in HIC is attributed to

the nature of their interaction with the protein. If the interaction is preferential, the salt causes salting-in as the ions cluster around the protein molecules, decreasing unfavorable interactions with water molecules. If the interaction is not preferential, salting-out is observed as the protein molecules reduce the hydrophobic surface area that is exposed to the mobile phase by adsorbing to ligands [72]. The preferential interaction and solvophobic theories are similar but differ, in that they attribute salting-in and salting-out to protein–salt interactions and the salt effects on surface tension, respectively.

Because neither of these models has been generally accepted, a different approach for modeling salt effects was used in this work (see Chapter 7) — an adaptation of Kirkwood's electrostatic theories on macromolecules in solution by Mollerup and colleagues [10]. This model also assumes that salting-in and salting-out, as well as the retention in HIC, are caused by the same phenomena. In this case, however, the effects of salt are described by the changes in electrostatic potentials.

RPC Models

There are few thermodynamic models that describe the retention in RPC. The solvophobic theory was discussed above, and models that are based on partitioning are not considered in this thesis. In many cases, empirical first- or second-degree polynomials of the modulator concentration are used to describe its effect on the natural logarithm of the retention factor [79-81]. This approach is simple and useful for case studies with a certain adsorbate–modulator–ligand system but does not allow for extrapolation and does not provide any information about the underlying phenomena. Quantitative structure–retention relationships can be used to correlate the retention RPC to various physical properties [82] but not to make conclusions on the adsorption mechanism. Molecular dynamics simulations can give insights into the adsorption mechanism in all types of chromatography, but the results cannot be linked directly to retention [83, 84].

A semi-thermodynamic approach has been introduced by Nikitas, Pappa-Louisi, et al. [12, 80], who assumed that the modulator is competitively adsorbed and that solvent molecules cluster on the ligands and are displaced when adsorbate or modulator molecules adsorb. The retention factor is correlated to the modulator concentration per the equilibrium equation, and power series of the amount-of-substance fractions of the various species describe the changes in activity coefficients. This approach results in a set of polynomials of the amount-of-substance fraction of the modulator with more parameters than can be determined from retention data. However, qualified assumptions can prompt simplifications to be made that yield useful models.

In this work, the changes in activity coefficients with shifts in modulator content are described by Wilson's equation [85]. Supplementary solubility data for the proteins and vapor–liquid equilibrium data for the modulator and water were used together

with the retention data to estimate the binary interaction parameters. More information on the RPC model can be found in Chapter 7.

4.2.2 Temperature Effects

Although the temperature also influences A indirectly — e.g., as a consequence of changes in density, permittivity, and interactions between species in the mobile phase — the temperature dependence is generally attributed primarily to that of the adsorption equilibrium constant (Equation 8).

$$K_{ads,P} = \exp\left(-\frac{\Delta G_{ads,P}}{RT}\right) \Rightarrow \ln K_{ads,P} = -\frac{\Delta G_{ads,P}}{RT} \tag{8}$$

$\Delta G_{ads,P}$ is the change in Gibbs free energy on adsorption, which in turn can be divided into changes in enthalpy ($\Delta H_{ads,P}$) and entropy ($\Delta S_{ads,P}$) on adsorption. A common assumption is that these parameters vary insignificantly with temperature, rendering $\ln(K_{ads,P})$ linearly dependent on the inverse of the temperature (Equation 9).

$$\ln K_{ads,P} = -\frac{\Delta H_{ads,P}}{RT} + \frac{\Delta S_{ads,P}}{R} \tag{9}$$

If the Van't Hoff plots — i.e., $\ln(k_P)$ versus $1/T$ — are curved, the variations in enthalpy and entropy with temperature can be included using Equation 10a [62] instead of Equation 9. Because the viscosity varies with temperature, the column pressure drop (p_{drop}) does, as well. To account for the effects of p_{drop} on $K_{ads,P}$, Equation 10b [86] can be used.

$$\ln K_{ads,P} = -\frac{\Delta C^{o}_{p,ads,P}}{R}\left(\frac{T_{H,P}}{T} - \ln\left(\frac{T_{S,P}}{T}\right) - 1\right) \tag{10a}$$

$$\ln K_{ads,P} = -\frac{\Delta E_{ads,P}}{RT} - \frac{p_{drop}\Delta V_{m,P}}{RT} + \frac{\Delta S_{ads,P}}{R} \tag{10b}$$

$\Delta C°_{p,ads}$ is the change in heat capacity on adsorption, and $T_{H,P}$ and $T_{S,P}$ are reference temperatures for the changes in enthalpy and entropy, respectively. $\Delta E_{ads,P}$ is the change in internal energy on adsorption, and $\Delta V_{m,P}$ is that of the molar volume.

4.3 Dynamic Models

Whereas equilibrium models are used to calculate the retention time or volume of an adsorbate as a function of process conditions, generally within the linear adsorption range, dynamic models are used to simulate an entire chromatographic run, generating the concentration of the adsorbate(s) as a function of time (t) and position in the column (z) as the output. There are 3D models that include wall effects [87, 88], but most models assume radial homogeneity of the column packing and negligible radial concentration gradients; thus, the position is only specified by the axial coordinate. Another common assumption is that the porosities, the

temperature, and all physical properties are homogeneous throughout the column. These models require a mathematical description of the adsorption process and the transport phenomena that affect the adsorbate inside of the column, such as dispersion and pore diffusion [89].

The most complex models — general rate models — include at least two mass transfer effects regarding the transport of adsorbates to or inside of the particles. The transport phenomena that are generally considered are adsorption kinetics, diffusion in the liquid and on the surface inside of the particle pores, and mass transfer through the stagnant film that surrounds the particles. Lumped rate models are slightly less detailed chromatography models that include only one of these mass transfer effects. Because lumped rate models neglect concentration gradients inside of the particles, the mass transfer rate is modeled as adsorption kinetics or diffusion through the film around the particles. In this work, the reaction-dispersive model — a lumped rate model that incorporates adsorption kinetics [90] — has been used.

A lumped rate model was chosen, because this work focused on the effects on the adsorption equilibrium, not on transport phenomena or kinetics. Also, general rate models are only needed for complex cases, and estimating all of their parameters requires extensive experimental data or calculations from correlations that are based on dimensionless numbers [90]. These tasks were beyond the scope of the studies on which this thesis is based. The reaction-dispersive model has been used to successfully describe the chromatographic purification of insulin [81, 91], and because the mobile phase velocity and particle size do not vary in this work, this model was considered to be suitable [41].

4.3.1 Transport Phenomena in the Mobile Phase

The transport of species *i* (adsorbate or modulator) in the mobile phase is governed by three overarching phenomena, described by the right-hand side of Equation 11: convection (first term), dispersion (second term), and transport into the stationary phase.

$$\frac{\partial c_i}{\partial t} = -\frac{v_{sup}}{\epsilon_{t,i}}\frac{\partial c_i}{\partial z} + D_{app}\frac{\partial^2 c_i}{\partial z^2} - \frac{(1-\epsilon_c)\epsilon_p k_{D,i}}{\epsilon_{t,i}}\frac{\partial q_i}{\partial t} \tag{11}$$

v_{sup} is the superficial velocity of the mobile phase, and D_{app} is the apparent axial dispersion coefficient. The axial dispersion coefficient (D_{ax}) describes deviations from plug flow, caused by the packed bed, and can be estimated from the Péclet number, given by Equation 12, where d_p is the particle diameter.

$$Pe = \frac{d_p v_{sup}}{D_{ax}\epsilon_c} \tag{12}$$

The apparent axial dispersion coefficient is a lumped parameter that also includes pore diffusion and mass transfer through the liquid film on the adsorbent particles. Because the equilibrium, not the kinetics, is the focus of this work, the Péclet number correlation was assumed to provide a sufficient estimation of D_{app}.

$\partial q_i/\partial t$ is the adsorption rate for species i, which in this model was assumed to be rate-limiting for transport into the stationary phase. The factor in front of it depends on the choice of the model for retention. In the work summarized in this thesis, the factor is related to the accessible pore volume for species i inside of adsorbent j, because the thermodynamic retention factor (A) was used as the measure of retention (Equation 5). The use of total porosity for species i as the denominator in the convection and adsorption terms does not imply convective flow through the particles but is merely a consequence of the selection of the model. Because the reaction-dispersive model lacks a description of the transport inside of the particles, the column model (Equation 11) must include the particle void to yield the correct residence volume.

4.3.2 Adsorption

The expression for the adsorption rate can be derived from the equilibrium equation for the reaction as the difference between the driving forces for the adsorption and desorption. Assuming a concave isotherm, the adsorption rate is often described as in Equation 13.

$$\frac{\partial q_i}{\partial t} = k_{ads,i}\Lambda^{\nu_i}\left(1 - \sum_{k=1}^{N}\frac{(\nu_k+\sigma_k)q_k}{\Lambda}\right)^{\nu_i} c_i - k_{des,i}q_i \tag{13}$$

$k_{ads,i}$ and $k_{des,i}$ are the adsorption and desorption rate constants, respectively. Λ is the ligand density of the adsorbent, σ_k is the shielding factor — i.e., the number of ligands that are covered by but not adsorbed to protein k — and N is the number of adsorbate types that are present. The expression in parentheses yields the fraction of available adsorption sites. Equation 13 also assumes that the activity coefficients are unity, or at least constant, because concentrations, not activities, are used to calculate the driving forces. Substitution of concentrations by activities and division of the right-hand side of Equation 13 by $k_{des,i}$ results in the form that is given by Equation 14, with the adsorption equilibrium constant and only one rate constant ($k_{kin,i}$). The relationships between A_i, $K_{ads,i}$, $k_{ads,i}$, $k_{des,i}$, and $k_{kin,i}$ are given by Equation 15.

$$\frac{\partial q_i}{\partial t} = k_{kin,i}\left(K_{ads,i}\left(\frac{\Lambda\gamma_L}{c_{tot}}\right)^{\nu_i}\left(1 - \sum_{k=1}^{N}\frac{(\nu_k+\sigma_k)q_k}{\Lambda}\right)^{\nu_i} c_i\gamma_i - q_i\gamma_{PL_v}\right) \tag{14}$$

$$k_{kin,i} = k_{des,i} \quad K_{ads,i} = \frac{k_{ads,i}}{k_{des,i}} \quad A_i \propto K_{ads,i} \tag{15}$$

The exact correlation between the thermodynamic retention factor and equilibrium constant depends on the adsorption mechanism, and Equation 14 is strictly valid only for the mechanism that is described in Equation 2a. If the modulator adsorbs to the ligands, as described by Equation 2b, Equation 16 should be used instead of Equation 14.

$$\frac{\partial q_i}{\partial t} = k_{kin,i}\left(K_{ads,i}\left(\frac{\Lambda\gamma_{LM_\xi}}{c_{tot}}\right)^{\nu_i}\left(1-\sum_{k=1}^{N}\frac{(\nu_k+\sigma_k)q_k}{\Lambda}\right)^{\nu_i} c_i\gamma_i - q_i\gamma_{PL_\nu}(\gamma_M x_M)^{\nu_i\xi_i}\right) \tag{16}$$

When the activity coefficients are neglected (Equation 13), the effects of the mobile phase modulator(s) are generally given by $k_{ads,i}$ and $k_{des,i}$ [92, 93] and otherwise (Equations 14 and 16) by γ_i [94]. The description of these effects depends on the theory that is applied. The adsorption model that is given by Equation 16 is similar to the steric mass-action (SMA) model of Brooks and Cramer [95]. The difference is that the SMA model describes IEX with salt being displaced by the adsorbate(s) and does not include variations in the activity coefficients.

4.3.3 Initial and Boundary Conditions

For the dynamic models that are described above, the initial conditions that are required are the initial concentrations of all species — i.e., both adsorbates and modulators — that are present in the mobile phase (c_{init}) or that are adsorbed to the particles (q_{init}) (Equation 17) [90].

$$c_i|_{t=0} = c_{init,i} \tag{17a}$$
$$q_i|_{t=0} = q_{init,i} \tag{17b}$$

In most cases, all initial adsorbate concentrations are 0, whereas the modulator concentration is at a level that promotes adsorption. If the modulator does not adsorb, q_i = 0 for all species. Boundary conditions are required for the inlet (Equation 18) and outlet (Equation 19) of the column [90].

$$c_i|_{z=0} = c_{in,i} - \frac{D_{ax}}{v_i}\frac{\partial c_i}{\partial z}\Big|_{z=0} \tag{18}$$
$$\frac{\partial c_i}{\partial z}\Big|_{z=L} = 0 \tag{19}$$

L is the column length, and $c_{in,i}$ is the inlet concentration of species i. The latter varies with time, and for the adsorbates, this relationship is generally described by a step function that equals the feed concentration during the injection and 0 at all other times. If the axial dispersion is low, which is common, the second term on the left-hand side of Equation 18 can be neglected, and the concentration at the column

boundary is set simply to that of the mobile phase that enters the column [90]. Equation 19 is actually a simplification of the more correct boundary condition that the outlet concentration must be finite. The finite outlet concentration is generally approximated by a concentration that only varies with time; thus, the simplified boundary condition is that there is no spatial concentration gradient.

Chapter 5

Implementation and Use of Models

As discussed in Chapter 4, an ideal chromatogram for linear-range adsorption can be constructed using direct calculations with an equilibrium model. This is generally insufficient for studies on preparative chromatography, in which the significance of transport phenomena between and inside of the particles and the adsorption kinetics cannot be neglected. Further, the high adsorbate load will affect the shape and position of the peaks — effects that a linear-range model fails to capture — necessitating simulations with a dynamic model to produce a realistic chromatogram.

Using an algorithm for simulating a dynamic model under various process conditions, that process can be optimized. The value of a quality measure, often the yield or productivity of the target adsorbate, is then maximized by varying a specified set of process conditions, while still fulfilling certain constraints, such as a minimum purity of the final product and a maximum level of specific impurities. Before the model can be used, it must be calibrated to mimic reality sufficiently well by minimizing the difference between the model output and experimental data by tuning the parameter values.

5.1 Simulation

The dynamic column model that is described by Equation 11 in the previous chapter is a partial differential equation (PDE), because it includes derivatives in time and a spatial coordinate, along the column axis. Ordinary differential equations (ODEs) contain derivatives with respect to only one variable — for example, time — and for some ODEs, there are analytical solutions. A solution for a specified interval of the independent variable can be estimated for practically any ODE using a suitable numerical method that is implemented in a computational program. A PDE in time and space can be transformed into a set of ODEs in time by discretization, enabling calculation of an approximate solution.

5.1.1 Discretization in Space

The spatial variation of one or more properties of a line, surface, or volume can be estimated by dividing it into small pieces and averaging the properties for each segment. This technique is called discretization, and the type that is used in this work is the method of lines — i.e., discretization is performed along all spatial dimensions, leaving only ODEs with respect to time [96]. The finite volume method (FVM) was applied, placing *N* grid points along the column axis, each one centered inside of a finite volume (Figure 5.1) [97].

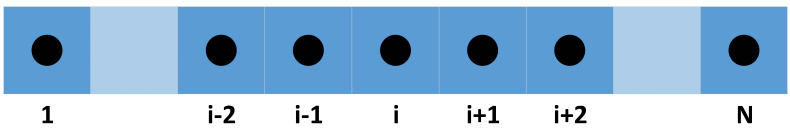

Figure 5.1: Division of a line into *N* cubical cells of equal size, using the finite volume method.

With the FVM, the time derivative of the dependent variable at grid point *i* is approximated as the volume average for the i^{th} cell by an integral along the discretized dimensions. The divergence theorem is used to substitute the volume integrals for the spatial derivatives for the difference between the values on the surfaces against the $i+1^{th}$ and $i-1^{th}$ cells [97, 98]. A one-dimensional example for convection inside of a column is given below (Equation 20).

$$\frac{\partial \bar{c}_i}{\partial t} = -\frac{v_{sup}}{\epsilon_{t,i}} \frac{1}{\Delta z_i} \left(c_{i+\frac{1}{2}} - c_{i-\frac{1}{2}} \right) \tag{20}$$

$\bar{c}_i$ is the volume average of the concentration, and Δz_i is the axial length of the i^{th} cell. Indices i-1/2 and i+1/2 refer to the surfaces of the neighboring cells before and after the i^{th} cell, respectively. There are two main alternatives to FVM: the finite differences and finite elements methods. The former approximates the spatial derivatives by Taylor series expansion, which is simpler but less accurate than the FVM approach. The latter uses simple equations, which are chosen as to minimize the error, to represent the PDEs in each element. The finite element method is better than the FVM for complex geometries but is more complex [99].

Because the value of the dependent variable — in this example, the concentration — is only evaluated at each grid point, the values on the surfaces are unknown. Consequently, the surface values ($c_{i+1/2}$ and $c_{i-1/2}$) must be approximated from those at the grid points. There are many discretization schemes for this purpose, differing in the number and location of grid points that are included. For models of chromatographic columns (Equation 11), it is common to use a 2-point backward approximation (Equation 21) for the first derivative and a 3-point central approximation (Equation 22) for the second derivative. For this simple geometry, it

is also routine to place the grid points equidistantly, rendering the index on the axial cell length superfluous.

$$\frac{\partial c_i}{\partial z} \approx \frac{c_i - c_{i-1}}{\Delta z} \tag{21}$$

$$\frac{\partial^2 c_i}{\partial z^2} \approx \frac{c_{i+1} - 2c_i + c_{i-1}}{2\Delta z} \tag{22}$$

For systems with very sudden changes, such as RPC, in which the injection of sample and rapid adsorption/desorption cause shockwaves in the adsorbate concentration, the approximation of the convection term (Equations 11 and 21) can induce oscillations in the solution. Problems that include such systems are called *stiff*. Because the simulation of an RPC system is a stiff problem, a more complex approximation than that given by Equation 21 was used in the optimization study (Paper IV) — the weighted essentially non-oscillatory (WENO) scheme. The WENO scheme uses a weighted polynomial of the concentrations in the included cells, and the weights are chosen to smooth the approximation as much as possible. The WENO scheme has been detailed by its developers, Liu et al. [100]. The use of the WENO scheme instead of 2-point backward approximation in the optimization study effected a fourfold reduction in the number of grid points, without any increase in numerical dispersion. Consequently, the computational time fell significantly.

5.1.2 Numerical Methods

When the PDE in Equation 11 has been transformed into a set of N ODEs, N being the number of grid points, a simulation can be performed with an ODE solver. There are many types of ODE solvers, all of which estimate the value of the dependent variable — often, time — for a certain interval of the independent variable — in this example, concentration. The estimation is performed stepwise by approximation of the time derivative, starting from an initial concentration at the beginning of the time interval. The methods differ in the number of steps that are included in the approximation of the derivative, the length of the steps (fixed or varying), and the formula that is used (explicit or implicit). Further, there are solvers for discrete and continuous problems.

In this work, the computational program MATLAB [101] was used for all calculations, simulations, and optimizations. The simulations were performed with the built-in ODE solver `ode15s`, which is based on numerical differentiation formulas [101, 102]. It is an implicit solver that entails several steps in the approximation of derivatives and varies the step length. `ode15s` was chosen primarily because it is suitable for stiff problems — hence, the suffix "s."

Two MATLAB-based chromatography simulators were used in this work: *Applied Chromatography Toolbox* (`act`) and *Preparative Chromatography Simulator*

(pcs) [103]. Both were developed by doctoral and master's students and postdoctoral fellows in the Department of Chemical Engineering, Lund University, Faculty of Engineering. act is a simulator that uses only the reaction-dispersive model and was applied in Papers I-III. pcs is a more advanced simulator in which any chromatography model can be implemented and was used for the optimizations in Paper IV. pcs was faster in addressing this problem, because WENO is implemented in it and because the code is more efficient for complex isotherms and many grid points.

5.2 Optimization

Optimization aims to minimize the value of an *objective function* by varying the value of a set of *decision variables*. The decision variables can have upper and lower *boundaries*, and their values can be further restricted by *constraints*. A mathematical description of an optimization problem is given by Equation 23.

$$\begin{aligned} &\min f_{obj}(\boldsymbol{p}) \\ &\text{w.r.t.} \quad \boldsymbol{p} = (p_1, p_2, \dots, p_N) \in \mathbb{R}^N \\ &\text{s.t.} \quad \boldsymbol{p}_L \leq \boldsymbol{p} \leq \boldsymbol{p}_U \\ &\qquad f_{con}(\boldsymbol{p}) \leq 0 \end{aligned} \tag{23}$$

The objective function (f_{obj}) is minimized with respect to (w.r.t.) the decision variables $\boldsymbol{p}$, and the decision variables are subject to (s.t.) the upper and lower boundaries (p_U and p_L) and the constraint function (f_{con}). Common objective functions in preparative chromatography are the yield Y (Equation 24), productivity P (Equation 25), and pool concentration of the target adsorbate, and the optimization is often constrained by the minimum purity X of the target adsorbate (Equation 26). In addition to the minimum purity of the target adsorbate, there can be maximum levels of certain impurities.

$$Y_{target} = \frac{Q}{n_{load,target}} \int_{t_c}^{t_f} c_{target}(t, z_f) dt \tag{24}$$

$$P_{target} = \frac{M_{target} n_{load,target}}{V_{col}(t_f + t_r)} Y_{target} \tag{25}$$

$$X_{target} = \frac{n_{load,target} Y_{target}}{\sum_{k=1}^{N} n_{load,k} Y_k(t_f)} \tag{26}$$

Q is the volumetric flow rate of the mobile phase, t_r is the time that is required for regeneration before the next chromatographic run can be initiated, and t_c and t_f are the cut points for the product. $n_{load,target}$ and M_{target} are the total amount of substance that is loaded and the molar weight, respectively, of the target adsorbate. Y and X are dimensionless, whereas P, in this case, is expressed as mass target adsorbate per unit column volume and unit time.

The values of the decision variables are limited by such factors as the process equipment, the stability of the product, and the solubility of the modulators. Some of these limiting factors can also be formulated as constraints. Equation 23 describes a simple optimization problem, and actual problems can have several levels and multiple objective functions.

5.2.1 Multi-Level Optimization

Optimization problems that concern preparative chromatography have two levels: 1. the main optimization — i.e., the upper-level optimization with, for example, productivity, yield, or pool concentration as the objective function and the process parameters $\boldsymbol{p}$ as the decision variables (Equation 23); and 2. the pooling — i.e., the lower-level optimization with productivity, yield, or pool concentration as the objective function; the cut points as the decision variables; and the minimum purity as a constraint [58, 104]. It is common to use yield as the objective function for the lower-level optimization, even if the upper-level optimization has another objective function [58]. Notably, this results in mixed-objective optimization. If the pooling of the actual process is designed to always maximize the yield, then the use of different objective functions is correct, but it should be taken into account when conclusions are drawn.

5.2.2 Multi-Objective Optimization

It is not always apparent whether the most desirable process conditions are those that maximize the yield, productivity, or pool concentration, and sometimes, a compromise is most suitable. In these cases, a weighted combination of multiple objectives can be used as the objective function. An example that combines productivity and yield is given by Equation 27, where ω is the weight factor for the productivity and has a value between 0 and 1.

$$f_{obj} = -\left(\omega \frac{P_{target}}{P_{target,max}} + (1-\omega) Y_{target}\right) \tag{27}$$

Because the productivity can reach any positive value while the yield is limited to the interval 0-1, P_{target} is often divided by the maximal productivity ($P_{target,max} = f_{obj}(\omega = 1)$) to achieve a fair distribution between the two objectives. By performing optimizations for different values of ω, a *Pareto front* can be created. A Pareto front is a plot of the optimal combinations of different objectives [105, 106]. Figure 5.2 shows a fictitious example, using productivity and yield.

Theoretically, there is no limit to the number of objectives that can be combined, but the combination of two objectives is the most common type. Because productivity and yield are competing objectives in preparative chromatography, they are often combined. There are studies in which, for example, pool concentration has been added as a third objective [57, 58, 107], but the use of over

three objectives is time-consuming, and the result is difficult to visualize in more than three dimensions.

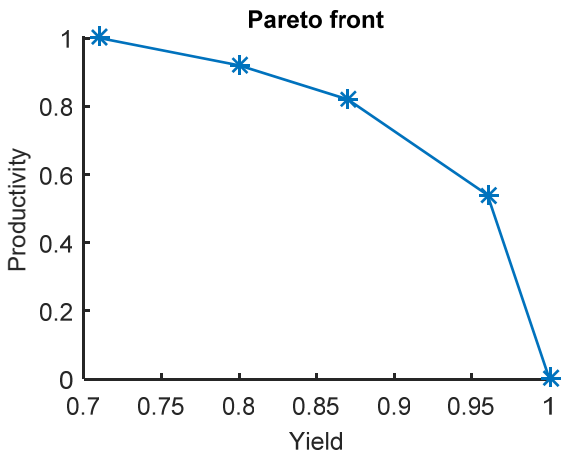

Figure 5.2: An example of the appearance of a Pareto front with productivity and yield as objectives.

5.2.3 Optimization Methods

Optimization methods can be classified according to their strategy for determining the values of the decision variables that correspond to a minimum of the objective function. All optimization strategies start from a set of initial values of the decision variables and move stepwise toward values that give a lower objective function output. There are three types of methods: 1. those that only evaluate and compare objective function values — e.g., simplex methods and genetic algorithms; 2. those that evaluate Jacobians (gradients — i.e., first derivatives of the objective function) and move in the direction of the most negative Jacobian — e.g., steepest descent methods; and 3. those that evaluate Jacobians and Hessians (second derivatives of the objective function) to identify stationary points of the objective function, such as Newton's method [108]. The computational cost for each *iteration* — i.e., the set of calculations that is performed to determine the direction and length of the next step — increases with the order of the derivatives that are included, but the number of iterations that are required to reach the optimum declines concomitantly.

The MATLAB function `fmincon` was used for the optimizations in Paper IV. `fmincon` is suitable for nonlinear objective functions and constraints, and it applies the third type of method — i.e., it uses Jacobians and Hessians. The specific algorithm that was selected is called sequential quadratic programming [101].

5.3 Model Calibration

The objective of model calibration or parameter estimation is to find a set of values of the model parameters ($\boldsymbol{p}$) that minimizes the difference between the model

responses ($\boldsymbol{y_{mod}}$) under process conditions $\boldsymbol{x}$ and the corresponding experimental results ($\boldsymbol{y_{exp}}$) — i.e., calibration is a special case of optimization, using model parameters as decision variables and an objective function that is a measure of the discrepancy between the model and reality. $\boldsymbol{x}$ should encompass the range of process conditions within which the model is to be used, ensuring that the model is valid for this range. Calibration can be performed with any of the optimization methods above, and its main difference from process optimization is the type of objective function that is applied. The most commonly applied objective function for calibrations is the least-squares function, which is described below.

There are many methods for analyzing the validity of the model structure and the parameter values that are given by the calibration. A comparison of the model response and experimental data for process conditions that were not included in the calibration can be used to evaluate the predictability of the model. Validation points can be chosen inside and outside of the intervals of the process conditions that are used for the calibration to test interpolation and extrapolation, respectively. Calculating statistics, such as confidence intervals and correlation matrices, for the model parameters is useful for determining whether the model is *over-parametrized* — i.e., whether the model describes effects in excess of what is observed in the experimental data. A simple example of an over-parametrized model is a fifth-degree polynomial of parameter p that is fitted to data points for four values of p. Simple statistical analyses of the model parameters were performed for the models in Papers I, II, and III.

5.3.1 Least-Squares Function

Model calibration in the least-squares sense means that the objective function is the sum of the squares of the difference between the model response and the experimental data for all N process conditions (Equation 28) [109].

$$\min_{\boldsymbol{p}} \sum_{i=1}^{N} \left(y_{mod,i}(\boldsymbol{p}, \boldsymbol{x}_i) - y_{exp,i} \right)^2 \tag{28}$$

If several data sets of various sizes are used and if the values of the experimental data vary widely, some type of weighting might be suitable. Weighting for calibration is a special case of multi-objective optimization, in which the sum of squares for each data set or data point is an objective. The purpose of weighting is to give each data set or data point the same impact on the calibration or to give those that are considered to be more important greater impact. Division of the sum of squares for each data set with N and the mean value of y_{exp} equalizes the impact of the data sets. However, the greater impact of data points that correspond to higher values of y_{exp} is retained, because an equally large relative difference results in a larger absolute difference for these data points. Division with the mean value of y_{exp} for each data point results in the equivalent impact of equally large relative differences.

In chromatography, the precision increases concomitantly with retention volume, which motivates maintaining the higher impact of data points with greater experimental value. Consequently, the objective function that is given by Equation 29 (f_{cal}) was used for calibration in Papers II and III, in which the retention data and solubility data were considered two separate data sets ($N = 2$).

$$f_{cal}(\boldsymbol{p}, \boldsymbol{x}) = \sum_{i=1}^{N} \left(\frac{1}{\bar{y}_{exp,i} N_i} \sum_{j=1}^{N_i} \left(y_{mod,i,j}(\boldsymbol{p}, \boldsymbol{x}_{i,j}) - y_{exp,i,j} \right)^2 \right) \tag{29}$$

The calibrations in this work were performed with the MATLAB function `lsqcurvefit`, which is designed for nonlinear curve-fitting in the least-squares sense. The optimization algorithm that was chosen was the default option, *trust-region-reflective*, which searches for stationary points using first and second derivatives of the objective function — i.e., the third type of optimization method above [101].

Chapter 6

Combined Modulator Effects on HIC

One of the aims of this PhD project was to examine the possibility of developing a common model for the effects of salt and organic modulators on HIC and RPC. Thus, the first subproject (Paper I) included an experimental study of linear-range retention in HIC. The dependence of the retention of three insulin variants on the concentration of KCl and ethanol in the mobile phase was studied for two HIC adsorbents. The insulin variants were insulin aspart, desB30 insulin, and an insulin ester, and the adsorbents were Toyopearl beads from Tosoh Bioscience GmbH (Stuttgart, Germany) with butyl (But) and phenyl (Ph) ligands, respectively. Three ethanol levels were evaluated — 0, 5, and 10 wt% — and the starting concentration of KCl was nearly 0, with an upper limit set by its solubility or the retention of desB30 insulin being in excess of 50 column volumes (CV).

6.1 Effects of KCl on Retention

The hypothesis was that variations in the retention of a protein in HIC are caused solely by changes in the mobile phase properties, altering the activity coefficient of the protein in solution. Neither of the species in the stationary phase — i.e., the ligands and protein–ligand complexes — were assumed to be significantly affected. Consequently, their activity coefficients, or at least their ratio, were constant. A constant ratio between the activity coefficients of the species in the stationary phase has been suggested and shown to be a fair assumption for HIC of lysozyme [10]. Starting from the equilibrium expression in Equation 3a, this assumption yields the last simplification in Equation 30.

$$K_{ads} = x_L^{-\nu} \frac{\gamma_{PL_\nu}}{\gamma_P \gamma_L^\nu} \frac{q_P}{c_P} \approx \left(\frac{c_{tot}}{\Lambda}\right)^\nu \frac{\gamma_{PL_\nu}}{\gamma_P \gamma_L^\nu} \frac{q_P}{c_P} \Rightarrow \ln(A) \approx \ln(A_0) + \ln(\gamma_P) \tag{30}$$

The first simplification is only valid for negligible protein loads, at which point approximately all ligands are free. c_{tot} is the total molarity of the mobile phase, and the stationary and mobile phases are assumed to be a single phase in the thermodynamic sense. The small effect of the salt on c_{tot} in HIC can generally be neglected, and the molarity can be approximated to that of water. A_0 is a lumped

parameter, comprising the constants K_{ads}, c_{tot}, and Λ^{v} and the activity coefficient ratio. More details on this derivation can be found in Paper II.

If the hypothesis is correct, a specific salt should affect the retention of a certain protein on any HIC adsorbent in the same manner. Consequently, plotting ln(A) versus the ionic strength of the mobile phase should generate a set of parallel curves with disparate intercepts, denoted ln(A_0), for different types of ligands, as has been shown for lysozyme on seven HIC adsorbents [10]. The aim of the work presented in this chapter was to: 1. determine whether this hypothesis is valid for the insulin variants that are modulated by KCl; 2. study the effect of ethanol on this system; and 3. model the combined effects of KCl and ethanol as mobile phase modulators. The influence of KCl on the retention of the insulin variants under ethanol-free conditions is shown in Figure 6.1.

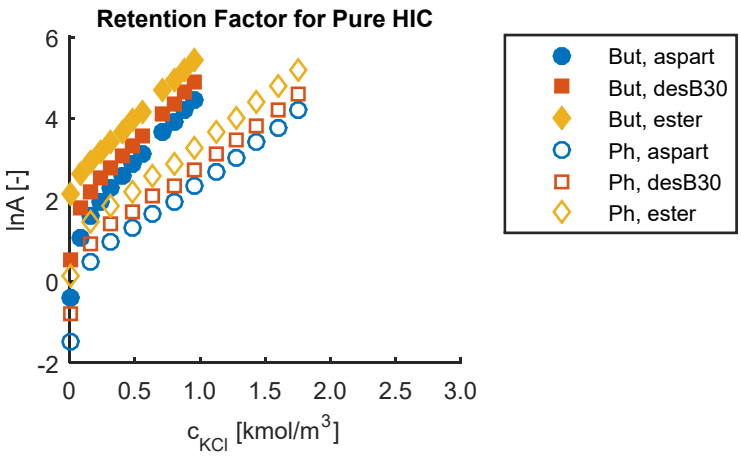

Figure 6.1: Logarithm of the thermodynamic retention factor as a function of KCl concentration for the two HIC adsorbents without any ethanol in the eluent.

As expected, ln(A) increased linearly with rising salt concentrations, and the butyl ligands effected greater retention than the phenyl ligands, due to their higher hydrophobicity. However, there were two unexpected observations: no salting-in occurred, and the curves for the same insulin variant were not parallel. Based on existing knowledge on the salting-in and salting-out of proteins [10], a minimum in ln(A) was anticipated, yielding a curve that would be similar in shape to the Nike logotype. Instead, it decreased linearly and concomitantly with the KCl concentration, approaching salt-free conditions, at which point it approached negative infinity as the retention volume was reduced to the non-retained volume.

The difference in slopes for the same adsorbate on the butyl and phenyl adsorbents suggests that the activity coefficients of the ligands or adsorbate–ligand complexes changed with the mobile phase composition. There are, however, other possible

explanations. Other phenomena, such as self-association and conformational changes in the adsorbates, might occur and affect the adsorption. Oscarsson [73] and Nunes et al. [110] have shown that conformational changes in proteins and peptides, respectively, affect their retention in HIC, and that the same salt can have disparate effects in combination with different adsorbents. Similar results for peptides on RPC adsorbents have been reported by Purcell et al. [111]. Studies on insulin have demonstrated that it forms dimers and hexamers at pH values of approximately 7 [112, 113], in the presence or absence of zinc ions [113]. Conformational changes and self-association are thus plausible explanations for this difference in slopes.

6.2 Effects of Ethanol on Retention

The addition of ethanol to the eluents resulted in weaker adsorption at the same salt concentration and reduced the retaining effect of the salt (Figure 6.2), consistent with a study of the effects of ethanol on lysozyme retention on HIC adsorbents [61].

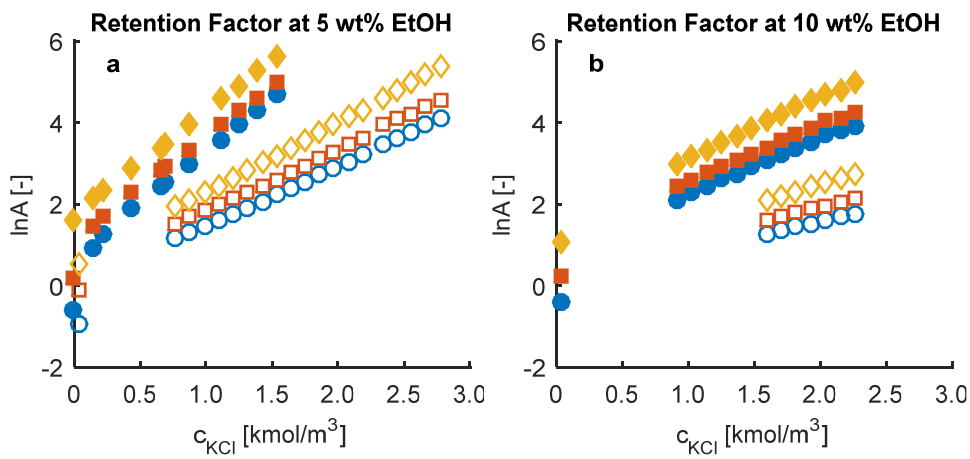

Figure 6.2: Logarithm of the thermodynamic retention factor as a function of KCl concentration for the two HIC adsorbents, with 5 and 10 wt% ethanol in the eluents, respectively.

Salting-in was not observed for either ethanol concentration, but the difference in slopes between the two adsorbents was reduced at higher ethanol concentrations, consistent with the concomitant decline in peak fronting (Figures 6.3-6.4). Thus, ethanol lessens the effect of the additional phenomenon — the changes in activity coefficients of species in the stationary phase or the conformational changes or self-association of adsorbates — that influences the retention.

Comparing the chromatograms in Figures 6.3 and 6.4, the separation of the insulin variants declined with increasing ethanol content, a trend that was confirmed on closer inspection of the curves in Figures 6.1-6.2. The conformation of proteins is

affected by the presence of an organic solvent, and ethanol impedes the self-association of proteins [114]. The difference in slopes for ln(A) versus salt concentration between adsorbents and the fronting peaks that were observed in this study thus might be attributed to conformational changes in or self-association of the adsorbates. Fronting per se does not effect a difference in slopes, because the retention factor is calculated from the first moment of each peak in the decomposed chromatogram — not from the peak maximum.

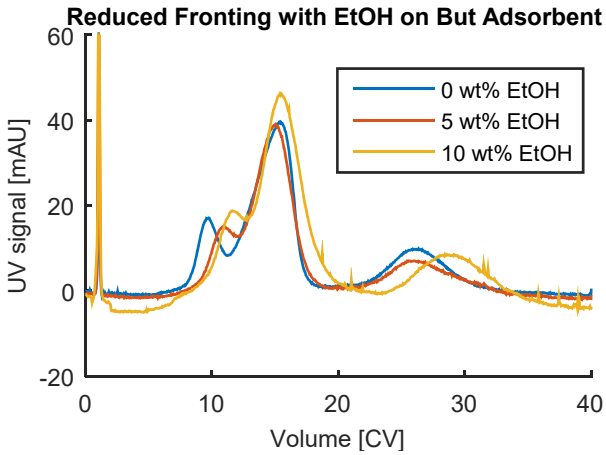

Figure 6.3: Transition from fronting to near-Gaussian peaks eluted from the butyl adsorbent as the ethanol content of the mobile phase increases. The chromatograms in this comparison were chosen based on their similar retention volume and were generated from experiments at various KCl concentrations.

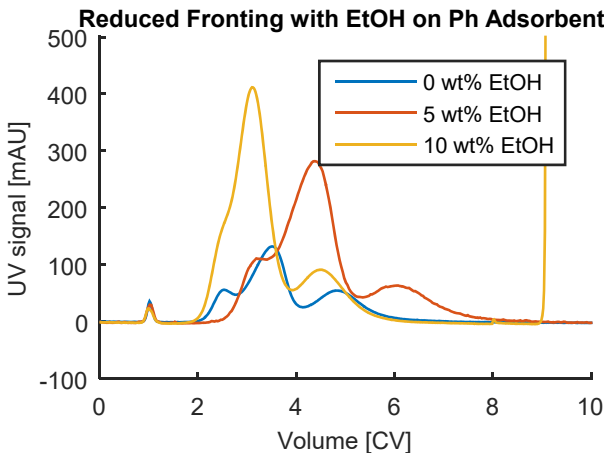

Figure 6.4: Transition from fronting to near-Gaussian peaks eluted from the phenyl adsorbent as the ethanol content of the mobile phase increases. The chromatograms in this comparison were chosen based on their similar retention volume and were generated from experiments at various KCl concentrations.

6.3 Cause of Fronting and Different Slopes for ln(*A*)

The cause of peak fronting and the difference in the effects of KCl on retention was examined in a number of experiments at high adsorbate load. The resulting chromatograms for the butyl and phenyl adsorbents are shown in Figures 6.5-6.6, respectively.

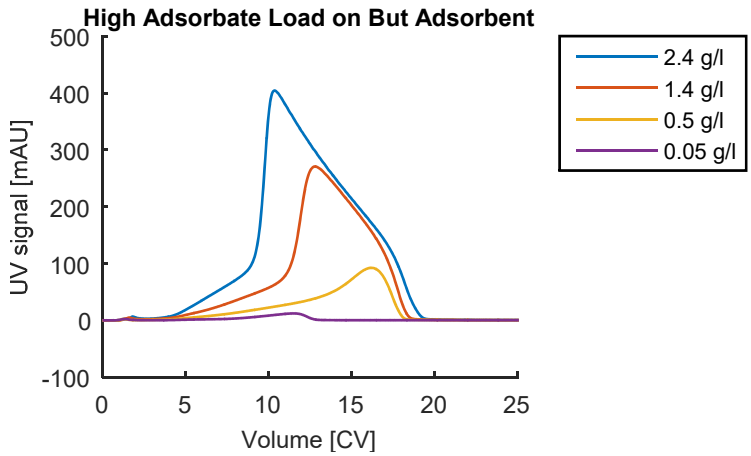

Figure 6.5: Change in peak shape with increasing adsorbate load of desB30 insulin on the butyl adsorbent. The adsorbate load per column volume is shown in the legend.

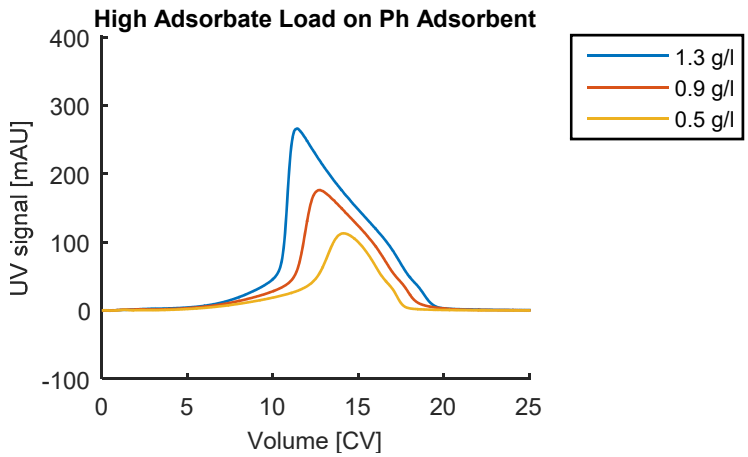

Figure 6.6: Change in peak shape with increasing adsorbate load of desB30 insulin on the phenyl adsorbent. The adsorbate load per column volume is shown in the legend.

This peak shape is characteristic of S-shaped isotherms [61, 115], which arises due to self-association of the adsorbate — through aggregation in the mobile phase prior to adsorption or the formation of a second layer on adsorbates that have already

adsorbed. The initial flat slope for both adsorbents is similar to several experimental and simulated chromatograms for dimer-forming insulin in the literature [61]. Consequently, the fronting and the different slopes for ln(A) can most likely be attributed to self-association of the adsorbates.

One of the aims of this project was to examine the possibility of developing a common model for the effects of KCl and ethanol on the chromatographic retention of insulin on hydrophobic adsorbents — i.e., the adsorbents that are used in HIC and RPC. The main differences that affect the adsorption between these two types of adsorbents are the hydrophobicity and coverage of ligands; thus, the same modulator should influence them similarly. However, only salting-out was observed for the HIC adsorbents, and for the RPC adsorbents, only salting-in occurred. Because these two phenomena are independent, there is no advantage in creating a combined model and no possibility of verifying that the same phenomenon has the same effect on both types of adsorbents.

Additionally, the unexpected fronting that was observed for both HIC adsorbents prevented the effect of KCl on the retention factor from being quantified, because the influence of these two phenomena cannot be separated based solely on retention data. It might be possible to discriminate between effects by fractionizing and analyzing the peaks. Nevertheless, there is a significant chance that the ratio of monomers to dimers and hexamers changes as a function of time and sample composition, rendering offline measurements impossible. Examination and modeling of the self-association of insulins were beyond the scope of this project; thus, modeling of HIC retention was not pursued further.

Chapter 7

Modeling of Modulator and Temperature Effects on RPC

In addition to studying the effects on the HIC adsorbents, the influence of the concentrations of KCl and ethanol (Papers I-II) on the adsorption to two RPC adsorbents was evaluated. The temperature dependence of these two systems was also studied (Paper III). The same insulin variants (insulin aspart, desB30 insulin, and an insulin ester) as in the HIC study were used, and the two adsorbents were silica particles from Novo Nordisk Pharmatech A/S (Køge, Denmark) with C_{18} and C_4 ligands. Although the retention at low adsorbate load — i.e., the equilibrium for linear-range adsorption — was the primary focus, the effects at high adsorbate load were also examined. Because there were no indications of self-association or conformational changes in the RPC studies, with near-Gaussian peaks for the C_{18} adsorbent and slightly tailing peaks for the C_4 adsorbent, these systems were considered to be suitable for modeling (Papers II-III). A linear-range equilibrium model and a dynamic model for varying levels of adsorbate load were developed, but the emphasis was placed on the former.

7.1 Retention at Low Adsorbate Load

The trends in retention factor for the three adsorbates with changing modulator concentrations was examined thoroughly in a series of isocratic experiments, with mobile phase compositions of 0.1–0.7 mol KCl/kg solution and 23–32 wt% ethanol. A less extensive study of the combined effects of temperature and modulator concentrations was performed in the range of 10–40°C.

7.1.1 Effects of Modulator Concentrations

As shown in Figures 7.1-7.2, the retention of all three adsorbates clearly decreased with rising concentrations of KCl and ethanol. The latter observation was expected, because ethanol increases the hydrophobicity of the mobile phase, the phenomenon that underlies separation by RPC. A shift from salting-in — i.e., increasing solubility and thus declining retention of the insulins with higher salt concentrations — toward salting-out was anticipated but did not occur in these concentration ranges. The

stronger tendency of salting-in in RPC and of salting-out in HIC, however, was consistent with predictions of the effects of ethanol on protein retention and solubility by Mollerup [61], based on Kirkwood's electrostatic theories on macromolecules in solution. According to this model, ethanol turns the entire Nike logotype-shaped salting-in and salting-out curve clockwise, resulting in more pronounced salting-in and less distinct salting-out [61].

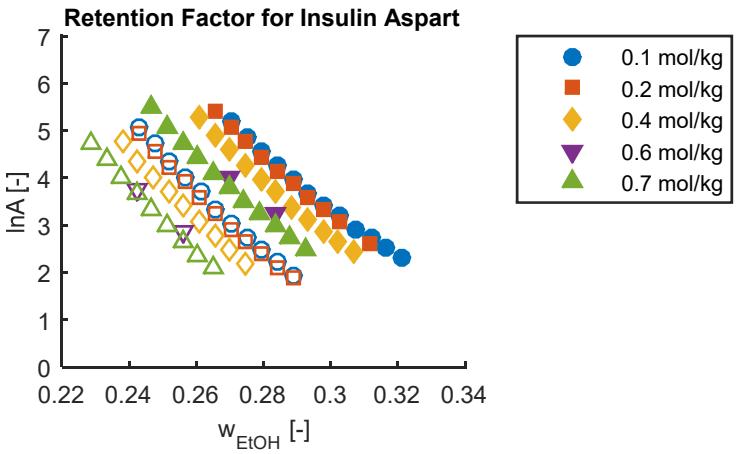

Figure 7.1: Results from isocratic runs on C_{18} (filled markers) and C_4 (open markers) adsorbents for insulin aspart at varying mobile phase compositions. The KCl concentrations are shown in the legend.

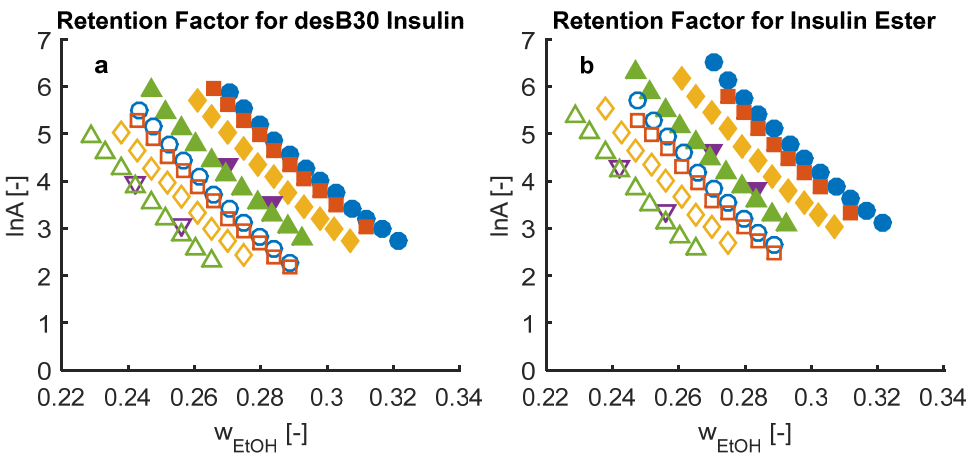

Figure 7.2: Results from isocratic runs on C_{18} (filled markers) and C_4 (open markers) adsorbents for a) desB30 insulin and b) the insulin ester at varying mobile phase compositions. The KCl concentrations are shown in the legend in Figure 7.1.

To determine whether salting-out of the insulin variants occurred at combinations of KCl and ethanol concentrations within the soluble range, a series of experiments

were performed at 27 wt% ethanol on the C_{18} adsorbent (Figure 7.3). The KCl concentration was maintained below 80% of its maximum solubility (1.5 kmol KCl/kg) at this ethanol concentration.

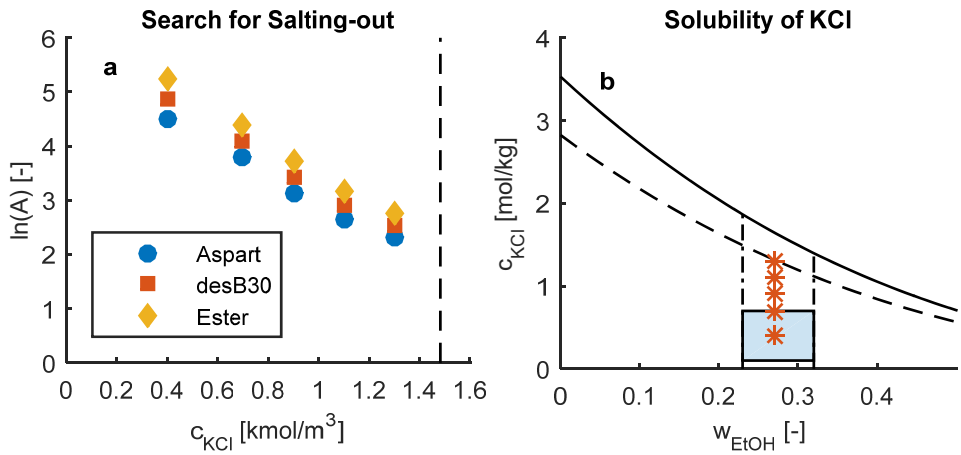

Figure 7.3: a) Results from isocratic runs on the C_{18} adsorbent at 27 wt% ethanol and b) solubility of KCl as a function of ethanol content [116]. The dashed lines indicate 80% of the maximum solubility of KCl at the specific ethanol content. The light blue area and asterisks in plot b represent the combinations of KCl and ethanol concentrations in the study in Paper II and the search for salting-out, respectively.

According to the results for HIC of lysozyme [61], the addition of 7.5 vol% ethanol caused a parallel shift in ln(A) versus ionic strength by -2, whereas the clockwise turn toward salting-in was barely detectable. Combining the parallel shift with the decrease in ln(A) at a certain ionic strength with higher ethanol content, caused by the clockwise turn presented by Mollerup [61], the change in ln(A) when shifting from salting-out to salting-in should be immense. Naturally, conclusions for another protein on HIC adsorbents cannot be applied directly to the insulin variants on RPC adsorbents. However, ethanol has a strong influence on ln(A) for these adsorbate–adsorbent systems, too, which supports the validity of making qualitative generalizations. Based on the results in Figure 7.3 and the discussion above, salting-out was concluded to have been unlikely to occur at an ethanol concentration that was sufficiently high to promote elution in a reasonable time (less than 100 CV). The KCl concentration that would be required to achieve salting-out under these conditions would likely exceed its solubility limit.

As shown in Figures 7.1-7.2, a change in KCl concentration merely induced a parallel shift in the curve, indicating that the synergistic effects of the modulator concentrations are small relative to the individual effects. Although the curves for the C_4 adsorbent appear to be slightly more linear than those for the C_{18} adsorbent, their slopes are similar, suggesting that the effect of the type of adsorbent can be

separated from the influence of the modulators. However, the data do not indicate whether exchange of adsorbed ethanol and adsorbate molecules occurred.

7.1.2 Effects of Temperature

The influence of temperature on the retention of the insulin variants was studied for a specific mobile phase composition, the set point, and for lower concentrations of KCl and ethanol. The set point for each adsorbent was chosen as the midpoint relative to the concentration ranges in the study of the effects of the modulators — 28.4 and 25.6 wt% ethanol for the C_{18} and C_4 adsorbents, respectively, and 0.4 mol KCl/kg for both adsorbents. Two other mobile phase compositions were tested: one with less KCl (0.1 mol KCl/kg) and one with less ethanol (27.5 and 24.7 wt% for the C_{18} and C_4 adsorbents, respectively). Figures 7.4-7.5 show the results of the temperature study.

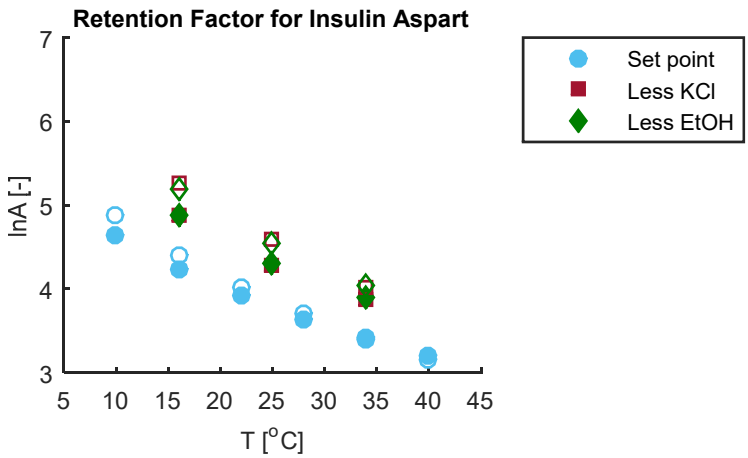

Figure 7.4: Results from isocratic runs on the C_{18} (filled markers) and C_4 (open markers) adsorbents for insulin aspart at varying temperatures. The difference in mobile phase composition between the three series is shown in the legend.

The series in Figures 7.4-7.5 appear to be linear, but there is a trace of concavity. Also, temperature has a stronger influence on retention on the C_4 adsorbent for all three insulin variants, regardless of the mobile phase composition, and the effects of modulators and adsorbents differ between adsorbates. For insulin aspart, the least hydrophobic adsorbate, reductions in the concentrations of KCl and ethanol affect the retention on each adsorbent similarly. For the two more hydrophobic adsorbates, the effects of less KCl and ethanol differ between adsorbents, albeit less extensively. Without information on the hydrophobic patches on the insulin molecules, with which they bind to the ligands, and on how they are affected by the mobile phase composition, it is impossible to determine whether this finding is a coincidence or an effect of the increasing hydrophobicity of the insulin variants.

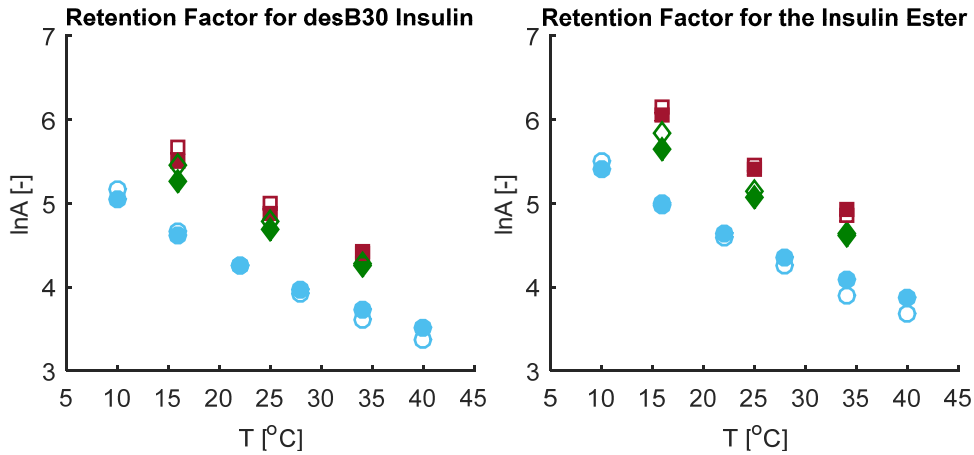

Figure 7.5: Results from isocratic runs on the C_{18} (filled markers) and C_4 (open markers) adsorbents for a) desB30 insulin and b) the insulin ester at varying temperatures. The difference in mobile phase composition between the three series is shown in the legend in Figure 7.4.

7.2 Solubility of desB30 Insulin

To discriminate between the effects of changes in the activity coefficient of the insulin variants and those of potential adsorption of ethanol, two minor studies on the solubility of desB30 insulin were performed. The first study focused on the influence of ethanol content, and the second study examined the influence of temperature. Dissolution of a protein can be described by Equation 31, where *(s)* and *(aq)* denote solid state and dissolved in a primarily aqueous solution, respectively.

$$P(s) \rightleftarrows P(aq) \tag{31}$$

Equation 31 is a simplified description of the actual process, because proteins are electroneutral only at their isoelectric point, and even then, they have point charges with varying signs and magnitudes. Depending on the pH, insulin participates in various dissociation reactions, and the development of a model that includes all such reactions would require an unreasonably large effort compared with the resulting increase in accuracy. Further, the rise in salt concentration due to the dissolution of desB30 insulin is negligible, based on an initial concentration of at least 0.1 mol KCl/kg. Consequently, the activity coefficient of the salt will also be approximately constant. In this simplified dissolution model, the equilibrium constant for this process ($K_{sol,P}$) is governed solely by the activity of the protein in solution, because the activity of a pure substance is unity (Equation 32).

$$K_{sol,P} = \frac{a_{P(aq)}}{a_{P(s)}} = a_{P(aq)} = x_P \gamma_P \implies \ln(x_P) = \ln\left(K_{sol,P}\right) - \ln(\gamma_P) \tag{32}$$

7.2.1 Influence of Ethanol Content

A comparison between Equations 29 (Chapter 6) and 31 reveals that under the same conditions, the curves for ln(A) and ln(x_P) versus ethanol content should have equal slopes but opposite signs, provided that the variations in the former are attributed solely to the effect of ethanol on γ_P. Thus, a short solubility study on desB30 insulin at pH 7.5, 0.4 mol KCl/kg, and a range of ethanol concentrations was performed. Details can be found in Paper II. The results from the solubility study are shown in Figure 7.6, with the corresponding findings from the linear-range retention study.

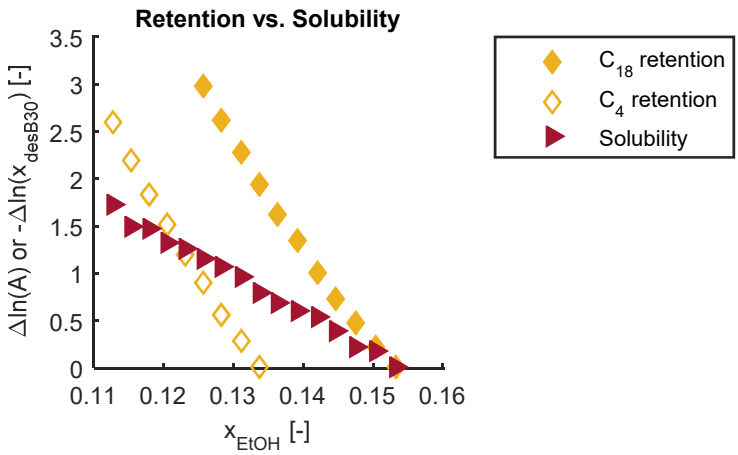

Figure 7.6: Comparison between the influence of ethanol on retention and solubility of desB30 insulin.

There is a clear difference in the influence of ethanol content on ln(A) and ln(x_P), wherein the slopes for the retention factor are more than twice as steep as that for solubility (Figure 7.6). Thus, the effect of ethanol on the adsorption of the insulin variants is not only a consequence of the influence on their activity coefficients. There are several likely explanations for this discrepancy: 1. displacement of adsorbed ethanol by the insulins; 2. the ratio between the activity coefficients of the insulin–ligand complexes and free ligands is not constant (Equation 30); 3. the concentration of desB30 insulin in the solubility experiments was too high to allow the simplifications to Wilson's equation that were made (see Paper II); and 4. one or more other phenomena affected the adsorption process — e.g., conformational changes in the insulin molecules.

One explanation that is not addressed in Paper II is the effect of changes in the pressure drop over the column between mobile phase compositions [86]. However, using the change in the molar volume of insulin due to adsorption onto an RPC adsorbent, as reported by Szabelski et al. [86], I found that this effect explained less than 1% of the variation in ln(A).

The amount-of-substance fraction of desB30 insulin in the solubility study was very low, and Explanation 3 is thus implausible, unless the activity coefficient of this species is very strongly influenced by its concentration. Explanation 2 is possible, but it is difficult to isolate the effects of the modulator on these activity coefficients from those on other phenomena in the adsorption process; such studies were clearly beyond the scope of this work. Explanation 4 is also conceivable, but recognized signs of conformational changes, such as peak broadening [111] and peak separation [110], were not observed, and insulin is small and rigid compared with other proteins. In addition to the arguments against Explanations 2–4, ethanol and other organic modulators adsorb onto RPC adsorbents [117-120], at least under certain conditions. In this work, the additional phenomenon is thus assumed to be the displacement of adsorbed ethanol by adsorbing insulin molecules.

Ideally, whether ethanol adsorbs to these RPC adsorbents should be determined experimentally. Nevertheless, it is not obvious how the adsorption of ethanol should be detected, especially at a high concentration of ethanol in the mobile phase. Attempts were made to measure the amount of ethanol that desorbed during insulin adsorption and that adsorbed during the elution of the insulin, using a refractive index (RI) detector. Variations in RI were observed for high-load runs, but the detector was sensitive to changes in the concentrations of KCl and insulin; consequently, a stable baseline was never achieved. Tests in which sample was not injected (blank runs) and only ethanol concentrations were varied confirmed that a stable signal could not be obtained with this experimental setup. Similar experiments, with radioactive isotope-containing ethanol and a detector that was based on radioactivity, were considered. However, due to the unreasonable cost and the high risk of generating inconclusive results, this option was not pursued.

7.2.1 Influence of Temperature

The influence of temperature on the solubility of desB30 insulin was evaluated at two ethanol concentrations — 25.6 and 28.4 wt% — which are representative levels for chromatographic runs on the C_4 and C_{18} adsorbents, respectively. The KCl concentration was maintained at 0.4 mol/kg. Figure 7.7 shows the unexpected results from this solubility study.

Below 20°C, the solubility increased exponentially with temperature, as expected, with the exception of the outlier for high ethanol content at 19°C. Above 20°C, the results were unusual. No dissolved desB30 insulin, other than at levels below 0.1 g/L in two samples at low ethanol content, could be detected in the samples that had been equilibrated at 25°C, despite repeated analysis and sampling and several runs of the entire experiment. The analyses and sampling were also recapitulated for some of the experiments at higher temperatures, yielding the same results.

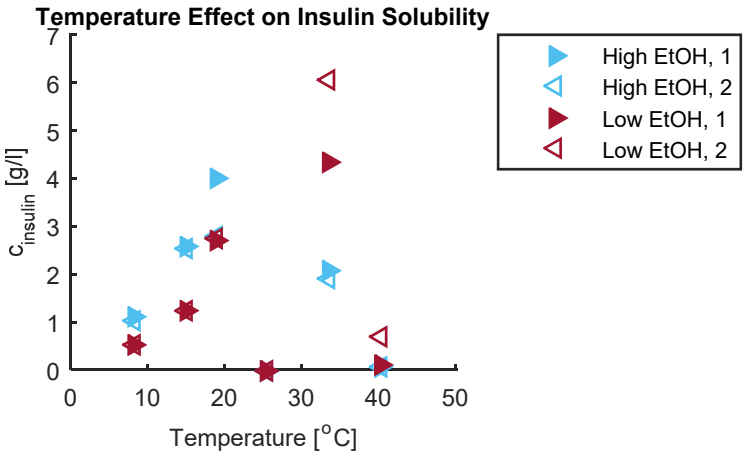

Figure 7.7: Influence of temperature on the solubility of desB30 insulin. High and low ethanol content refers to 28.4 and 25.6 wt%, representative for chromatographic runs on the C_{18} and C_4 adsorbents, respectively. "1" and "2" refer to the first experiment and its replicate, respectively.

Random errors were thus precluded, raising the possibility of a systematic error in the method. Because the same material and methods were used for all temperatures, the presumed systematic error must be related to the handling of the samples. The temperature control in the climate cabinet might have been faulty, but the temperature reported for each experiment was measured independently with a separate thermometer. After incubation in the climate cabinet, the samples were centrifuged at room temperature, which could have caused additional precipitation for the samples that were incubated at above-ambient temperatures. Such an event, however, should only have resulted in a halted rise in solubility with temperature compared to what would have been observed with centrifugation at the incubation temperature.

Another possibility is that the actual complexity of the dissolution, with many coupled equilibria, effected less predictable behavior at above-ambient temperatures. Insulin is prone to forming dimers and hexamers, generally via reversible reactions, but fibrillation can also occur. The latter type of aggregation is irreversible and is often caused by mechanical stress and elevated temperature [13, 113, 121]. The combination of elevated temperatures and centrifugation might have induced irreversible aggregation and is thus a reasonable explanation for the confusing results in Figure 7.7.

Consequently, none of the data in Figure 7.7 was considered to be reliable, and all of the findings were excluded from the calibration of the adsorption equilibrium model. Fortunately, the solubility data from the second solubility study were less important for the calibration than those from the first study, because the

stoichiometric coefficients between ethanol and the insulin variants ($\nu\zeta$) were assumed to be temperature-independent.

7.3 Models

In accordance with the assumption that ethanol was displaced by the insulin variants, to explain the stronger effect of ethanol on retention than on solubility, the models were based on the mechanism and corresponding equilibrium expression per Equations 2b and 3b, respectively, and the dynamic model in Equation 16 was used for the simulations. All ligands were assumed to be occupied by the insulin variants or ethanol. Consequently, the model is similar to the SMA model [95] but with ethanol molecules instead of counter-ions.

The model was developed and calibrated in two steps. First, equilibrium and dynamic models for the influence of the concentrations of KCl and ethanol were derived and calibrated (Paper II), and then, these models were expanded to include the temperature dependence of the adsorption process (Paper III). This subsection describes the final models, which encompass the effects of modulator concentrations and temperature.

7.3.1 Equilibrium Model

The main structure of the linear-range equilibrium model that was developed in this work is given by Equation 33, from which the thermodynamic retention factor for adsorbate i on adsorbent j can be calculated. Only the first and last terms are adsorbent-specific, whereas all of them are adsorbate-specific. Based on the assumptions, the activity of the species in the mobile phase is unaffected by the adsorbent, and the mobile phase properties do not affect the species in the stationary phase.

$$\ln\left(A_{i,j}\right) = \ln\left(A'_{0,i,j}\right) + \ln(\gamma_i(c_{salt})) + \ln(\gamma_i(x_M)) - \nu_{i,j}\xi_{i,j}\ln(x_M\gamma_M) \qquad (33)$$

Under isothermal conditions, the first term is constant. $A'_{0,i,j}$ is a lumped parameter (Equation 34), comprising the adsorption equilibrium constant and all other factors that vary negligibly with the mobile phase composition — e.g., the lumped parameter ζ_i (denoted ω'_i in Paper II), which contains the constant terms from Wilson's equation for ternary solutions. The simplified version of this formula is given by Equation 38. The ratio between the activity coefficients of the species in the stationary phase and the total molarity of the mobile phase are assumed to vary insignificantly with the modulator concentrations. Also, the fraction of occupied ligands is neglected under linear-range conditions. The motivations for these assumptions can be found in Paper II.

$$A'_{0,i,j} = K_{ads,i,j}\left(\frac{\Lambda_j}{c_{tot}}\right)^{\nu_{i,j}}\frac{\gamma_{LM_\xi}^{\nu}}{\gamma_{PL_\nu}}\zeta_i \qquad (34)$$

The theoretical temperature dependence of $K_{ads,i,j}$ is given by Equation 8 in Chapter 4, and based on the near-linear Van't Hoff plots, the changes in enthalpy and entropy were assumed to be temperature-independent. On performing approximate calculations, the variation in column pressure drop with temperature was negligible in this case, and thus, Equation 9 could be used to describe the effects of temperature on the adsorption equilibrium constant. All of the other parameters that were lumped in $A'_{0,i,j}$ were assumed not to have varied significantly with temperature. The premise for these assumptions can be found in Paper III.

The second term in Equation 33 describes the influence of salt concentration on the activity coefficient of adsorbate *i*. It is a simplified version of the salting-in potential from Kirkwood's electrostatic theories on macromolecules in solution, used to model HIC by Mollerup and colleagues [10] (Equation 35).

$$\ln(\gamma_i(c_{salt})) = -\frac{3N_A}{64\pi\epsilon_D RT}\left(\kappa^2\psi_i + \frac{\beta_i^2 F^2}{\epsilon_D RT}\sum_{j=1}^{N} c_j\psi_j\right) \tag{35}$$

N_A and F are Avogadro's and Faraday's numbers, respectively, and R is the ideal gas constant. The mobile phase properties are given by the permittivity (ε_D), temperature (T), and inverse of the Debye length (κ), which is a measure of ionic strength (Equation 36).

$$\kappa^2 = \frac{F^2}{\epsilon_D RT}\sum_{j=1}^{N} c_j\beta_j^2 \tag{36}$$

c_j and β_j are the concentration and valence, respectively, of ion *j*. In Equation 35, index *j* represents the *N* types of adsorbates, whereas it denotes the *N* types of ions in the mobile phase in Equation 36. In the linear-range equilibrium model, the concentrations of the adsorbates in the mobile phase were assumed to be sufficiently low to omit the last term in Equation 35 and neglect their contribution to κ. The parameter ψ_i (denoted $(\eta\tau^2)_i$ in Paper II) is a combination of two parameters that are related to the size and dipole moment of adsorbate *i* and varies with the permittivity of the mobile phase (Equation 37).

$$\psi_i = \psi_{0,i}\frac{4}{\left(2+\frac{\epsilon_0}{\epsilon_D}\right)^2} = \eta_{0,i}\tau_{0,i}^2\frac{4}{\left(2+\frac{\epsilon_0}{\epsilon_D}\right)^2} \tag{37}$$

ε_0 is the permittivity of vacuum. One of these parameters ($\tau_{0,i}$) was assumed to be small enough to allow the use of a Maclaurin series — i.e., a Taylor series around 0 — thereby enabling a reduction of the number of parameters. Because no indication of conformational changes in the insulin variants was observed in the temperature study, the size and dipole moment of each adsorbate should not vary significantly with temperature, and temperature affects ψ_i solely with regard to permittivity. Paper II details the derivation of Equation 35.

Although there is a slight variation in the salting-in potential versus ethanol concentration, due to its impact on permittivity, the main effect of ethanol on the activity coefficients of the adsorbates is given by the third term in Equation 33. This term is a simplified version of Wilson's equation for ternary solutions (Equation 38), assuming infinite dilution of adsorbate *i*. The concentrations of the insulin variants are not negligible, especially outside of the linear range, but the amount-of-substance fractions are insignificant compared with those of ethanol and water, which justifies this assumption. In addition, some terms have been assumed to vary insignificantly (see Paper II).

$$\ln(\gamma_i(x_M)) = -\frac{\alpha_i x_M}{\chi x_M^2 + \delta x_M + E_{W,M}} \tag{38}$$

α_i, χ, and δ are lumped parameters that are functions of the binary interaction parameters for the water–ethanol–insulin system. Two of them, $E_{W,M}$ and $E_{M,W}$, are parameters for the water–ethanol system and are also used in Wilson's equation for binary solutions (Equation 39), which is applied to estimate the influence of ethanol content on the activity coefficient of ethanol. χ and δ can be calculated from $E_{W,M}$ and $E_{M,W}$, whereas α_i includes parameters for the interaction between insulin and water or ethanol.

$$\ln(\gamma_M) = -\ln\left(x_M + E_{M,W} x_W\right) + x_W \left(\frac{E_{M,W}}{x_M + E_{M,W} x_W} - \frac{E_{W,M}}{x_W + E_{W,M} x_M}\right) \tag{39}$$

x_W is the amount-of-substance fraction of water, and the temperature dependence of the binary interaction parameters is given by Equation 40, where V_m is the molar volume and $\Delta U_{i,j}$ is a system-specific constant.

$$E_{i,j} = \frac{V_{m,i}}{V_{m,j}} \exp\left(-\frac{\Delta U_{i,j}}{RT}\right) \tag{40}$$

The effect of temperature on α_i was assumed to have the same form as that of $E_{W,M}$ and $E_{M,W}$ but with an empirical constant instead of the ratio between molar volumes. The empirical constant was determined from the previously calibrated values of α_i at 22°C (Paper II) and the system-specific constant for α_i, henceforth denoted $\Delta U_{\alpha,i}$, was calibrated against retention data.

Estimates for $E_{W,M}$ and $E_{M,W}$ were based on data from a publication regarding the vapor–liquid equilibrium (VLE) of mixtures of water and ethanol at 25°C [122]. These values were used to calibrate the model that describes the effects of modulator concentrations but not temperature (Paper II). The same VLE data were also applied to estimate $\Delta U_{i,j}$ for the temperature-dependent model (Paper III). To separate the effects of ethanol concentration on the two last terms in Equation 33, this model and the solubility model that is given by Equation 32 were calibrated simultaneously,

using the correlation for the activity coefficient in Equation 38 for both models. In the solubility model, the constant ζ was lumped with K_{sol}.

The presence of the salt and its potential effects were neglected when Wilson's equation was used, primarily because it does not account for electrostatic interactions and is thus unsuitable for ionic compounds. It is possible to combine electrostatic interactions — e.g. per Debye and Hückel — with Wilson's equation, but these interactions have a minor effect on uncharged species, such as ethanol and water. Therefore, the increased accuracy of a combination model was not considered to motivate the increased complexity of such a model.

Effects of Modulator Concentrations

The parameters that were calibrated were ψ_i and α_i, which are only adsorbate-specific, and $A'_{0,i,j}$, $\nu_{i,j}$, and $\xi_{i,j}$, which are adsorbate-specific and adsorbent-specific. However, in the final model, the effect of ethanol concentration on the activity coefficient was assumed to be the same for all three insulin variants — i.e., α was not considered to be adsorbate-specific in this case — based on the similarities in the structure and properties of the adsorbates and in the influence of ethanol on their retention (Figures 7.1-7.2 and 7.8). It is more likely that they differ with regard to the surface with which they adsorb to the stationary phase; thus, the difference in the effect of ethanol was modeled using individual stoichiometric coefficients ($\nu_{i,j}$ and $\xi_{i,j}$) for the insulin variants.

Only the product of the stoichiometric coefficients is relevant in the linear-range equilibrium model, and thus, $\nu_{i,j}\xi_{i,j}$ was considered to be a single parameter. All of the data in Figures 7.1-7.2 were included in the calibration, but for clarity, only the results for the lowest and highest KCl concentrations are shown in Figure 7.8. The calibration results for all KCl concentrations, those for the solubility of desB30 insulin, and the calibrated parameter values are presented in Paper II.

As shown in Figure 7.8, the model fit well for all combinations of adsorbents and adsorbates. However, the agreement between the experimental data and the response of the model was better for lower KCl concentrations and for more strongly retained adsorbates. The model describes $\ln(A)$ as being slightly more linearly dependent on the amount-of-substance fraction of ethanol compared with the experimental data. The resulting lack of fit occurs at the data points that correspond to lower retention volumes, because the calibration was performed for A, not its logarithm (Paper II). This approach was chosen due to the inherently lower precision of these points. Regarding the solubility of desB30 insulin, the model fit is comparable with that of the retention model. All of the calibrated parameters were statistically significant.

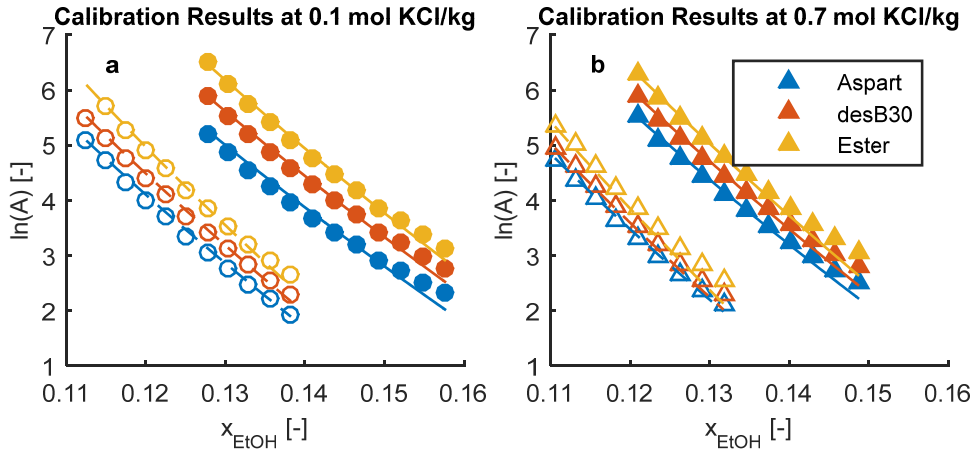

Figure 7.8: Comparison of experimental data (markers) and equilibrium model response (lines) for linear-range adsorption on the C_{18} (filled markers) and C_4 (open markers) adsorbents at a) 0.1 mol KCl/kg and b) 0.7 mol KCl/kg.

Effects of Temperature

The parameters that were calibrated were $\Delta H'_{i,j}$ and $\Delta S'_{i,j}$, which are adsorbate-specific and adsorbent-specific, and $\Delta U_{\alpha,i}$, which is adsorbate-specific. Because α_i was presumed to have the same value for all three insulin variants, the same assumption was made for $\Delta U_{\alpha,i}$. The calibrated parameter values are listed in Paper III, and the model fit is shown in Figures 7.9-7.10.

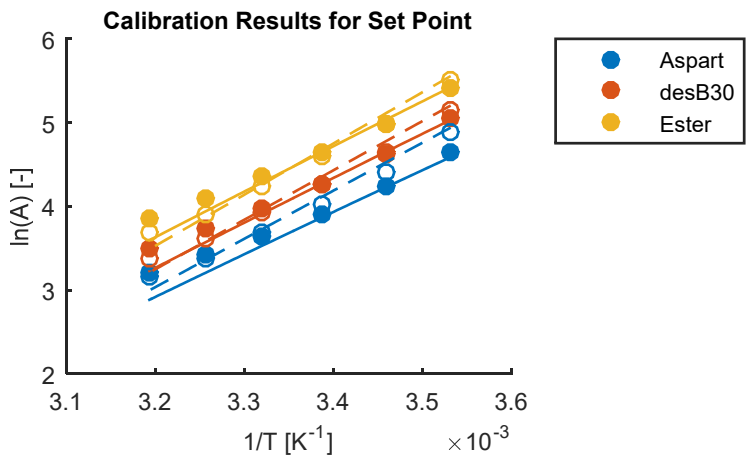

Figure 7.9: Comparison of experimental data (markers) and equilibrium model response (lines) for linear-range adsorption on the C_{18} (filled markers) and C_4 (open markers) adsorbents. Results for the set point concentrations (28.4 and 25.6 wt% for the C_{18} and C_4 adsorbents, respectively, and 0.4 mol KCl/kg) are shown.

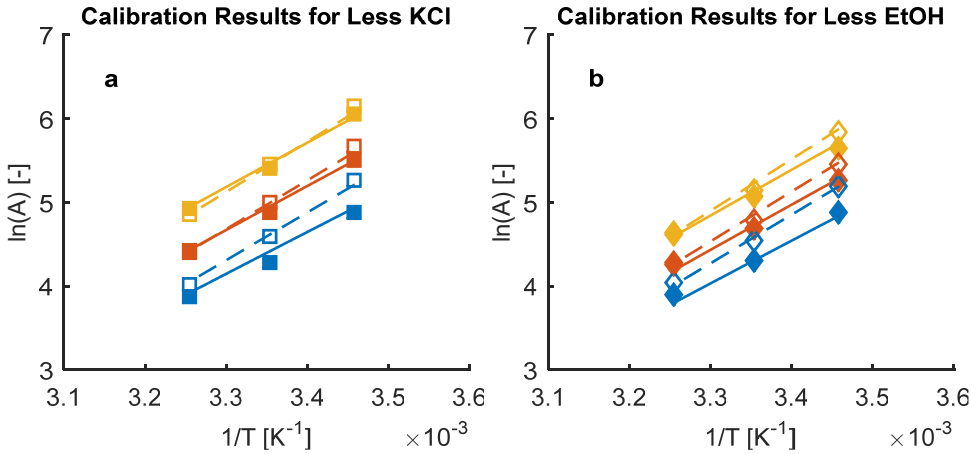

Figure 7.10: Comparison of experimental data (markers) and equilibrium model response (lines) for linear-range adsorption on the C_{18} (filled markers) and C_4 (open markers) adsorbents. Results for the a) lower KCl concentration (0.1 mol/kg) and b) lower ethanol content (27.5 and 24.7 wt% for the C_{18} and C_4 adsorbents, respectively) are shown. The colors for the various adsorbates are as in Figure 7.9.

As shown in Figures 7.9-7.10, the model fit is comparable with that of the model that only includes modulator effects (Figure 7.8). Ideally, the lines could have been slightly curved, but the discrepancies were not considered to be large enough to warrant the use of Equation 10a and the addition of one parameter per adsorbate–adsorbent combination. All calibrated parameters were statistically significant (Paper III).

7.3.2 Dynamic Model

The structure of the dynamic model that was used in this work is described in Section 4.3 (Equations 11 and 16-19), and the thermodynamic retention factor was included in the model, as described by Equation 41.

$$K_{ads,i}\left(\frac{\Lambda\gamma_{LM_\xi}}{c_{tot}}\right)^{\nu_i}\gamma_i = A_i(x_M\gamma_M)^{\nu_i\xi_i} = A'_{0,i}\gamma_i(c_{salt})\gamma_i(x_M) \tag{41}$$

Because the activity coefficient is included in $A'_{0,i,j}$, this parameter was moved to outside of the term in large parentheses in Equation 16, resulting in the final adsorption rate expression in Equation 42.

$$\frac{\partial q_i}{\partial t} = k_{kin,i}\left(A'_{0,i}\gamma_i(c_{salt})\gamma_i(x_M)\left(1-\sum_{k=1}^{N}\frac{(\nu_k+\sigma_k)q_k}{\Lambda}\right)^{\nu_i}c_i - q_i(\gamma_M x_M)^{\nu_i\xi_i}\right) \tag{42}$$

Effects of Modulator Concentrations

The remaining parameters that were to be calibrated for this model were those that described the capacity effects (Λ, ν_i, and σ_i) and adsorption kinetics ($k_{kin,i}$). Because the capacity parameters correlate strongly, parameter reduction was performed by estimating the number of ligands that were covered by an insulin molecule to be 7, using literature data for representative RPC adsorbents [30, 31], and setting $\sigma_i = 7 - \nu_i$. The remaining parameters were calibrated by iterative adjustment of the values and visual comparison of the experimental and simulated chromatograms for high-load runs with only desB30 insulin (Figures 7.11-7.12). To determine the parameters Λ and ν_i, the chromatograms that were generated at 12 g insulin/L column were used, whereas $k_{kin,i}$ was fitted to the chromatograms that were produced at 1.2 g insulin/L column. The calibrated parameter values and details on the estimations are presented in Paper II.

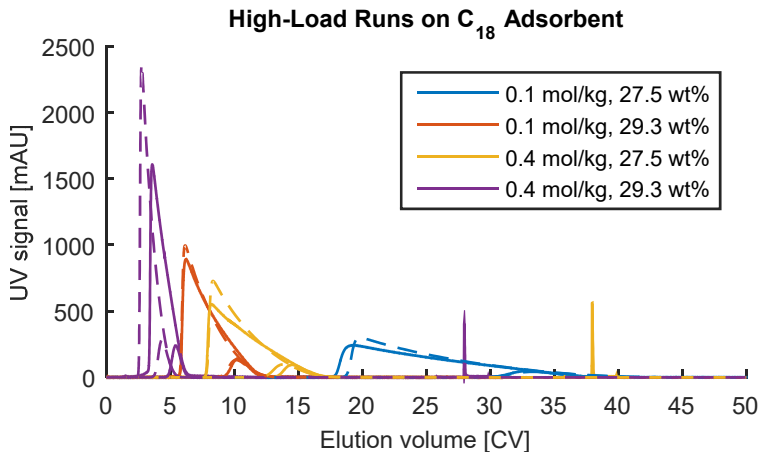

Figure 7.11: Comparison of experimental data (full lines) and simulation results for the dynamic model (dashed lines). For each mobile phase composition, 12 and 1.2 g desB30 insulin/L column were loaded onto the C_{18} adsorbent. The small, narrow peaks at the end of some of the experimental chromatograms were caused by regeneration.

Experiments were also performed at 28.4 and 25.6 wt% ethanol on the C_{18} and C_4 adsorbents, respectively, and used for the calibration but were excluded from Figures 7.11-7.12 for readability. The study included the corresponding experiments at 0.7 mol KCl/kg, but none of them was included in the calibration, because the retention volumes were very low, causing partial flow-through.

As shown in Figures 7.11-7.12, the model fit was acceptable, but there were clearly minor effects that the model could not capture. The lack of fit at 0.4 mol KCl/kg and the highest ethanol concentration for both adsorbents (purple lines) was most likely caused by a lack of fit for the equilibrium model, because the discrepancies for the two protein loads were comparable. Also, the peaks in the experimental

chromatograms for 12 g insulin/L column on the C_{18} adsorbent were nearly triangular, whereas the corresponding simulated peaks had the expected curved trailing edge. There were, however, no obvious effects of modulator concentrations on adsorption capacity, supporting the assumption that the species in the stationary phase are insignificantly affected by the mobile phase composition.

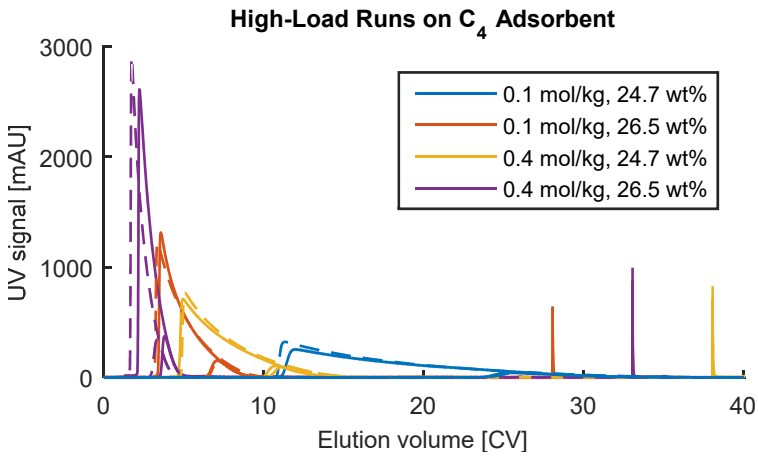

Figure 7.12: Comparison of experimental data (full lines) and simulation results for the dynamic model (dashed lines). For each mobile phase composition, 12 and 1.2 g desB30 insulin/L column were loaded onto the C_4 adsorbent. The small, narrow peaks at the end of some of the experimental chromatograms were caused by regeneration.

Effects of Temperature

The capacity parameters Λ and ν should not vary with temperature, although the latter might change if the conformation of the adsorbate is altered. Because no signs of conformational changes were observed, such changes were assumed not to have occurred; thus, Λ and ν should have remained constant. A clear effect of temperature on peak shape was nonetheless seen, as evidenced by the wider and more rounded peaks at lower temperatures (Figures 7.13-7.16). This finding was anticipated as a consequence of the increased viscosity at lower concentrations, causing slower mass transfer. Because the mass transfer effects — i.e., diffusion through the stagnant film around the particles and inside of the particle pores — are clustered with the desorption rate in k_{kin}, the influence of temperature should be attributed to this parameter.

An exponential function of $1/T$, similar to the Arrhenius equation for reaction rates, and a linear function of T, similar to the Stoke–Einstein and Wilke–Chang correlations for diffusion constants, were tested. However, a change in k_{kin} primarily affects the peak height, not its roundness. Consequently, k_{kin} was kept constant, and the conclusion was reached that a more advanced dynamic model would be required to describe the effects of temperature on peak shape correctly. Details can be found

in Paper III, and the experimental and simulated chromatograms from the temperature study for the C_{18} and C_4 adsorbents are compared in Figures 7.13-7.14 and 7.15-7.16, respectively.

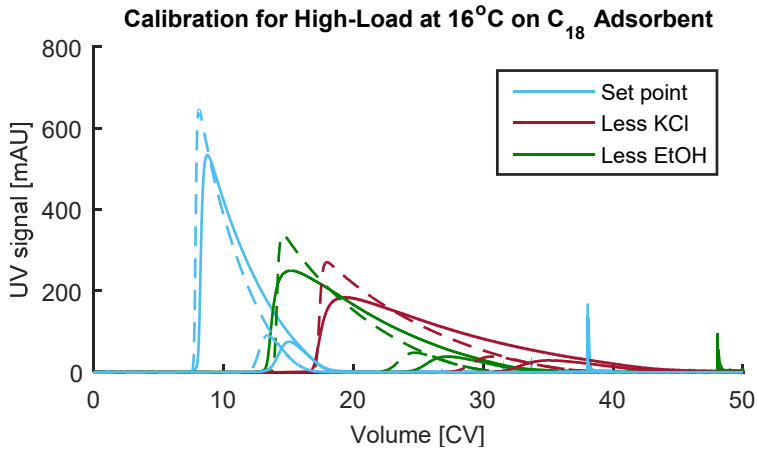

Figure 7.13: Comparison of experimental data (full lines) and simulation results for the dynamic model that includes the temperature dependence (dashed lines) at 16°C on the C_{18} adsorbent. The load levels are the same as in the study of the modulator effects.

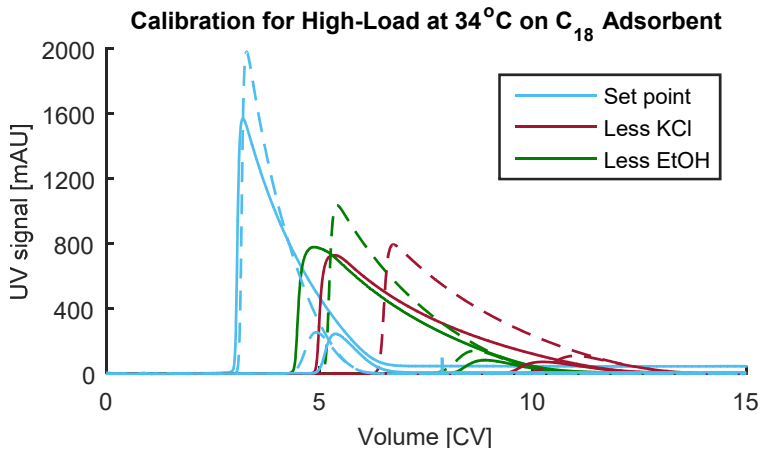

Figure 7.14: Comparison of experimental data (full lines) and simulation results for the dynamic model that includes the temperature dependence (dashed lines) at 34°C on the C_{18} adsorbent. The load levels are the same as in the study of the modulator effects.

The fit of the model that includes the temperature dependence is worse at high adsorbate loads (Figures 7.13-7.16) than that of the model that only includes the effects of the modulator concentrations (Figures 7.11-7.12). As discussed, the model fails to capture the roundness of the peaks, and there are clear discrepancies in the

retention volume between the experiments and simulations. These differences appear to be random and cannot be explained by a lack of fit of the linear-range equilibrium model.

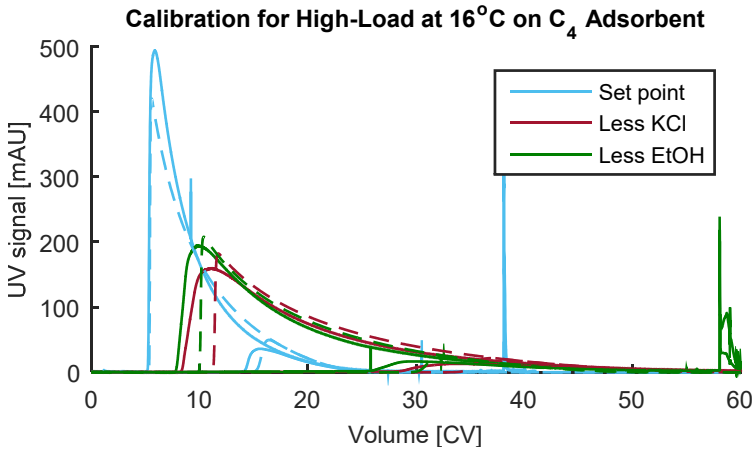

Figure 7.15: Comparison of experimental data (full lines) and simulation results for the dynamic model that includes the temperature dependence (dashed lines) at 16°C on the C_4 adsorbent. The load levels are the same as in the study of the modulator effects.

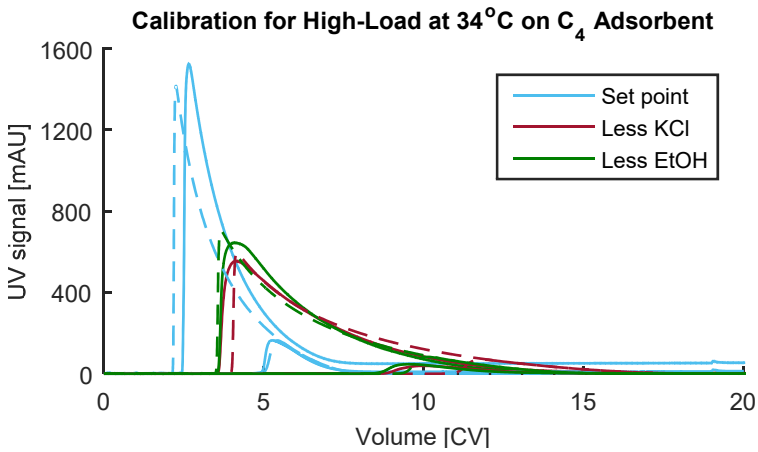

Figure 7.16: Comparison of experimental data (full lines) and simulation results for the dynamic model that includes the temperature dependence (dashed lines) at 34°C on the C_4 adsorbent. The load levels are the same as in the study of the modulator effects.

Notably, the modulator concentration had a pronounced effect on peak roundness, which was not observed in the first study, as evidenced by a comparison between Figures 7.11, 7.13, and 7.14 for the C_{18} adsorbent and Figures 7.12, 7.15, and 7.16 for the C_4 adsorbent. A reduction in the values of Λ from Paper II by 25% and 50%

for the C_{18} and C_4 adsorbents, respectively, improved the results with regard to the position of the peaks. Thus, the lack of fit was concluded to have been caused primarily by wear of the adsorbents.

7.3.3 Predictions for Other Systems

The greater complexity of a mechanistic versus empirical model is often warranted by the possibility of extrapolating and making predictions for conditions outside of the ranges that are examined and for other systems — i.e., other combinations of adsorbates, adsorbents, and modulators. Few predictions can be made with the models that are presented in this thesis without any experimental data for the new system, but a limited number of experiments can suffice for re-calibration of the models.

Change in Adsorbents — Three Experiments

The simplest prediction that can be made from the model is how adsorption will be affected by a change in adsorbents. The C_4 and C_{18} adsorbents cover most of the range of ligand types for RPC adsorbents, and the linear-range retention on, for example, a C_8 adsorbent should lie between those on the C_4 and C_{18} adsorbents but reside closer to that of the former. The parameters that are related to the adsorbent are A_0, $\Delta H^{'}$, $\Delta S^{'}$, ξ, ν, σ, Λ, and k_{kin}, but not all of them need to be re-calibrated. ν and σ were estimated from literature data and are not specific for the systems in this work. Two linear-range chromatographic experiments at 0.4 mol KCl/kg and various ethanol concentrations and one experiment at high adsorbate load should be satisfactory to estimate new values for A_0, ξ, Λ, and k_{kin}. For the inclusion of temperature dependence — i.e., the calibration of $\Delta H^{'}$ and $\Delta S^{'}$ — one linear-range chromatographic experiment each at 16°C and 34°C should suffice.

Change in Salts — Six Experiments

Only two of the calibrated parameters, A_0 and ψ, are related to the salt modulator, but another salt might cause both salting-in and salting-out within the soluble range of modulator concentrations. Consequently, three linear-range chromatographic experiments, distributed evenly over the solubility range for the salt, should be performed for each of two ethanol concentrations — e.g., 27 and 29 wt%. The resulting data will be sufficient to determine whether salting-out occurs and re-calibrate A_0 and ψ — or A_0, η, and τ, if salting-out is observed. If the temperature-dependent model is used, $\Delta H^{'}$ is re-calibrated instead of A_0; the other effects of temperature are already given by the model. However, if the salt differs significantly from KCl, another correlation for the effect of the salt on mobile phase density is required. Possible effects on mobile phase permittivity should also be taken into account.

Change in Organic Modulators — Five Experiments

In addition to the calibrated parameters A_0 or $\Delta H^{'}$, ξ, and α, a change in organic modulators affects the density and permittivity of the mobile phase. Further, the

binary interaction parameters for the water–organic modulator system will have other values. Adaptation of the model to another organic modulator thus requires literature data for its influence on density and permittivity and for its vapor–liquid equilibrium with water. A solubility study for one of the insulin variants, at a minimum of three concentrations of the organic modulator, is required to separate the effects of ξ and α. However, only two linear-range chromatographic experiments at 0.4 mol KCl/kg, with various concentrations of the organic modulator, are needed for subsequent re-calibration of these two parameters and A_0 or $\Delta H^{'}$.

Change in Adsorbates — Thirteen Experiments

A change in adsorbates requires the most extensive re-calibration. The only parameter values that remain unchanged are ξ and Λ, but all literature data for the modulators can be reused. New values for σ and $\nu+\sigma$ must be estimated from the size of the adsorbate molecules. The probability of salting-out is lower than when the salt is exchanged, but it is still advisable to perform three linear-range chromatographic experiments, distributed over the solubility range for the salt, for each of two ethanol concentrations. A solubility study for the new adsorbates — or one of them if they have similar properties — at a minimum of three different ethanol concentrations is also needed. Re-calibration of ψ (or η and τ), A_0, $\nu\xi$, and α can be performed against the six linear-range chromatographic experiments and the three solubility experiments. Linear-range chromatographic experiments should be conducted at a minimum of three temperatures for re-calibration of $\Delta H^{'}$ and $\Delta S^{'}$. At least one chromatographic experiment at a high load of the intermediately retained adsorbate must be performed for the re-calibration of Λ and k_{kin}. However, if the properties of the adsorbates differ significantly, one experiment for each is recommended.

Chapter 8

Optimal Conditions for RPC Separation

Although it is interesting to study and model various effects on chromatographic retention, models are seldom developed without a specific field of application. The most common applications are the design of a new process and optimization or robustness analysis of an existing process. One of the aims of the work presented in this thesis was to demonstrate the applicability of the model that was described in the previous chapter in an optimization study (Paper IV). The effects of temperature and the concentrations of KCl and ethanol on the selectivity between the insulin variants will first be evaluated, because several conclusions with regard to suitable process conditions can be drawn from these relationships.

8.1 Selectivity

Notable observations regarding the separation of the insulin variants on the RPC adsorbents were made in the studies on which Papers II and III are based (Figures 8.1-8.2).

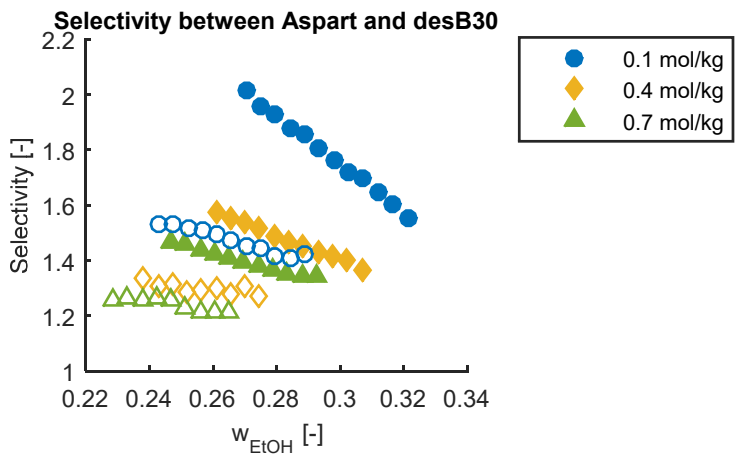

Figure 8.1: Selectivity between the two most weakly retained insulin variants at various modulator concentrations on the C_{18} (filled symbols) and C_4 (open symbols) adsorbents.

As discussed in the previous chapter, the C_{18} adsorbent yielded near-Gaussian peaks, whereas the peaks that were eluted from the C_4 adsorbent were tailing. Combined with a lower selectivity, the tailing resulted in poorer separation of the insulin variants on the C_4 adsorbent. Further, concerning the separation on the RPC adsorbents, the selectivity declined with increasing KCl concentration. These observations were made directly from the chromatograms but were supported by calculations that revealed that greater selectivity is achieved at lower concentrations of KCl or ethanol and that there is a clear synergistic effect (Figures 8.1-8.2).

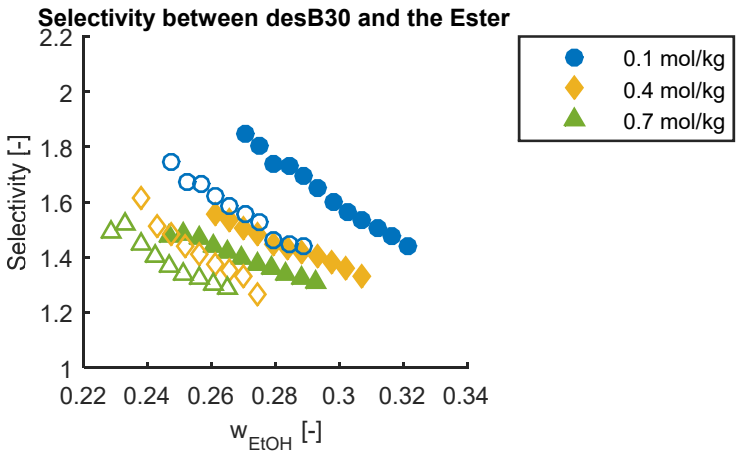

Figure 8.2: Selectivity between the two most strongly retained insulin variants at various modulator concentrations on the C_{18} (filled symbols) and C_4 (open symbols) adsorbents.

As suspected, the selectivity was significantly lower on the C_4 versus C_{18} adsorbent at the same modulator concentrations. The dependence of the selectivity on KCl was substantial and stronger at lower concentrations for all cases, whereas the dependence on ethanol varied between adsorbate pairs and adsorbents. For the most weakly retained adsorbates (Figure 8.1), ethanol had a strong effect on selectivity on the C_{18} adsorbent but barely affected that on the C_4 adsorbent. For the two most strongly retained adsorbates (Figure 8.2), however, the effect of ethanol was moderate and did not differ significantly between adsorbents. The effects of modulator concentrations and adsorbent type on the selectivity above were confirmed by the findings in Paper III (Figures 8.3-8.4).

Within the ranges of mobile phase compositions and temperatures that were examined, the KCl concentration had the strongest influence on the selectivity between both adsorbate pairs on both adsorbents, whereas the influence of the ethanol concentration and temperature were similar in magnitude. The selectivity between the two most weakly retained insulin variants (Figure 8.3) clearly increased with falling temperature, and the effect was more pronounced at the lower KCl concentration (0.1 mol/kg) on the C_{18} adsorbent. For the C_4 adsorbent at 0.1 mol

KCl/kg (open burgundy squares), the data point at 16°C is an outlier — or the selectivity peaks at approximately 25°C. The former explanation is more likely, but neither interpretation can be excluded without performing additional experiments.

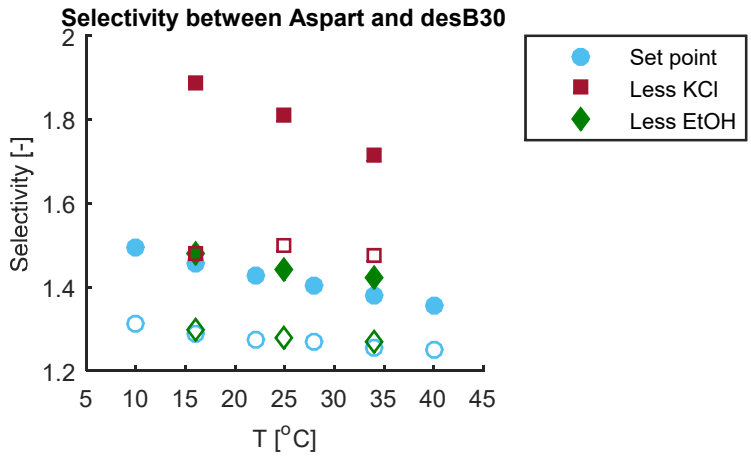

Figure 8.3: Selectivity between the two most weakly retained insulin variants at various temperatures and modulator concentrations on the C_{18} (filled symbols) and C_4 (open symbols) adsorbents.

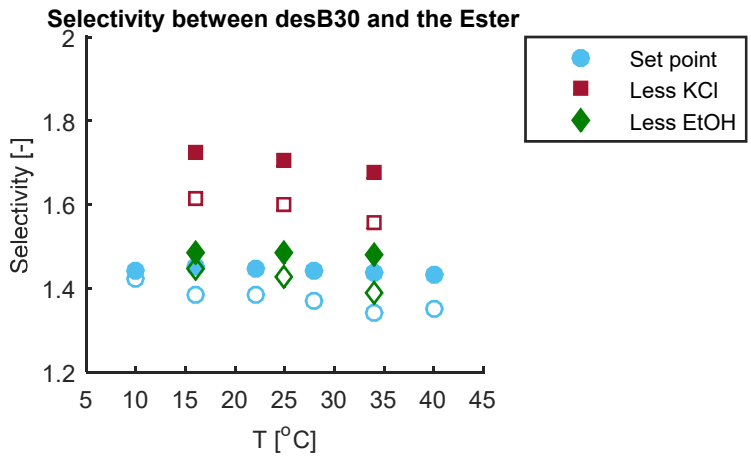

Figure 8.4: Selectivity between the two most strongly retained insulin variants at various temperatures and modulator concentrations on the C_{18} (filled symbols) and C_4 (open symbols) adsorbents.

The influence of temperature on the selectivity between the two most strongly retained insulin variants (Figure 8.4) was less pronounced, and there are indications of maxima for the two series at 0.4 mol KCl/kg (filled light-blue circles and green diamonds). In summary, a decline in temperature or the concentration of either modulator increases the selectivity. There are also synergistic effects, improving the results further if the values of two or all three of the parameters are reduced. Because

the retention rises with decreasing temperature and modulator concentrations, a balance between maximum selectivity and a reasonable retention time must be maintained.

8.2 Optimization Study

Four Pareto fronts were determined — with and without a solubility constraint for both adsorbents. The weighted sum of the productivity and yield (Equation 27 in Chapter 5) was used as the objective function, and the intermediately retained adsorbate, desB30 insulin, was chosen as the target adsorbate. The solubility constraint that was applied was an upper limit of the total insulin concentration in the eluate, corresponding to 90% of the maximum solubility at the current ethanol concentration, according to the solubility function that was given by Equations 32 and 38 (Paper II). A lower limit for the purity of the target adsorbate and upper limits for the concentrations of the impurities were also set. The minimum purity was 96%, and a maximum of 3% and 1% of insulin aspart and the insulin ester, respectively, was allowed. 2 CV were added to the total cycle time for regeneration and equilibration.

Due to the lack of fit of the dynamic model that included the effects of temperature at high adsorbate loads, the model that only included the influence of the modulator concentrations was used for the optimization study. Many possible decision variables that had similar effects on retention remained. Consequently, isocratic elution was chosen, and the remaining decision variables were the load factor, the concentration of KCl and ethanol during elution, and the cut points for pooling. The load factor was defined as the ratio between the adsorbate load and the maximum amount of adsorbates that could be adsorbed per unit volume of the column. Upper and lower bounds were applied for the load factor and the modulator concentrations to avoid establishing process conditions that were too unrealistic. Details can be found in Paper IV.

8.2.1 Pareto Fronts

The significant difference in selectivity between the C_{18} and C_4 adsorbents was expected to impact the possibility of improving the separation of the insulin variants. As shown in Figure 8.5, the maximum productivity that could be achieved with the C_{18} adsorbent is more than twice that with the C_4 adsorbent for the constrained optimization, and the difference is even larger for the unconstrained optimization. Here, the term “unconstrained optimization” is defined as optimization without the solubility constraint, although the constraints on the purity and impurity levels were applied for all cases.

There was a pronounced effect of the solubility constraint on the Pareto front (Figure 8.5), wherein the maximum productivity was over threefold higher when this constraint was not applied, and a sudden deviation appeared between the constrained

and unconstrained Pareto fronts at yields of approximately 98% and 90% for the C_{18} and C_4 adsorbents, respectively. Despite the difference in the achievable productivity levels, the Pareto fronts for the two adsorbents were similar in shape.

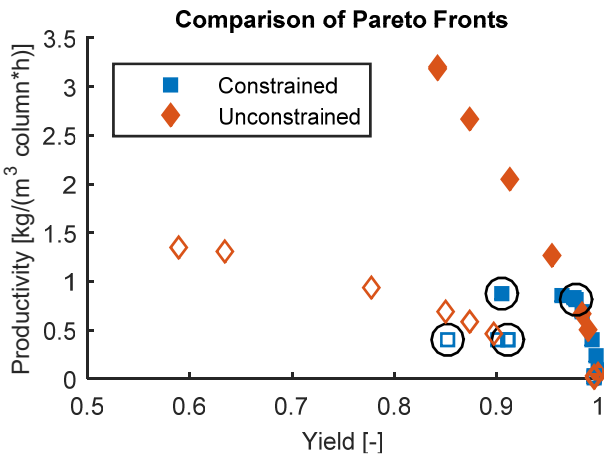

Figure 8.5: Pareto fronts for constrained and unconstrained optimization of purification of desB30 insulin on the C_{18} (filled markers) and C_4 (open markers) adsorbents. The encircled Pareto points are compared in the next subsection.

8.2.2 Comparison of Suitable Operating Points

Due to the significantly limiting effect of the solubility constraint on productivity, only two reasonable alternative operating points arose for each adsorbent (encircled in Figure 8.5); the corresponding chromatograms are shown in Figures 8.6-8.7.

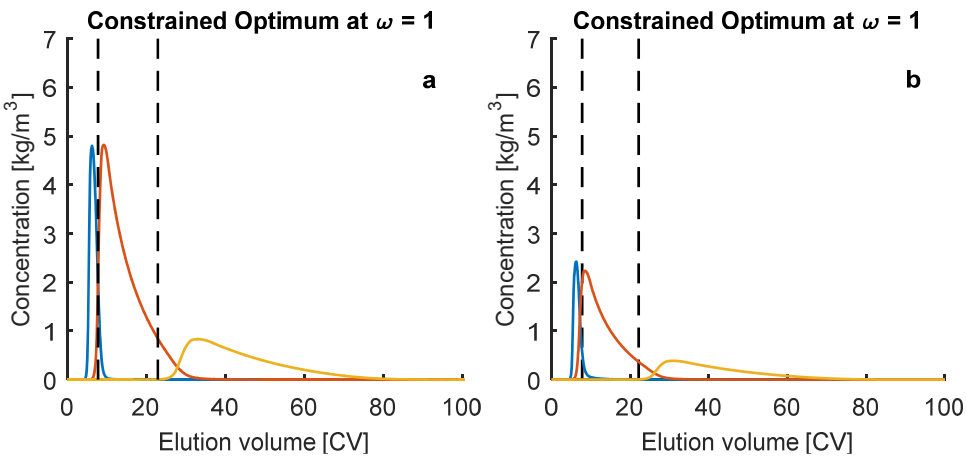

Figure 8.6: Chromatograms for maximum productivity, when the insulin concentration is limited by the solubility constraint, for separation on the a) C_{18} and b) C_4 adsorbents. These chromatograms correspond to the encircled points at the lower yields in Figure 8.5.

The principal difference between the chromatograms in Figure 8.6 is the scale of the concentrations. Because the solubility of the insulin variants decreased concomitantly with the ethanol content of the mobile phase, the lower ethanol content that is required for elution on the C_4 adsorbent decreases the concentration limit. The productivity for the C_4 adsorbent is thus limited primarily by the solubility constraint, despite the lower selectivity between the most weakly retained impurity (insulin aspart) and the target adsorbate (desB30 insulin) resulting in a loss of product on the leading edge, where the concentration peaks.

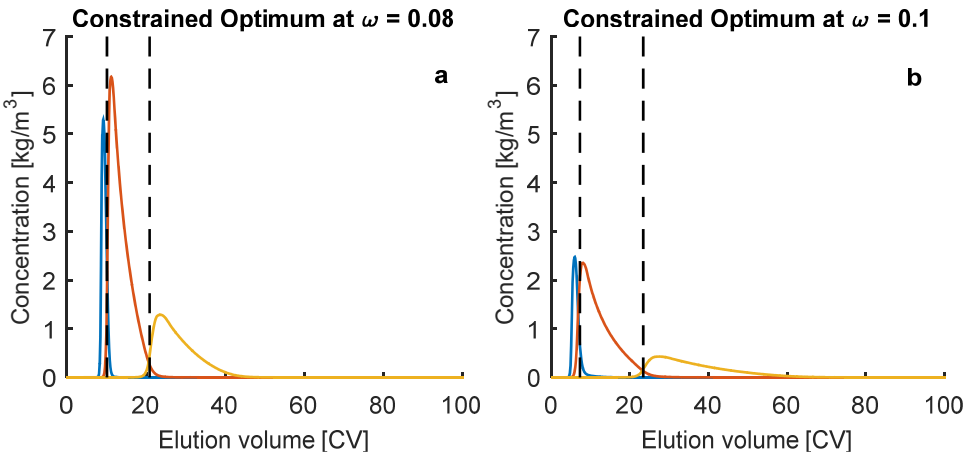

Figure 8.7: Chromatograms for the suggested operating points for separation on the a) C_{18} and b) C_4 adsorbents. These chromatograms correspond to the encircled points at the higher yields in Figure 8.5.

Comparing the chromatograms in Figures 8.6 and 8.7, the concentration of each insulin variant is slightly higher at the lower value of ω, especially for the C_{18} adsorbent, due to a higher ethanol content, which increases the solubility of insulin. At $\omega = 1$, the load factor is higher, and the greater overlap raises the total insulin concentration. Due to the constraint, the peaks must be flattened, which is achieved with a lower ethanol concentration. Thus, it appears to be more efficient to lower the ethanol content to widen the peaks than to increase it to enhance the solubility of insulin.

Another notable difference between the high and low values of ω is that the constraint on the concentration of the most strongly retained impurity (the insulin ester) is only limiting in the latter case. At maximum productivity, the concentration of the target adsorbate (desB30 insulin) in the tail of the peak is not sufficiently high for its inclusion in the product pool to improve productivity. Consequently, the purity is 1.0 percentage point above the minimum at maximum productivity for both adsorbents. As seen in Table 8.1, the little gain in productivity is outweighed by the loss in yield if the operating points that correspond to maximum productivity are chosen.

Table 8.1: Productivity, yield, and product purity for the four encircled operating points in Figure 8.1.

Adsorbent	**C_{18}**		**C_4**	
ω	1	0.05	1	0.1
Y [%]	90.4	97.7	85.1	91.0
P [kg/(m³·h)]	0.87	0.82	0.41	0.40
X [%]	97.0	96.0	97.0	96.0

8.2.3 An Alternative Approach

The constrained optimizations require the maximum total concentration of insulin that exits the column to be determined for each simulation. When standard optimization algorithms are used, the simulation must be performed twice or the optimization algorithm must be modified. The latter was chosen for the study presented here, but for this type of optimization problem, there is a third alternative.

As concluded above, the point at which the constrained and unconstrained Pareto fronts diverged corresponds to suitable operating conditions, because the solubility constraint limits the productivity to a greater extent than selectivity. This point can be approximated using the unconstrained Pareto front and the solubility limit. It is shown in Paper IV that the intersection between the maximum total insulin concentration for each unconstrained Pareto-optimal point and the 90% solubility limit, plotted against ethanol concentration, coincides with this point. However, this method has limitations — it only works well for continuous Pareto fronts, as demonstrated in Figure 8.8 and Table 8.2, which compare the operating conditions that are determined by the two methods.

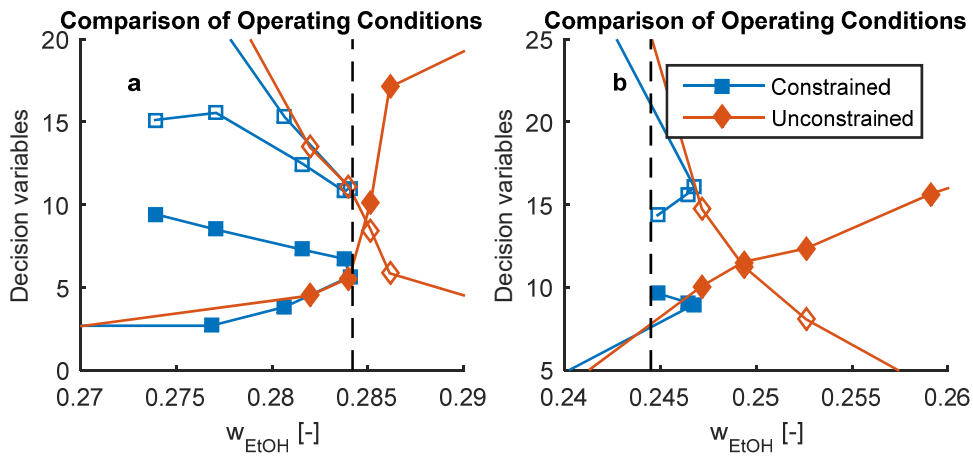

Figure 8.8: Evaluation of the alternative approach for estimating a suitable operating point for the a) C_{18} and b) C_4 adsorbents. Filled and open markers denote the load factor and pool volume, respectively, and the black dashed line marks the ethanol concentration, as determined with the alternative approach.

Based on Figure 8.8 and Table 8.2, the alternative method is applicable to the separation on the C_{18} but not C_4 adsorbent, due to the lack of Pareto points for yields between 91% and 99% for the latter (Figure 8.1).

Table 8.2: Operating conditions as determined from the constrained Pareto front (alt. 1) and the alternative approach (alt. 2).

Adsorbent	**C_{18}**		**C_4**	
Approach	Alt. 1	Alt. 2	Alt. 1	Alt. 2
f_{load} *[%]*	6.7	6.3	9.0	7.8
w_{EtOH} *[wt%]*	28.4	28.4	24.7	24.5
V_{pool} *[CV]*	10.8	10.7	16.1	25.2

The concentration of KCl in the eluent was also included as a decision variable, but the optimal value for all tested values of ω and both adsorbents was 0.1 mol/kg (±0.001) for both adsorbents, which was also the lower bound for this variable, because lower concentrations had not been examined experimentally. This trend was anticipated, because the KCl concentration has a much stronger influence on the selectivity between the insulin variants than on their retention.

Chapter 9

Summary of Findings

The findings from the work on which this thesis is based are summarized below in the conclusions, and a short discussion about the uncertainties in the investigations is presented. The thesis concludes with suggestions for future work.

9.1 Conclusions

The HIC experiments show that salting-in of the insulin variants does not occur within the soluble range of KCl concentrations, at least not with the butyl and phenyl adsorbents that were examined in this work. Different results might be obtained with other types or densities of ligands, but it is likely that another type of salt is required to achieve salting-in. The lack of a salting-in effect is unaffected by the addition of ethanol, but ethanol weakens the salting-out effect and lowers the retention time. All three adsorbates yield fronting peaks on both HIC adsorbents, but the fronting is more pronounced with butyl ligands — i.e., with the more hydrophobic adsorbent. The retention time and fronting tendency decline with an increasing ethanol concentration in the mobile phase, likely due to the higher solubility in a more hydrophobic solution.

In contrast to the influence of salt on the retention in HIC, salting-out was not observed during RPC of the insulin variants. A rise in the concentration of either modulator lowered the retention — a pattern that held for the entire range of feasible combinations of KCl and ethanol concentrations. Compared with the solubility of desB30 insulin, ethanol had a substantially stronger effect on the chromatographic retention of this insulin variant — indicating that the influence of ethanol concentration on the adsorption of desB30 insulin in RPC cannot be attributed solely to variations in the activity coefficient of the adsorbate. There are several plausible explanations for this finding, but in this work, the additional phenomenon was assumed to be the displacement of adsorbed ethanol molecules on adsorption of the insulin variants. The mechanism is presumed to be analogous to that of the steric mass-action (SMA) model for ion-exchange chromatography — i.e., all “free” ligands are occupied by ethanol.

The retention of the insulin variants on the RPC adsorbents decreased with rising temperature. The influence of temperature was stronger for the C_4 versus C_{18} adsorbent and at lower concentrations of KCl and ethanol. The effect of temperature also increased concomitantly with the hydrophobicity of the adsorbate.

A model that describes the effects of temperature and modulator concentrations was developed from existing thermodynamic theories, simplified and calibrated against experimental data for the RPC systems. The influence of salt concentration was based on the adaptation of Kirkwood's electrostatic theories on macromolecules in solution to HIC by Mollerup and colleagues, and that of ethanol content was derived from Wilson's equation. The final calibrated model describes the linear-range equilibrium well and makes good predictions on high-load dynamics. Because the focus was on the equilibrium, more time was spent on the development of that component of the model, which is reflected by its better fit.

Using the final equilibrium model, conclusions about the different contributions to the temperature dependence of ln(A) could be drawn. As suspected, the decrease in retention at higher temperatures was attributed to negative changes in enthalpy and entropy on adsorption of each adsorbate. However, the decline of the lumped parameter ln(A'_0) with increasing temperature, which includes the equilibrium constant, was more than twice that of ln(A), because the contributions from the changes in the activity coefficients of the adsorbates and ethanol were significant and had the opposite sign. The assumption that the changes in the equilibrium constant with temperature were the sole cause of the temperature dependence of the retention would have led to a gross underestimation of ΔH and ΔS.

I acknowledge that A'_0, in addition to the equilibrium constant, includes factors for the activity coefficients of the adsorbates and the ratio between the activity coefficients of the ethanol–ligand and adsorbate–ligand complexes. One or both of these factors might vary with temperature. Consequently, I do not claim to have made a good estimation of the actual values of ΔH and ΔS — only that of the lumped parameters $\Delta H'$ and $\Delta S'$. Nevertheless, it is unlikely that the sign of the actual and lumped parameters differs; thus, I conclude that the adsorption is enthalpy-driven and that a practically applicable model has been derived.

The selectivity between the closely eluting insulin variants varied substantially with mobile phase composition and temperature. A reduction in temperature or the concentration of KCl or ethanol increased the selectivity with significant synergistic effects. Compared with its influence on retention, the concentration of KCl had a significantly stronger effect on selectivity than temperature and ethanol concentration. The effects of temperature and modulator concentrations were more noticeable for the C_4 versus C_{18} adsorbent and affected the selectivity between insulin aspart and desB30 insulin to a greater extent than that between desB30 insulin and the insulin ester.

As expected, based on the calculated selectivity values, significantly greater productivity could be achieved with the C_{18} versus C_4 adsorbent for the same yield and using the same constraints. When the solubility constraint was applied, the productivity for the C_4 adsorbent was further limited by its lower hydrophobicity, decreasing the ethanol concentration during elution. Because the solubility of insulin increased concomitantly with the ethanol concentration, the lower ethanol concentrations required for the C_4 adsorbent correspond to a stricter solubility constraint compared with the C_{18} adsorbent. Due to the solubility constraint, the difference in ethanol concentration affected the productivity more than that in selectivity.

The Pareto fronts for optimization with and without the solubility constraint diverged when the constraint became active, and the productivity ceased to rise with decreasing yield for the constrained Pareto fronts. For continuous Pareto fronts, an alternative approach could be used to determine suitable operating conditions, instead of constructing a Pareto front from constrained optimizations. The operating conditions that correspond to the ethanol concentration at which the solubility limit and the maximum total insulin concentrations from the unconstrained optimizations coincide constituted a good estimate of the operating conditions that were determined from the constrained Pareto front.

9.2 Uncertainties

The certainty of the observations and conclusions in the text above varies, and I have summarized the main uncertainties below.

The cause of the fronting peaks on the HIC adsorbents remains unknown but was attributed to self-association of the adsorbates, as supported by the findings at high adsorbate load. The effects of self-association were more pronounced at high adsorbate loads, but this phenomenon will also occur in linear-range experiments, despite the low adsorbate concentrations. Another explanation is that conformational changes in the insulin variants arose during the adsorption/desorption process, but the low hydrophobicity of the adsorbent and mobile phase should not have induced such shifts. This explanation is especially unlikely for insulin, which is a robust protein with a stable ternary structure. A third possibility, which is not discussed in Paper II, is that self-association of the insulin variants occurred at low ethanol concentrations (below 10 wt%) due to their poor solubility under these conditions.

The peculiar peak shapes that were observed for RPC at high adsorbate loads and the tailing at low adsorbate loads on the C_4 adsorbent might have originated from self-association or a similar phenomenon. This possibility could have been examined by fractionation and analysis of the eluted peaks, but the potential on-column dimerization might be reversed during elution.

It is also difficult to study the possible effects of modulator concentrations and temperature on the activity coefficients of the adsorbate–ligand and ethanol–ligand complexes experimentally. Independent experiments, equivalent to solubility studies on the effects on the activity coefficients of the insulin variants in solution, are difficult, if not impossible, to design. The validity of the assumption that the ratio between the activity coefficients of the adsorbate–ligand and ethanol–ligand complexes is invariant thus remains unknown.

That ethanol adsorption caused ethanol to have a stronger influence on the chromatographic retention than on the solubility of insulins is plausible, but this effect could also be explained by the invalidity of the assumption in the previous paragraph. If ethanol is adsorbed and desorbed during RPC of the insulin variants, the corresponding decrease and increase in ethanol concentration should be possible to measure experimentally, but this project had insufficient resources for such experiments.

9.3 Future Work

The effects of other modulators on the retention of the insulin variants and those of KCl and ethanol on other proteins or peptides should be examined and compared. Studies that use other adsorbents are less interesting, because C_{18} and C_4 ligands cover the RPC range well, and butyl and phenyl ligands are representative for HIC. The effects of temperature should be included in such studies. A more detailed investigation of the influence of temperature and the concentrations of KCl and ethanol on the solubility of insulin can enable refinement of the model, generating useful results for process development and resolving the strange findings from the study on the effects of temperature on the solubility of desB30 insulin.

The cause of peak fronting and the disparate slopes of $\ln(A)$ for the HIC systems should also be determined. Although the potential dimers and hexamers might revert to monomers during the elution, a first step could be to fractionize and analyze the peaks. Molecular dynamics simulations could also provide insights into the underlying phenomena. There is a slight possibility that the unexpected peak shapes in the HIC study were caused by non-specific binding, which would be interesting to examine for the HIC and RPC adsorbents. In the latter case, it should be easy to obtain adsorbent particles without ligands for such a study.

One of the main conclusions of this work is that ethanol adsorbs onto the ligands and is displaced by adsorbing insulin molecules. Although other studies support the adsorption of ethanol, it is desirable to demonstrate that it also occurs for the adsorbents used in this work. A better setup with an RI detector, the use of ethanol with a radioactive isotope, or an improved experimental design might enable measurement of ethanol adsorption.

The optimization study in this work only tested the possibilities with regard to simultaneously varying the concentrations of the two modulators — not temperature. By fixing the KCl concentration at the value that yielded the highest selectivity according to this study, temperature could be added as a decision variable — preferably after improving the temperature-dependent model. A linear, or more complex, gradient of the ethanol concentration for this process could be optimized.

References

1. Ditz, R., *Chapter 1: Introduction*, in *Preparative Chromatography of Fine Chemicals and Pharmaceutical Agents*, H. Schmidt-Traub, Editor. 2005, WILEY-VCH Verlag GmbH & Co.: Weinheim, Germany. p. 1-8.
2. Livengood, J., *Why was M. S. Tswett's chromatographic adsorption analysis rejected?* Studies in History and Philosophy of Science, 2009. **40**(1): p. 57-69.
3. Guiochon, G., et al., *Chapter 1: Introduction, Definitions, Goal*, in *Fundamentals of Preparative and Nonlinear Chromatography*. 2006, Elsevier Inc.: San Diego, CA, USA. p. 1-18.
4. *The Nobel Prize in Chemistry 1952*. Nobel Prizes and Laureates, Nobel Media AB, 2017, [cited March 7, 2017]; Available from: http://www.nobelprize.org/nobel_prizes/chemistry/laureates/1952/press.html.
5. Johnson, I.S., *Human Insulin from Recombinant DNA Technology.* Science, 1983. **219**(4585): p. 632-637.
6. Ersson, B., L. Rydén, and J.-C. Janson, *Chapter 1: Introduction to Protein Purification*, in *Protein Purification: Principles, High Resolution Methods, and Applications*, J.-C. Janson and L. Rydén, Editors. 1998, John Wiley & Sons, Inc.: New York, NY, USA. p. 3-40.
7. ICH, *Pharmaceutical Development Q8 (R2)*, in *ICH Harmonised Tripartite Guideline*. 2009.
8. Roth, C.M., K.K. Unger, and A.M. Lenhoff, *Mechanistic model of retention in protein ion-exchange chromatography.* J. Chromatogr. A, 1996. **726**(1): p. 45-56.
9. Xu, X. and A.M. Lenhoff, *A Predictive Approach to Correlating Protein Adsorption Isotherms on Ion-Exchange Media.* J. Phys. Chem. B, 2008. **112**(1): p. 1028-1040.
10. Mollerup, J.M., et al., *Simultaneous correlation of hydrophobic interactions in HIC and protein solubility in aqueous salt solutions and mixed solvents.* Fluid Phase Equilibria, 2011. **301**(2): p. 163-170.
11. Horváth, C., W. Melander, and I. Molnár, *Solvophobic Interactions in Liquid Chromatography with Nonpolar Stationary Phases.* J. Chromatogr., 1976. **125**: p. 129-156.
12. Nikitas, P., A. Pappa-Louisi, and P. Agrafiotou, *Effect of the organic modifier concentration on the retention in reversed-phase liquid chromatography I. General semi-thermodynamic treatment for adsorption and partition mechanisms.* J. Chromatogr. A, 2002. **946**: p. 9-32.

References

13. Mollerup, I., et al., *Insulin Purification*, in *Encyclopedia of Industrial Biotechnology*, M.C. Flickinger, S.W. Drew, and R.E. Spier, Editors. 2010, John Wiley & Sons, Inc.
14. Janson, J.-C. and J.-Å. Jönsson, *Chapter 2: Introduction to Chromatography*, in *Protein Purification: Principles, High Resolution Methods, and Applications*, J.-C. Janson and L. Rydén, Editors. 1998, John Wiley & Sons, Inc.: New York, NY, USA. p. 43-78.
15. Schulte, M. and A. Epping, *Chapter 2: Fundamentals and General Terminology*, in *Preparative Chromatography of Fine Chemicals and Pharmaceutical Agents*, H. Schmidt-Traub, Editor. 2005, WILEY-VCH Verlag GmbH & Co.: Weinheim, Germany. p. 9-50.
16. Wewers, W., et al., *Chapter 4: Selection of Chromatographic Systems*, in *Preparative Chromatography of Fine Chemicals and Pharmaceutical Agents*, H. Schmidt-Traub, Editor. 2005, Wiley-VCH Verlag GmbH & Co.: Weinheim, Germany. p. 107-172.
17. Yamamoto, S., K. Nakanishi, and R. Matsuno, *Chapter 2: Theoretical Aspects*, in *Ion-Exchange Chromatography of Proteins*. 1988, Marcel Dekker, Inc.: New York, NY, USA. p. 35-106.
18. Sellberg, A., et al., *Discretized multi-level elution trajectory: A proof-of-concept demonstration.* J. Chrom. A, 2017. **1481**(1): p. 73-81.
19. Holmqvist, A. and F. Magnusson, *Open-loop optimal control of batch chromatographic separation processes using direct collocation.* J. Process Control, 2016. **46**(1): p. 55-74.
20. Carlsson, J., J.-C. Janson, and M. Sparrman, *Chapter 10: Affinity Chromatography*, in *Protein Purification: Principles, High Resolution Methods, and Applications*, J.-C. Janson and L. Rydén, Editors. 1998, John Wiley & Sons: New York, NY, USA. p. 375-442.
21. Karkov, H.S., L. Sejergaard, and S.M. Cramer, *Methods development in multimodal chromatography with mobile phase modifiers using the steric mass action model.* J. Chromatogr. A, 2013. **1318**: p. 149-155.
22. Holstein, M.A., et al., *Effects of Urea on Selectivity and Protein−Ligand Interactions in Multimodal Cation Exchange Chromatography.* Langmuir, 2012. **29**(1): p. 158-167.
23. Chilamkurthi, S., et al., *Thermodynamic description of peptide adsorption on mixed-mode resins.* J. Chromatogr. A, 2014. **1341**: p. 41-49.
24. Ordoñez, E.Y., et al., *Computer assisted optimization of liquid chromatographic separations of small molecules using mixed-mode stationary phases.* J. Chromatogr. A, 2012. **1238**: p. 91-104.
25. Yang, Y. and X. Geng, *Mixed-mode chromatography and its applications to biopolymers.* J. Chrom. A, 2011. **1218**(1): p. 8813-8825.
26. Mant, C.T. and R.S. Hodges, *Mixed-mode hydrophilic interaction/cation-exchange chromatography (HILIC/CEX) of peptidesand proteins.* J. Sep. Sci., 2008. **31**(1): p. 2754-2773.

27. Ohyama, K. and N. Kuroda, *Capillary Electrochromatography of Charged Biomolecules with Mixed-Mode Stationary Phases.* J. Liq. Chromatogr. Relat. Technol., 2007. **30**(1): p. 833-851.
28. Eriksson, K.-O., *Chapter 7: Hydrophobic Interaction Chromatography*, in *Protein Purification: Principles, High Resolution Methods, and Applications*, J.-C. Janson and L. Rydén, Editors. 1998, John Wiley & Sons, Inc.: New York, USA.
29. Deitcher, R.W., et al., *A new thermodynamic model describes the effects of ligand density and type, salt concentration and protein species in hydrophobic interaction chromatography.* J. Chromatogr. A, 2010. **1217**: p. 199-208.
30. AkzoNobel., in *Kromasil 100 Å Data Sheet*. 2014.
31. AkzoNobel., in *Kromasil 300 Å Data Sheet*. 2014.
32. Dill, K.A., *The Mechanism of Solute Retention in Reversed-Phase Liquid Chromatography.* J. Phys. Chem., 1987. **91**: p. 1980-1988.
33. Vailaya, A. and C. Horváth, *Retention in reversed-phase chromatography: partition or adsorption?* J. Chromatogr. A, 1998. **829**: p. 1-27.
34. Hearn, M.T.W., *Chapter 6: High-Resolution Reversed-Phase Chromatography*, in *Protein Purification: Principles, High Resolution Methods, and Applications*, J.-C. Janson and L. Rydén, Editors. 1998, John Wiley & Sons, Inc.: New York, NY, USA. p. 239-282.
35. Melander, W. and C. Horváth, *Salt Effects on Hydrophobic Interactions in Precipitation and Chromatography of Proteins: An Interpretation of the Lyotropic Series.* Arch. Biochem. Biophys., 1977. **183**: p. 200-215.
36. To, B.C.S. and A.M. Lenhoff, *Hydrophobic interaction chromatography of proteins II: Solution thermodynamic properties as a determinant of retention.* J. Chromatogr. A, 2007. **1141**: p. 235-243.
37. Langmuir, I., *The adsorption of gases on plane surfaces of glass, mica and platinum.* J. Am. Chem. Soc., 1918. **40**: p. 1361-1403.
38. Guiochon, G., et al., *Chapter 3: Single-Component Equilibrium Isotherms*, in *Fundamentals of Preparative and Nonlinear Chromatography*. 2006, Elsevier Inc.: San Diego, CA, USA. p. 67-149.
39. O'Haver, T., *Peak Fitter*. 2012, MATLAB CENTRAL.
40. Johansson, K., et al., *Combined effects of potassium chloride and ethanol as mobile phase modulators on hydrophobic interaction and reversed-phase chromatography of three insulin variants.* J. Chromatogr. A, 2015. **1381**(1): p. 64-73.
41. Lenhoff, A.M., *Significance and estimation of chromatographic parameters.* J. Chromatogr. A, 1987. **384**(1): p. 285-299.
42. Unger, K.K., C. du Fresne von Hohenesche, and M. Schulte, *Chapter 3: Columns, Packings and Stationary Phases*, in *Preparative Chromatography of Fine Chemicals and Pharmaceutical Agents*, H. Schmidt-Traub, Editor. 2005, WILEY-VCH Verlag GmbH & Co.: Weinheim, Germany. p. 51-105.

References

43. Speybrouck, D. and E. Lipka, *Preparative supercritical fluid chromatography: A powerful tool for chiral separations.* J. Chrom. A, 2016. **1467**(1): p. 33-55.
44. Patel, D.C., et al., *Advances in high-throughput and high-efficiency chiral liquid chromatographic separations.* J. Chrom. A, 2016. **1467**(1): p. 2-18.
45. Freitag, R., *Chapter 25: Chromatographic Techniques in the Downstream Processing of Proteins in Biotechnology*, in *Animal Cell Biotechnology - Methods in Molecular Biology*, R. Pörtner, Editor. 2014, Humana Press: New York, NY, USA. p. 419-458.
46. Walsh, G., *Biopharmaceuticals: recent approvals and likely directions.* Trends Biotechnol., 2005. **23**(11): p. 553-558.
47. Walsh, G., *Second-generation biopharmaceuticals.* Eur. J. Pharm. Biopharm., 2004. **68**: p. 185-196.
48. *Chapter 2: Chemicals from Metabolic Pathways*, in *Bioreaction Engineering Principles*, J. Villadsen, J. Nielsen, and G. Lidén, Editors. 2011, Springer Science+Business Media, LLC: New York, NY, USA.
49. Freed, S. *New Oral GLP-1 Promising for Type 2 Diabetes*. Diabetes In Control, 2016.
50. Jungbauer, A., *Chromatographic media for bioseparation.* J. Chromatogr. A, 2005. **1065**: p. 3-12.
51. *The Nobel Prize in Physiology or Medicine 1923*. Nobel Prizes and Laureates, Nobel Media AB, 2017, [cited March 15, 2017]; Available from: http://www.nobelprize.org/nobel_prizes/medicine/laureates/1923/press.html.
52. *Diabetes - Fact sheet*. WHO Media centre, 2016, [cited February 15, 2017]; Available from: http://www.who.int/mediacentre/factsheets/fs312/en/.
53. Vargesson, N., *Thalidomide-induced teratogenesis: History and mechanisms.* Birth Defects Research, 2015. **105**(2): p. 140-156.
54. Klatt, K.-U., et al., *Model-based optimization and control of chromatographic processes.* Comput. Chem. Eng., 2000. **24**(1): p. 1119-1126.
55. Citoglu, G.S. and Ö.B. Acikara, *Chapter 2: Column Chromatography for Terpenoids and Flavonoids*, in *Chromatography and Its Applications*, S. Dhanarasu, Editor. 2012, InTech: Rijeka, Croatia. p. 13-50.
56. Agostini-Costa, T.d.S., et al., *Chapter 8: Secondary Metabolites*, in *Chromatography and Its Applications*, S. Dhanarasu, Editor. 2012, InTech: Rijeka, Croatia. p. 131-164.
57. Knutson, H.-K., *Robust Multi-objective Optimization of Rare Earth Element Chromatography*, Doctoral thesis, Department of Chemical Engineering, Lund University, 2016.
58. Knutson, H.-K., A. Holmqvist, and B. Nilsson, *Multi-objective optimization of chromatographic rare earth element separation.* Journal of Chromatography A, 2015. **1416**: p. 57-63.

59. Andersson, N., et al., *Model-Based Comparison of Batch and Continuous Preparative Chromatography in the Separation of Rare Earth Elements.* Industrial & Engineering Chemistry Research, 2014. **53**(42): p. 16485-16493.
60. Mollerup, J.M., et al., *Quality by design-Thermodynamic modelling of chromatographic separation of proteins.* J. Chromatogr. A, 2008. **1177**(2): p. 200-206.
61. Mollerup, J.M., *Chemical Engineering Thermodynamics and Protein Adsorption Chromatography.* J. Chem. Eng. Data, 2014. **59**(4): p. 991-998.
62. Vailaya, A. and C. Horváth, *Retention Thermodynamics in Hydrophobic Interaction Chromatography.* Ind. Eng. Chem. Res., 1996. **35**(9): p. 2964-2981.
63. Mollerup, J.M., *Chapter 2: Adsorption Isotherms*, in *Preparative Chromatography for Separation of Proteins*, A. Staby, A.S. Rathore, and S. Ahuja, Editors. 2017, John Wiley & Sons, Inc.: Hoboken, NJ, USA.
64. Guiochon, G., et al., *Glossary of Terms*, in *Fundamentals of Preparative and Nonlinear Chromatography*. 2006, Elsevier Inc.: San Diego, CA, USA. p. 949-968.
65. Mollerup, J.M., *Applied thermodynamics: A new frontier for biotechnology.* Fluid Phase Equilib., 2006. **241**(1-2): p. 205-215.
66. Fausnaugh, J.L., L.A. Kennedy, and F.E. Regnier, *Comparison of hydrophobic-interaction and reversed-phase chromatography of proteins.* J. Chromatogr., 1984. **317**: p. 141-155.
67. Marqusee, J.A. and K.A. Dill, *Solute partitioning into chain molecule interphases: Monolayers, bilayer membranes, and micelles.* J. Chem. Phys., 1986. **85**: p. 434-444.
68. Chen, J., T. Yang, and S.M. Cramer, *Prediction of protein retention times in gradient hydrophobic interaction chromatographic systems.* J. Chromatogr. A, 2008. **1177**: p. 207-214.
69. Chung, P.-L., et al., *A parallel pore and surface diffusion model for predicting the adsorption and elution profiles of lispro insulin and two impurities in gradient-elution reversed phase chromatography.* J. Chromatogr. A, 2010. **1217**: p. 8103-8120.
70. Nikitas, P. and A. Pappa-Louisi, *Retention models for isocratic and gradient elution in reversed-phase liquid chromatography.* J. Chromatogr. A, 2009. **1216**: p. 1737-1755.
71. Melander, W.R., S. El Rassi, and C. Horváth, *Interplay of hydrophobic and electrostatic interactions in biopolymer chromatography: Effects of salts on the retention of proteins.* J. Chromatogr., 1989. **469**: p. 3-27.
72. Arakawa, T., *Thermodynamic analysis of the effect of concentrated salts on protein interaction with hydrophobic and polysaccharide columns.* Arch. Biochem. Biophys., 1986. **248**: p. 101-105.

References

73. Oscarsson, S., *Influence of salts on protein interactions at interfaces of amphiphilic polymers and adsorbents.* J. Chromatogr. B: Biomedical Applications, 1995. **666**: p. 21-31.
74. Lienqueo, M.E., et al., *Current insights on protein behaviour in hydrophobic interaction chromatography.* J. Chromatogr. B, 2007. **849**: p. 53-68.
75. Fausnaugh, J.L. and F.E. Regnier, *Solute and Mobile Phase Contributions to Retention in Hydrophobic Interaction Chromatography of Proteins.* J. Chromatogr., 1986. **359**: p. 131-146.
76. To, B.C.S. and A.M. Lenhoff, *Hydrophobic interaction chromatography of proteins: I. The effects of protein and adsorbent properties on retention and recovery.* J. Chromatogr. A, 2007. **1141**(2): p. 191-205.
77. Shukla, A.A., et al., *Preparative Purification of a Recombinant Protein by Hydrophobic Interaction Chromatography: Modulation of Selectivity by the Use of Chaotropic Additives.* Biotechnol. Prog., 2002. **18**: p. 556-564.
78. Perkins, T.W., et al., *Protein retention in hydrophobic interaction chromatography: modeling variation with buffer ionic strength and column hydrophobicity.* J. Chromatogr. A., 1997. **766**: p. 1-14.
79. Baczek, T., et al., *Linear and Quadratic Relationships between Retention and Organic Modifier Content in Eluent in Reversed Phase High-Performance Liquid Chromatography: A Systematic Comparative Statistical Study.* J. High Resol. Chromatogr., 2000. **23**(12): p. 667-676.
80. Nikitas, P., A. Pappa-Louisi, and P. Agrafiotou, *Effect of the organic modifier concentration on the retention in reversed-phase liquid chromatography II. Tests using various simplified models.* J. Chrom. A, 2002. **946**(33-45).
81. Westerberg, K., et al., *Supporting Design and Control of a Reversed-Phase Chromatography Step by Mechanistic Modeling.* Chem. Eng. Technol., 2012. **35**(1): p. 169-175.
82. Put, R. and Y.V. Heyden, *Review on modelling aspects in reversed-phase liquid chromatographic quantitative structure–retention relationships.* Analytica Chimia Acta, 2007. **602**(2): p. 164-172.
83. Lindsey, R.K., et al., *Molecular simulation studies of reversed-phase liquid chromatography.* J. Chromatogr. A, 2013. **1287**: p. 60-82.
84. Sykora, D., J. Vozka, and E. Tesarova, *Chromatographic methods enabling the characterization of stationary phases and retention prediction in high-performance liquid chromatography and supercritical fluid chromatography.* J. Sep. Sci., 2016. **39**(1): p. 115-131.
85. Wilson, G.M., *Vapor-liquid equilibrium. XI. A new expression for the excess free energy of mixing.* J. Am. Chem. Soc., 1964. **86**: p. 127-130.
86. Szabelski, P., et al., *Experimental studies of pressure/temperature dependance of protein adsorption equilibrium in reversed-phase high-performance liquid chromatography.* Journal of Chromatography A, 2002. **950**(1): p. 41-53.

87. Stute, B., V. Krupp, and E. von Lieres, *Performance of iterative equation solvers for mass transfer problems in three-dimensional sphere packings in COMSOL.* Simul. Model. Pract. Theory, 2013. **33**(1): p. 115-131.
88. Schnittert, S., R. Winz, and E. von Lieres. *Development of a 3D Model for Packed Bed Liquid Chromatography in Micro-columns*. Presented at *2009 Third UKSim European Symposium on Computer Modeling and Simulation* in 2009. Athens, Greece: IEEE.
89. Guiochon, G., et al., *Chapter 16: Kinetic Models and Multicomponent Problems*, in *Fundamentals of Preparative and Nonlinear Chromatography*. 2006, Elsevier Inc.: San Diego, CA, USA.
90. Michel, M., A. Epping, and A. Jupke, *Chapter 6: Modeling and Determination of Model Parameters*, in *Preparative Chromatography of Fine Chemicals and Pharmaceutical Agents*, H. Schmidt-Traub, Editor. 2005, WILEY-VCH Verlag GmbH & Co.: Weinheim, Germany. p. 215-312.
91. Degerman, M., N. Jakobsson, and B. Nilsson, *Modeling and optimization of preparative reversed-phase liquid chromatography for insulin purification.* J. Chromatogr. A, 2007. **1162**(1): p. 41-49.
92. Karlsson, D., et al., *Methodologies for model calibration to assist the design of a preparative ion-exchange step for antibody purification.* J Chromatogr.A, 2004. **1033**(1): p. 71-80.
93. Jakobsson, N., M. Degerman, and B. Nilsson, *Optimisation and robustness analysis of a hydrophobic interaction chromatography step.* J. Chromatogr. A, 2005. **1099**: p. 157-166.
94. Arkell, K., et al., *Mechanistic Modeling of Reversed-Phase Chromatography of Insulins with Potassium Chloride and Ethanol as Mobile-Phase Modulators.* ACS Omega, 2017. **2**(1): p. 136-146.
95. Brooks, C.A. and S.M. Cramer, *Steric Mass-Action Ion Exchange: Displacement Profiles and Induced Salt Gradients.* AIChE J., 1992. **38**(12): p. 1969-1978.
96. Villadsen, J. and M.L. Michelsen, *Solution of differential equation models by polynomial approximation*. 1978, Englewood Cliffs, NJ, USA: Prentice Hall.
97. Versteeg, H.K. and W. Malalasekera, *Chapter 4: The Finite Volume Method for Diffusion Problems*, in *An Introduction to Computational Fluid Dynamics - The Finite Volume Method*. 1995, Longman Group Ltd.: Harlow, England, U.K. p. 85-102.
98. Farlow, S.J., *Partial Differential Equations for Scientists and Engineers*. Dover Books on Advanced Mathematics. 1993, Mineola, NY, USA: Dover Publications Inc.
99. Davis, M.E., *Chapter 4: Parabolic Partial Differential Equations in One Space Variable*, in *Numerical Methods & Modeling for Chemical Engineers*. 1984, John Wiley & Sons, Inc.: New York, NY, USA. p. 127-176.

100. Liu, X.-D., S. Osher, and T. Chan, *Weighted Essentially Non-oscillatory Schemes.* J. Comput. Phys., 1994. **115**(1): p. 200-212.
101. *MATLAB Release 2015a*. The MathWorks, Inc.: Natick, Massachusetts, USA.
102. Conte, S.D. and D.K. Kahaner, *Numerical analysis*, in *Encyclopedia of Computer Science*, A. Ralston, E.D. Reilly, and D. Hemmendinger, Editors. 2003, John Wiley and Sons Ltd.: Chichester, UK. p. 1260-1273.
103. *Preparative Chromatography Simulator (pcs)*. Department of Chemical Engineering, Lund University, [cited September 20, 2016,]; Available from: www.chemeng.lth.se/pcs.
104. Sreedhar, B., et al., *Optimal cut-times finding strategies for collecting a target component from overloaded elution chromatograms.* Computers & Chemical Engineering, 2013. **49**: p. 158-169.
105. Dutta, S., *Chapter 8: Some Advanced Topics on Optimization*, in *Optimization in Chemical Engineering*. 2016, Cambridge University Press: New Dehli, India. p. 180-221.
106. Stadler, W., *A Survey of Multicriteria Optimization or the Vector Maximum Problem, Part I: 1776-1960.* J. Optim. Theory. Appl., 1979. **29**(1): p. 1-52.
107. Nagrath, D., et al., *Multiobjective optimization strategies for linear gradient chromatography.* AIChE J., 2005. **51**: p. 511-525.
108. Davis, M.E., *Chapter 1: Initial-Value Problems for Ordinary Differential Equations*, in *Numerical Methods & Modeling for Chemical Engineers*. 1984, John Wiley & Sons, Inc.: New York, NY, USA. p. 1-52.
109. Coleman, T.F. and Y. Li, *An Interior Trust Region Approach for Nonlinear Minimization Subject to Bounds.* SIAM J. Optim., 1996. **6**(2): p. 418-445.
110. Nunes, C.A. and A.C.M. Dias-Cabral, *Angiotensin I retention behavior on Butyl-Sepharose under linear loading chromatographic conditions.* J. Chromatogr. A, 2009. **1216**: p. 2332-2338.
111. Purcell, A.W., M.-I. Aguilar, and M.T.W. Hearn, *High-Performance Liquid Chromatography of Amino Acids, Peptides, and Proteins. 123. Dynamics of Peptides in Reversed-Phase High-Performance Liquid Chromatography.* Anal. Chem., 1993. **65**: p. 3038-3047.
112. Hvidt, S., *Insulin association in neutral solutions studied by light scattering.* Biophys. Chem., 1991. **39**: p. 205-213.
113. Brange, J., *Stability of Insulin - Studies on the physical and chemical stability of insulin in pharmaceutical formulation*, Dr. Pharm. thesis, Royal Danish School of Pharmacy, 1994.
114. Brange, J., *Galenics of Insulin*. 1987, Berlin, Germany: Springer Berlin Heidelberg.
115. Diack, M. and G. Guiochon, *Adsorption Isotherm and Overloaded Elution Profiles of Phenyldodecane on Porous Carbon in Liquid Chromatography.* Anal. Chem., 1991. **63**: p. 2608-2613.

116. Pinho, S.P. and E.A. Macedo, *Solubility of NaCl, NaBr, and KCl in Water, Methanol, Ethanol, and Their Mixed Solvents.* J. Chem. Eng. Data, 2005. **50**(1): p. 29-32.
117. Bocian, S., et al., *Solvent excess adsorption on the stationary phases for reversed-phase liquid chromatography with polar functional groups.* J. Chrom. A, 2008. **1204**(1): p. 35-41.
118. Gritti, F., Y.V. Kazakevich, and G. Guiochon, *Effect of the surface coverage of endcapped C18-silica on the excess adsorption isotherms of commonly used organic solvents from water in reversed phase liquid chromatography.* J. Chrom. A, 2007. **1169**(1): p. 111-124.
119. Chan, F., et al., *Interpretation of the excess adsorption isotherms of organic eluent components on the surface of reversed-phase phenyl modified adsorbents.* J. Chrom. A, 2005. **1082**(1): p. 158-165.
120. Vajda, P., A. Felinger, and G. Guiochon, *Evaluation of surface excess isotherms in liquid chromatography.* J. Chrom. A, 2013. **1291**(1): p. 41-47.
121. Librizzi, F. and C. Rischel, *The kinetic behavior of insulin fibrillation is determined by heterogeneous nucleation pathways.* Protein Sci., 2005. **14**(1): p. 3129-3134.
122. Yamamoto, H., et al., *Vapor-Liquid Equilibria for Methanol + Ethanol + Calcium Chloride, + Ammonium Iodide, and + Sodium Iodide at 298.15 K.* J. Chem. Eng. Data, 1995. **40**: p. 472–477.

Karolina Arkell started her doctoral studies at the Department of Chemical Engineering, Lund University in 2011. Her work has been focused on investigation and modeling of the influence of the temperature and the concentrations of mobile phase modulators on reversed-phase chromatography (RPC) of proteins.

Many of today's pharmaceuticals have active ingredients that are peptides, proteins or antibodies. These are called biopharmaceuticals, and are generally made to compensate for a human deficiency to produce that particular substance, or act as a tailor-made treatment for an illness that is otherwise difficult to treat.

In the production of biopharmaceuticals, preparative chromatography is a key method for purification of the active ingredients. Optimization of existing processes and efficient development of new ones require knowledge about the effects of different process conditions, which can be obtained by studying the underlying phenomena.

The aim of the work presented in this thesis was to investigate and model the effects of the temperature and the concentrations of KCl and ethanol on the chromatographic separation of three types of insulin. Existing thermodynamic models were combined to create a semi-empirical model that has a clear connection with the phenomena that affect the process, as well as with the process conditions and the properties of the insulins.

Finally, the possibilities offered by this kind of model are demonstrated in a model-based optimization study, focusing on the effect of a solubility constraint on the purified solution.

Printed by Media-Tryck, Lund 2017 NORDIC ECOLABEL, 3041 0903

LUND UNIVERSITY

350

ISBN: 978-91-7422-547-1

Department of Chemical Engineering
Faculty of Engineering, LTH
Lund University

9 789174 225471